

MASTERARBEIT

Evaluation of microparticle based multiplexed applications for minimal invasive diagnostics

durchgeführt am
Austrian Institute of Technology
zur Erlangung des akademischen Grades

Diplomingeneur

vorgelegt am Institut für Angewandte Genetik und Zellbiologie
Universität für Bodenkultur Wien

von
Anda Kostov, BSc

Wien, Juni 2016

Betreuer
Priv.-Doz. DI Dr. Andreas Weinhäusel
Mag. Dr. Walter Pulverer



Acknowledgment

I would first like to thank my thesis adviser Priv.-Doz. DI Dr. Andreas Weinhäusel for giving me the chance to do my master thesis in his group at AIT and for his generous advice and inspiring guidance throughout my research for this work.

Moreover, I am indebted to my supervisor Mag. Dr. Walter Pulverer for his continuous help, for all explanations and the patience he had with me.

I would also like to thank my colleagues Gabriel Beikircher, Lisa Milchram and Melanie Hammerl, for their support and the good times we spent together.

Finally, I must express my very profound gratitude to my parents Eleonora and Aurel Farcas, and to my spouse Plamen Kostov for their patience, for providing me with unfailing support and continuous encouragement throughout my years of study and through the process of researching and writing this thesis. This accomplishment would not have been possible without them. Thank you!

Abstract

DNA-methylation and protein-biomarkers have been recognized as very useful tools for minimal invasive diagnostics. These can be detected in volumes of patient's blood or serum, thus allowing integration into pre-symptomatic screening programs. The aim of this work was to evaluate the suitability of Evaluation™, a microparticle based multiplexing platform from MyCartis, to investigate protein and DNA methylation based biomarkers.

Assays design was based on a set of 48 colon cancer specific biomarkers targeting aberrantly methylated DNA, identified and validated previously by AIT. Aiming multiplexed analysis of DNA-methylation markers upon PCR amplification from patient samples by microparticle based hybridization, PCR assays were qualified according MIQE guidelines. Then hybridization conditions were optimized using synthetic oligonucleotides. After establishment of an optimized detection protocol, the per-experiment run time was reduced to 1 h. Further optimisation using different hybridization buffers enabled improved detection sensitivity (LOD <10 nM) and reduced cross-hybridization.

The second part of the thesis was a proof of principle study for autoantibody based diagnostics using the Evaluation™ platform. Therefore an indirect immunoassay was setup; therefore auto-antibodies from human serum were bound to the antigenic proteins immobilized on microparticles and detected by a labeled secondary antibody. Coupling and detection protocols were set which demonstrated the suitability of the platform for autoantibody testing.

Evaluation™ demonstrated its ability of specific detection with short assay times by means of microfluidic channels operated in the reaction limited regime, dynamic control of assay condition and real-time read-out. In this work we could successfully confirm that this platform is a valuable alternative to other methods used for multiplexed protein detection. For DNA based assay detection the current version of the platform has to be improved.

Zusammenfassung

DNA-Methylierungs- und Proteinbiomarker eignen sich besonders zur minimal-invasiven Diagnostik. Unter Verwendung von geringen Blut und Serum- Probenmengen ermöglichen diese die Früherkennung von Krankheiten und Implementierung in präsymptomatische Screening Programme. Im Zuge dieser Arbeit wurde die Eignung der EvaluationTM Plattform von MyCartis zur Multiplex-Detektion von DNA- und Protein-Biomarkern überprüft.

Mit einem am AIT identifizierten Set von 48 Kolon-Karzinom spezifischen DNA Methylierungsmarkern wurde die Multiplex-Analyse mittels Mikropartikel-basierter Hybridisierung nach PCR-Amplifikation evaluiert. Für diese Marker wurden qPCR-Tests entsprechend den MIQE Richtlinien erfolgreich qualifiziert. Hybridisierungskonditionen wurden mittels synthetischer Oligonukleotide optimiert, und durch Entwicklung eines verbesserten Detektionsprotokolls die Test-Laufzeit auf 1 h reduziert. Weitere Optimierungen unter Verwendung verschiedener Hybridisierungspuffer ermöglichten eine Steigerung der Nachweisempfindlichkeit ($LOD < 10 \text{ nM}$) und Reduktion der Kreuzhybridisierung.

Im zweiten Teil dieser Arbeit wurde die prinzipielle Eignung der Plattform zur Autoantikörper-basierten Diagnostik getestet. Ein indirekter Immunoassay wurde implementiert, wobei Serum-Auto-Antikörpern durch Bindung an Mikropartikel gekoppelte Protein-Antigene detektiert wurden. Kopplungs- und Detektionsprotokolle wurden erfolgreich getestet und die Eignung der EvaluationTM Plattform für dieses diagnostische Prinzip bestätigt.

Die Multiplex-analyse mit kodierten Mikropartikeln in mikrofluidischen Kanälen mittels der EvaluationTM Plattform, und der in dieser Arbeit optimierten Protokolle, ist aufgrund kurzer Analysezeiten, dynamischer Laufparameter Steuerung und der Echtzeitdarstellung der Messsignale eine wertvolle Alternative zu anderen Multiplex- Detektionsmethoden. Auf Basis der durchgeführten Arbeiten ist die Eignung der Plattform besonders für Protein-basierte Tests gegeben, während für DNA basierte Tests eine Verbesserung der aktuellen Version notwendig ist.

Table of contents

Acknowledgment	ii
Abstract	iv
Zusammenfassung	vi
Table of contents	x
List of abbreviation	xii
1 Introduction	2
1.1 Personalized Medicine	2
1.2 Molecular diagnostics in personalized medicine	3
1.2.1 DNA methylation as a cancer specific biomarker	4
1.2.2 Molecular diagnostic technologies	5
1.2.3 PCR and real-time PCR microarrays	6
1.3 Multiplex Assays	8
1.3.1 MyCartis Evaluation™ multiplexed detection platform	8
1.4 Aim of the thesis	11
2 Material and Methods	14
Nucleic acid assay	14
2.1 Assay design for Evaluation™ platform	14
2.1.1 Primer design	15
2.1.2 qPCR assay validation	16
2.1.3 Experimental setup for the qPCR assay	18
2.2 Experimental setup for detection on Evaluation™	21
2.2.1 Coupling of Streptavidin on the microparticles	21

2.2.2	Loading the cartridge	22
2.2.3	Streptavidin functional test	23
2.2.4	Attaching of biotinylated DNA probes	23
2.2.5	Flow rate assessment	25
2.2.6	Optimization of Streptavidin-Phycoerythrin concentration	26
2.2.7	Optimization of exposure time for detection	28
2.3	Nucleic acid assay feasibility study	28
2.3.1	Detection optimization using synthetic targets	29
2.3.2	Hybridization of qPCR products on different probes	32
Protein assay		35
2.4	pH screening for antigen coupling	36
2.5	Immunoassay feasibility study of Evalution™	38
2.5.1	Antigen coupling in tubes	38
2.5.2	Non-functional test	40
2.5.3	Human serum IgG detection	41
3	Results	46
Nucleic acid assay		46
3.1	Design and performance of the qPCR assay	46
3.2	Experimental setup for DNA hybridization	50
3.2.1	Flow rate assessment	50
3.2.2	Streptavidin functional test	51
3.2.3	Streptavidin R-Phycoerythrin detection	52
3.2.4	Optimal exposure time	54
3.3	Nucleic acid assay feasibility study	55
3.3.1	Detection optimization using 4 synthetic targets	55
3.3.2	Hybridization optimization in formamide buffer	56
3.3.3	Alternative hybridization buffers	57

0. Table of contents

3.3.4	Assay specificity and sensitivity	59
3.3.5	Hybridization of qPCR products on different probes	60
3.3.6	Limit of detection	64
Protein assay		66
3.4	pH screening for antigen coupling	66
3.5	Antigens coupling confirmation	67
3.6	Purified IgG vs. Serum IgG detection	67
3.7	LowCross and PBST-1%BSA buffers	70
4 Discussion		74
4.1	Nucleic acid assay	74
4.2	Protein assay	79
4.3	Conclusion	81
List of Figures		83
List of Tables		84
References		86
Eigenständigkeitserklärung		92
Appendix		94

List of abbreviations

a.u.	Fluorescence intensity arbitrary units
bp	Base pairs
cfDNA	Cell free DNA
Cp	Crossing point
DMSO	Dimethylsulfoxid
dNTPs	Deoxynucleotide
EDC	N-(3-Dimethylaminopropyl)-N-ethylcarbodiimide hydrochloride
GC	Guanine-cytosine content
LOD	Limit of detection
MES	2-(N-morpholino)ethanesulfonic acid
MIQE	Minimum Information for Publication of Quantitative Real-Time PCR Experiments
MSREs	Methylation Sensitive Restriction Enzymes
PBST	Phosphate-buffered saline buffer with 0.3% Tween [®] 20
PCR	Polymerase Chain Reaction
preAMP	Preamplification
qPCR	Real Time Quantitative PCR
R ²	Correlation coefficient of the standard curves
RXN	Reaction
SAPE	Streptavidin-R-phycoerythrin
SBR	Single to Background Ratio
SNP	Single Nucleotide Polymorphism
SNR	Single to Noise Ratio
ssDNA	Single stranded DNA
STA	Specific Target Amplification
sulfo-NHS	N-Hydroxysulfosuccinimide sodium salt
TBE	TRIS-Borate-EDTA
TE-buffer	Tris-EDTA buffer
T _m	Melting temperature
TMAC	Tetramethylammonium chloride

1 Introduction

1.1 Personalized Medicine

Human are all equal, but definitely different from each other. It's not just the skin color, body shape, eye color or our personality. A person's risk of disease and response to certain treatment is also unique. Even apparently similar diseases may have various causes and manifest themselves in different ways.

Almost all current treatments rely on the traditional standardized "one-size-fits-all" approach, universal drugs for certain diseases. Such a drug is the result of various randomized clinical trials addressed to one particular clinical problem and has to fit to a broader patient population. This ineffective and nonspecific treatment is based on statistically data resulted from research done on thousands of people. In this case of evidence-based medicine the doctors can only poorly predict susceptibility of the patients to a certain diseases and their responses to the applied treatment [Najeeb et al., 2012]. Patients have often lower chances of success in fighting against serious diseases. Beside this in conventional medicine, when a disease has the possibility of multiple pharmacotherapies, the choice of the right treatment is usually left to the experience and preference of the doctor [Jain, 2009].

Knowing the strong possibility of a patient developing diabetes disease or cancer, it would allow doctors to make the treatment more specific in a way that tailors each individual patient. To achieve this the unique properties of the patient, like the genetic map or the profile of the patient's genetic variation, should be well known. Even through that the clinicians and scientists supposed since long time that there is a complex relation between human genes, disease and response to a prescript treatment, the first steps towards individual medicine were set with the mapping of the human genome [Najeeb et al., 2012]. Using the HGP database together with other publicly available resources such as HapMap, a database of common genetic variation in human, researchers were able to identify a variety of

genes that are associated with human diseases. Rapid developments in genomics combined with other fields like computational biology or bioinformatics has given scientists both past and present the possibility of developing tools for personalized diagnosis and treatment. Already more than 1800 genes are known to be responsible for diseases, around 2000 genetic tests for human conditions are available and at least 350 biotechnology-based products are currently in clinical trials [National Institute of Health, 2010]. These extraordinary developments of the last few years led to a revolutionary therapeutic approach in clinical research and medical care – namely, personalized medicine. This concept states that the genotype as well as other individual characteristics of the patient had to be taken into consideration in order to design the right treatment for the right patient [Platforma europeana de dezvoltare, 2013].

Epigenetics has an important role in development of personalized therapies as well as molecular diagnostics. Modifications in gene expression of higher organisms that do not involve changes in the DNA sequence of a gene are called epigenetic alterations. These are associated with aging, environment exposure and pathological conditions. DNA methylation, small interfering RNAs, and histone modification initiate and maintain epigenetic regulation. Unlike genetic modifications, epigenetic alterations are not stable, but rather changeable and can lead to a variety of epigenetic related diseases ([Tost, 2010]). Distinct cancer types are frequently associated with aberrant epigenetic alterations, which can be used as potential biomarkers [Jain, 2009].

1.2 Molecular diagnostics in personalized medicine

The clinical-chemical laboratory diagnostics are a main part of the medicine today. It is assumed that up to 80% of diagnostic decision in the clinical practice relies on laboratory data. Molecular diagnostic is that area of the laboratory diagnostic which is based on detection and study of genetic material or proteins associated with a specific disease [Wink, 2011]. Thanks to modern diagnostic and molecular tests to look at the genetic profile (including epigenetics) of a patient and the

1. Introduction

biomarkers of disease, new pathways are opening up in order to better match therapies to the individual characteristics of the patients, facilitating the practice of personalized medicine. Diagnostic tests can identify a disease, predisposition of a person for a disease, or the progress of a treatment by detecting specific molecules like DNA, RNA and proteins [Pothier et al., 2013].

1.2.1 DNA methylation as a cancer specific biomarker

Molecular diagnostics used in personalized medicine aim generally to identify the presence, amount or absence of a biomarker in tissue, blood, or other body fluids. These are key tools for pharmaceutical research and drug development.

The term "biomarker" (biological marker) referred originally just to simple physiological indicators such as body temperature, heart rate, blood pressure or blood glucose that serve to identify an imbalance of the body or the presence of a disease [Strimbu and Tavel, 2010]. Today many different biomarkers are already known. Modern definition describes a biomarker as any specific measurable molecular alteration of a cell either on DNA, RNA, metabolite, or protein level, that can be used to detect, predict and prognose a disease [Jain, 2010]. There are several definitions of biomarkers in the literature, but the standardized definition of the National Institute of Health working group is now mostly used. They defined a biomarker as “a characteristic that is objectively measured and evaluated as an indicator of normal biological processes, pathogenic processes, or pharmacologic responses to a therapeutic intervention” [Biomarkers Definitions Working Group, 2001].

Research in the biomarker field helped not only to speed up of the diagnosis process, monitoring and development of therapies, but also to reduce the overall costs of therapy. Today biomarker-based molecular diagnostics tests are already available on the market [Schmitz and Anz, 2008].

Analysis of DNA Methylation using cfDNA circulating in peripheral blood can facilitate the development of accurate biomarker for certain diseases [Jung et al.,

2010]. Even though that the release of extracellular DNA into blood is not well understood it is thought to occur due to necrosis, apoptosis, as well as due to active release via secretion [Schwarzenbach et al., 2011]. The presence of high levels of cfDNA in bloodstream of the patients suffering from several carcinoma types was already shown. Genetic alterations of tumoural origin in cfDNA, such as aberrant methylation, were found to be identical with alterations present in the primary tumor [Gormally et al., 2007]. It was estimated that from a tumor weighting 100 g up to 3.3% of its DNA enter daily into the bloodstream. The fragment size of this DNA was found to vary between 70 base pairs up to 21 kilobases. It is known that the clearance of tumor DNA from peripheral blood occurs vary fast and therefore the DNA amount of tumoural origin represents only a fraction of the total cfDNA [Schwarzenbach et al., 2011]. Even though the detection and analysis of methylation patterns for cancer of different organs is possible due to modern molecular technologies.

DNA methylation is the most explored epigenetic modification in tumors. It refers to the enzymatic, post synthetic addition of methyl group to the 5' position of a cytosine ring. In mammals, 70-80% of the CpG dinucleotide are methylated. In the CpG dinucleotides C (cytosine) and G (guanine) are connected by a phosphodiester bond. Most of the unmethylated CpGs are found in GC-rich sequences, the so called CpG island (CGI). Disturbing the specific methylation pattern of a tissue due to hypermethylation or hypomethylation of CpG islands has been linked to different diseases, especially cancer [Levenson, 2011]. ^5mC can be used as a biomarker for detection of aberrant methylation patterns associated with a certain diseases, including early detection of tumors and their classification and characterization into different subentities [Costello et al., 2000].

1.2.2 Molecular diagnostic technologies

Development of sensitive and specific biomarkers is a complex process, carried out on different levels including genome, proteome and transcriptome. Besides of biomarkers, molecular diagnostic requires novel technologies able to analyze in

1. Introduction

parallel a big volume of data obtained from different biomolecules. There is large number of techniques involved in modern molecular diagnostics used to detect and quantify specific DNA or RNA sequences, or certain proteins. Some of this, relevant to the personalized medicine, are presented in Figure 1.1 [Debnath et al., 2010].

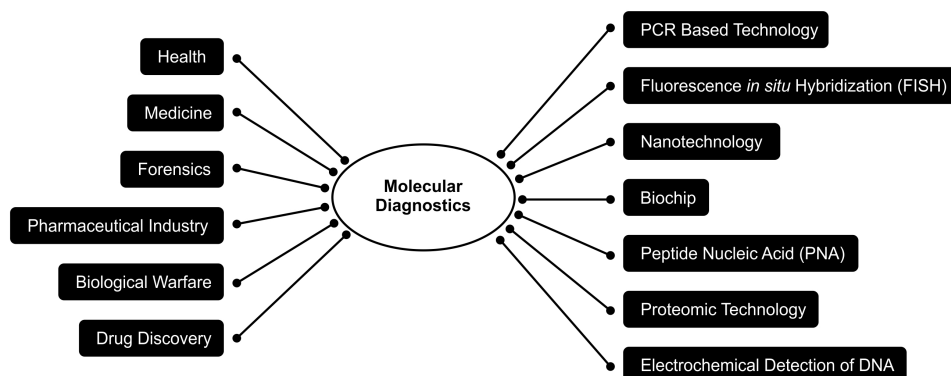


Figure 1.1: Application of molecular diagnostics in clinical field. Adapted after Debnath “Molecular Diagnostics: Promises and Possibilities” [Debnath et al., 2010].

1.2.3 PCR and real-time PCR microarrays

Methods for nucleic acids analysis include microarrays, polymerase chain reaction (PCR) and quantitative polymerase chain reaction (qPCR). These technologies are highly sensitive and allow specific measurement of genomic factors, which are necessary for diagnosis assays or biomarker screening. Polymerase chain reaction or PCR is one of the key techniques used in molecular diagnostics today. It allows the amplification *in vitro* of a specific region of DNA from a limited amount of DNA, generating a large amount of copies, which can be detected and quantified. Chemically synthesized primers (short DNA fragments) ensure the specific replication by determining the sequence of the DNA which has to be amplified. The primers hybridize in a 5' to 3' orientation to one specific strand of the double stranded DNA target. A complementary DNA strand is produced by adding

nucleotides (deoxynucleotide triphosphates – dNTPs) to each primer. The PCR reaction requires a thermostable polymerase, which is not damaged by repeated heat treatments. Every amplification cycle has three basic steps: denaturation, annealing, and extension. During the denaturation step, the two DNA strands are physically separated by heating the DNA to 95 °C. Secondly, the temperature is lowered in order to allow the primer to hybridize to the complementary sequence. Afterwards, the mixture is heated to 72 °C, the optimal temperature of the DNA polymerase, which extends the primers, adding nucleotides sequentially to the primers, using the target DNA as a template. As shown in Figure 1.2, these cycles are repeated, theoretically doubling the DNA copies at every cycle [Alberts et al., 2008].

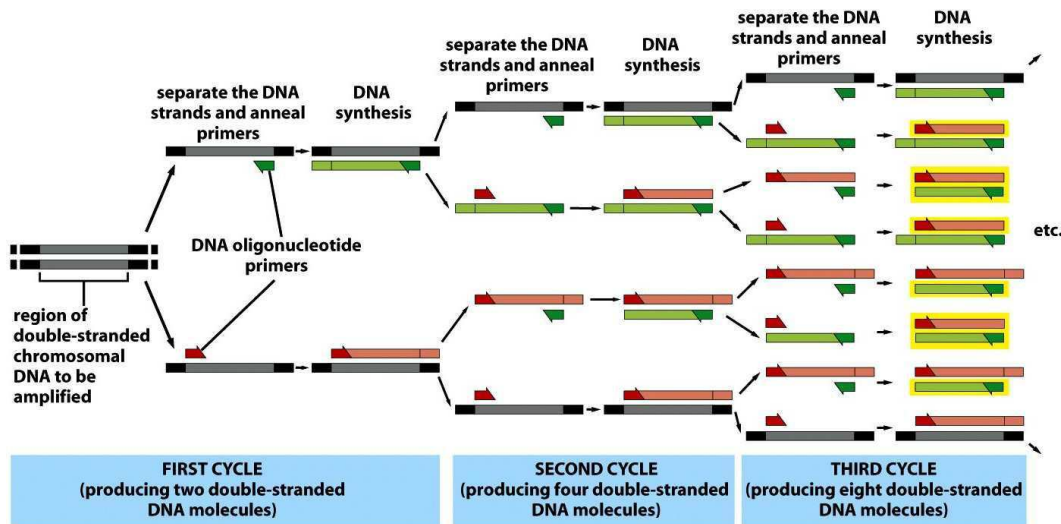


Figure 1.2: Amplification of DNA by PCR technique. The number of the DNA copies doubles after each cycle, and increases by 2^n folds after N cycles. Taken from “Molecular Biology of the Cell” from Alberts [Alberts et al., 2008].

In the conventional PCR, the amplicons are detected at the final phase or end-point of PCR by agarose gel electrophoresis. In recent years the real time PCR, also known as qPCR, has become a valuable alternative to the traditional PCR, where the detection occurs at the final phase, after reaction has already stopped [Mackay, 2007]. Real time PCR monitors the progress of DNA amplification in real time. In contrast to the end-point detection, real-time PCR monitors the

1. Introduction

amplification of the PCR by using florescent dyes. The detection of qPCR is based on fluorescence produce by a reporter molecule, which is proportional to the amount of PCR product accumulated with each cycle of amplification. Comparing the exponential phase of the curve with a known standard, qPCR is able not just to identify the target DNA sequence, but also to quantify the amount of target DNA found in the original sample [Pothier et al., 2013]. Reporter molecules can be fluorescent dyes which bind to the DNA strand (SYBR[®] Green) or fluorescent labeled primer or probes (TaqMan[®]). Although more expensive, fluorescent DNA primers and probes offer advantages over a DNA-binding dye, because they bind more specific and enable multiplexed application [Filion, 2012].

1.3 Multiplex Assays

Highly specific and fast multiplexed detection methods are essential for patient stratification and monitoring of disease progression. The most popularly and commercial available multiplexed assays are bead based assays. They are able to evaluate simultaneously multiples of up to 500 analytes such as proteins or nucleic acids. Screening in parallel of multiple biomarkers requires relatively small amount of samples, reagents, and time [Falconnet et al., 2015]. The potential cost- and time-savings that could be achieved using multiplexed bead assay in comparison to other methods, can provide a highly effective routine use of these in the biomarker research as well as for diagnosis in clinical laboratories [Filion, 2012].

1.3.1 MyCartis EvaluationTM multiplexed detection platform

Platforms and technologies allowing for multiplexing are various, but all of them are fundamentally limited by the rate at which target molecules bind to the surface, especially at low concentration of biomolecules. One of the main advantages of EvaluationTM System compared to other multiplex technologies is the significant reduction of hybridization time achieved by the diffusion-limited reaction kinetics. Planar arrays and bead-based system are mainly driven by diffusion and

show slow binding kinetics. Hybridization occurring in microfluidic channels reduces significantly the diffusional distances between the probes immobilized onto the microparticles surface and flowing targets, reducing also the detection time [Falconnet et al., 2015].

Evaluation™ is a rapid, flexible and sensitive platform based on digitally encoded microparticles in microfluidic channels that allow multiplexed analysis in real-time. It is a novel multiplex platform that it's able to analyze a high range of nucleic acid and protein based biomarkers in a single, simple integrated work flow. In order to ensure short assay times, Evaluation™ system was designed as a semi-automated process, where everything is integrated into a single piece of equipment [Falconnet et al., 2015]. Evaluation™ is compatible with a wide range of surface chemistries for multifunctional usage as shown in Figure 1.3.

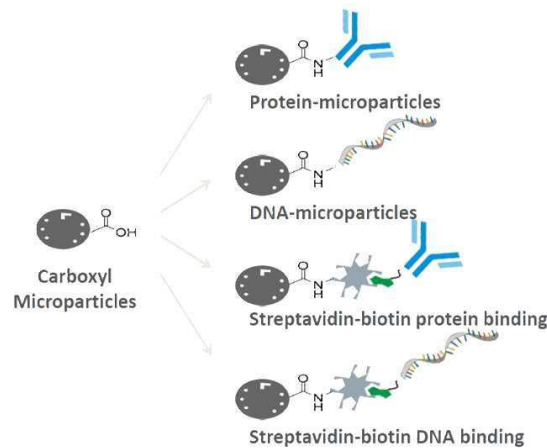


Figure 1.3: Evaluation™ detection schemes. DNA sequences and proteins can bind the carboxylated microparticles directly via amide link or can be coupled via streptavidin-biotin binding. Graphic provided by MyCartis.

The system is built on digitally encoded disc-shaped silicon microparticles that are arranged as a mono-layer on microfluidic assay plate for an optimal readout (Figure 1.4). The robust encoding strategy consists in the presence or absence of engraved bar code in the microparticles, which cannot be influenced by chemical degradation or light. The microparticles make up also the binding support for different biomolecules like antibodies, peptides or nucleic acid probes [Falconnet

1. Introduction

et al., 2015].

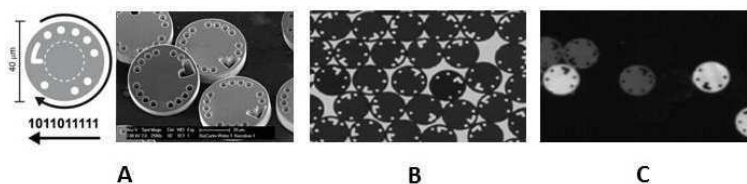


Figure 1.4: Digitally encoded microparticles(A), image used for automated decoding (B), fluorescent image for quantification (C). Adapted after Demierre “The new generation of biomarker analysis for personalized healthcare application”.

An assay plate, shown in Figure 1.5, is composed of 16 independent microfluidic channels, which can be run simultaneously or sequentially on different days. Each channel (700 nL) is 11 mm long, 400 μm wide, 16 μm high and connects an inlet well (130 μl) and a waste well (200 μl). The particles are pushed through the channel by customizable pressure (0 mbar up to 2000 mbar) between inlet and outlet. These are retained statically in the microchannel by a filter placed on the end of the channels, allowing the flow of the reagents and samples. Up to 3000 micro particles can be loaded per channel. With 20 microparticles per population a multiplex level of 150 can be achieved in a fully loaded channel [Falconnet et al., 2015].

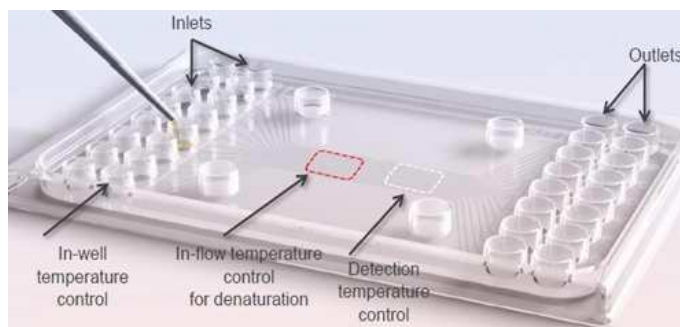


Figure 1.5: Microfluidic assay plate. The cartridge consisting of 16 independent channels, enables individual adjustment of the temperature in three different temperature zones. Image provided by MyCartis

The read out of fluorescent signals is performed by a device that interfaces the cartridge. This allows a dynamic control of the assay and real-data processing. This bench-top instrument (Figure 1.6) allows imaging of the microparticles, pumps

the fluids into the channels, and controls the temperature during the run. Real-time image processing detects and identifies particles, quantifies the fluorescence of each population and display the data. A main advantage of the EvaluationTM is that the system enables temperature control between 25 °C and 95 °C, which can be individually set in 3 zones on the cartridge (Figure 1.5). First zone is represented by the inlet temperature, where the samples and all necessary reagents are added. The second one, the transit zone, can be used for example by denaturation of double stranded DNA. The third zone on the detection zone contains the microparticles where the hybridization takes demand. This zone is also used for signal read out [Falconnet et al., 2015].

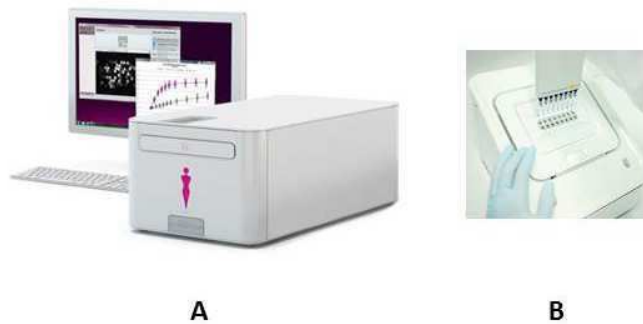


Figure 1.6: Bench top instrument with automated controls and green laser optics for imaging (A), and separate microparticles loading station (B). Adapted after Demierre

1.4 Aim of the thesis

This master thesis, performed at Austrian Institute of Technology (AIT) in collaboration with MyCartis, aimed to evaluate if the EvaluationTM system is suitable for minimal invasive sampling based on DNA methylation read out.

The first part of the thesis comprised the qPCR redesign of a biomarker panel consisting of a 48 targets, differentially methylated in colorectal cancer, with the aim to analyze the panel using the EvaluationTM system. Further, a standard protocol for streptavidin coupling and probes attachment on the microparticles, cartridge

1. Introduction

loading and for detection of EvaluationTM nucleic acid assays had to be established in order to assure an optimal target detection. Optimizations of hybridization temperatures and buffers were also performed and the dynamic range of the EvaluationTM system for nucleic acid detection was assessed.

The second part of the thesis focused on capture and detection of auto-antibodies isolated from human serum using EvaluationTM. Therefore, standard antigen coupling and autoantibody detection protocols were set, followed by optimizations of target concentrations and detection buffers, in order to evaluate the suitability of the system for protein detection.

2 Material and Methods

Nucleic acid assay

2.1 Assay design for Evaluation™ platform

In a previous project AIT have identified several methylation based biomarkers, which allow the identification of patients suffering from colorectal cancer with up to 100% diagnostic accuracy. This identified gene classifiers are best suited for minimal invasive diagnostic testing as well as for assays developing on the Evaluation™ platform, which is based on digitally encoded microparticles provided by MyCartis. AIT's colon-candidate DNA methylation marker panel was derived from targeted microarray based screening. In order to enable a streptavidin-R-phycoerythrin (SAPE) based quantitative detection on Evaluation™; the assay has to be adapted to the microparticle based platform by applying biotinylated probes in combination with biotinylated primer. An illustration of the Evaluation™ design concept is given in Figure 2.1. In this assay, biotinylated DNA probes are attached over Streptavidin-Biotin linkage to the carboxylated microparticles. The surface carboxyl group of the microparticles has to be first activated by adding EDC and sulfo-NHS, in order to yield intermediate esters that will then bind to the amino groups of the Streptavidin being conjugated to the microparticles. To enrich the targets of interest using reversed biotinylated primers, a preamplification (preAmp) step was included. Preamplified DNA targets are finally added into the cartridge, where they undergo an in flow denaturation. The resulted single stranded DNA (ssDNA) can bind complementary to the attached probe on the microparticle contained in the cartridge. Followed by a streptavidin-R-phycoerythrin treatment, the detection of the target is performed by measuring the fluorescence of the R-phycoerythrin bounded on the biotinylated end of the hybridized target.

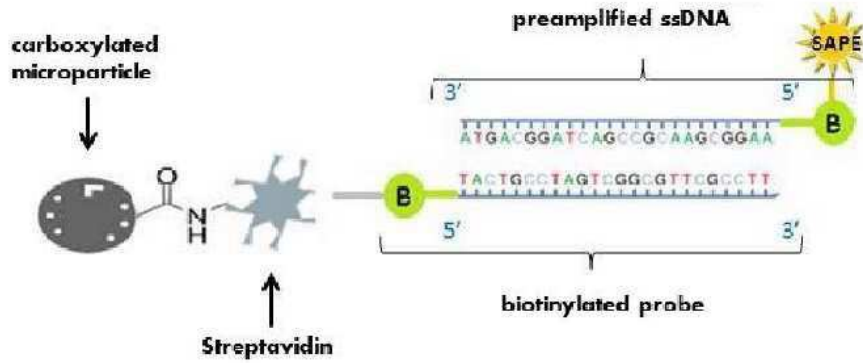


Figure 2.1: Design of the nucleic acid for Evaluation™ platform. Nucleic acid probes, labeled with biotin, are attached to streptavidin coated, carboxylated silicon-based microparticles. After denaturation in flow directly in the cartridge, single stranded PCR products can bind complementary to the attached probes. Finally, detection of the targets is based on fluorescence read out and performed using a streptavidin- phycoerythrin conjugate, which binds the biotin of the captured targets.

2.1.1 Primer design

As already mentioned before, the assay design is based on data from a previous study investigating 360 cancer associated 5'UTR gene regions. 48 optimal targets identified with aberrant modification in colorectal cancer were selected for multiplex assay design on Evaluation™. These had to be adapted to the microfluidic condition of the Evaluation™ system, which requires shorter amplification products between 80 and 150 bp. For that, a redesign of the forward primer and reverse primer was conducted, while the probe sequence remained the same. The primer design was performed with the online tool Primer3 from the University of Massachusetts (http://biotools.umassmed.edu/bioapps/primer3_www.cgi, June 2014). Primers with a length of 18 up to 30 bases and a GC content that range between 20% and 100% were chosen. One of the main aspects to consider when designing primers for multiplex PCR is the melting temperature (T_m). This was set to be between 68 °C and 72 °C for the primers. A T_m variation between forward and reverse primer of 2 °C was accepted so that each primer anneals with comparable efficiency.

2. Material and Methods

With regard to a later, possible method comparison with a MSRE-qPCR approach, the presence of at least two cut sites for the methylation restriction enzymes (MSREs) *AciI*, *HpaII*, *HpyCH4IV* and *Hin6I* in the PCR products was taken in consideration for the assay design. The presence of the desired cut sites, the absence of repetitive elements in the assay and SNPs in the primer sequence were checked by running *In Silico* PCRs. These were conducted using the In-Silico PCR tool from UCSB Genome Browser (<https://genome.ucsc.edu/cgi-bin/hgPcr>, versionHg19, June 2014), which allows the input of a primer pair and display of the amplified sequence in the human genome.

All oligonucleotides used in this work were synthesized by Microsynth (Microsynth, Switzerland) and dissolved in the amount of aqua destillata (as from now referred briefly as water) specified on the manufacture data sheet to adjust the concentration to 100 μ M. This stock solutions were stored at -20 °C.

2.1.2 qPCR assay validation

To ensure reliable experimental data, the assay set up and its quality control were performed running standard qPCR experiments on the LightCycler[®] 480 (Roche Applied Science, Switzerland), following the MIQE guidelines (Minimum Information for Publication of Quantitative Real-Time PCR Experiments) [Bustin et al., 2009]. Specificity, PCR efficiency, precision and linear range were calculated using serial dilutions of DNA.

PCR efficiency

The efficiency of the qPCR reaction is correlated with the robustness and precision of a PCR assay. It was determined by generating standard curves, using DNA standard serial dilutions over a range of four \log_{10} [Bustin et al., 2009]. Therefore, the standard curve was constructed by plotting the log of the starting quantity of the template versus crossing point (Cp) obtained during amplification of each dilution. The Cp value is defined as the number of cycles necessary for

the fluorescent signal to cross the threshold, the background level. Following the assumption of a perfect doubling of the number of DNA template molecules in each step of the PCR, the equation presented in Figure 2.2 was used to calculate the PCR efficiency. An ideal amplification efficiency of 100% is the equivalent of a -3.32 slope. Only efficiency values ranking from 80% to 120% were accepted [Sveca et al., 2015].

$$E = \left(10^{\left(-\frac{1}{\text{slope}} \right)} - 1 \right) * 100$$

Figure 2.2: PCR efficiency equation [Sveca et al., 2015]

Linear dynamic range

The correlation coefficient (R^2), obtained from the calibration curves, describes how well the linear regression fits the experimental data, in other words, it reflects the linearity of the standard curve. In ideal case R^2 has a value of one. According to the MIQE guidelines, the criteria for the acceptance of the linearity was a correlation coefficient R^2 equal or higher than 0.95. For the calculation of R^2 four \log_{10} concentration series for each target were used [Bustin et al., 2009].

Specificity

Assay specificity ensures that the likelihood of annealing to sequences other than the chosen target is very low. Prior to the empirical testing, the uniqueness of the PCR products were tested by running a BLAST search under the UCSC Genome Browser, mentioned in chapter 2.1.1. Another important parameter for the specificity of a PCR assay is the melting temperature, which depends on GC content (guanine-cytosine content), length, sequence composition of the PCR product and salt content of the reaction. Melting curve analysis, used for the identification of the products, including nonspecific products, was acquired on LightCycler[®] 480 (Roche Applied Science, Switzerland), which generated a melting curve after amplification reaction by increasing the temperature gradually and monitoring the

2. Material and Methods

fluorescent signal of each step. Fluorescent data was converted into characteristic melting peaks with a T_m (temperature at which 50% of the ds strands are separated), characteristic for each primer. T_m helps to distinguished the specific product from other products, such as primer dimers, which show other melting temperatures [Worm et al., 2001]. Primer pairs with two melting points were scored negative as a result of the presence of one nonspecific products.

The PCR efficiency varies thorough the reaction and can reach the plateau phase at high cycle numbers. In order to achieve accurate results data, it is very important to quantify qPCR experiments at the beginning of exponential reaction phase, when the DNA polymerase is highly efficient and the amplification reaction does not compete with primer annealing. Therefore, to ensure the specificity of the assay, the maximum value of the first standard point (10 ng/ μ l) was set to be at a C_p smaller than 30 [Karlen et al., 2007].

Precision of the assays

Repeatability and reproducibility of the assays are affected by intra-assay (short-term precision) and inter-assay variation respectively (long-term precision). For evaluation of assay's reproducibility, the presence of each target was measured by running first three standard qPCR experiments, followed by two qPCR experiments with prior enrichment of the targets amount by implementation of a preamplification step. As required by MIQE guidelines, the experiments were conducted on two different days with identical design, but different blood DNA dilution series, which were freshly prepared on the day of the experiment [Bustin et al., 2009].

2.1.3 Experimental setup for the qPCR assay

Standard qPCR parameters were determined to evaluate the quality of the assay. Therefore, a serial dilution was applied and singleplex PCR were performed on LightCycler[®] 480 (Roche Applied Science, Switzerland). The results were used

to generate a standard curve, like that described in subsection 2.1.2, in order to determinate the efficiency, reproducibility and dynamic range of the assay. The designed targets were amplified using genomic DNA extracted out from human peripheral blood mononuclear cells (PBMC), whereby serial dilution with 10 ng/RXN down to 0.16 ng/RXN (dilution factor 4; 4 calibration points). QIAamp Circulating Nucleic Acid Kit (Qiagen, Germany) was used for the extraction of DNA from 1 ml human blood according to the manufacturer's protocol. NanoDrop™ ND-1000 Spectrophotometer (PepLab) was used for the DNA quantification upon absorbency (A_{260}/A_{280}) measurements.

Before starting the qPCR experiments, reverse and forward primers (100 μ M) of each 48 targets were mixed at a 1:1 ratio in a 96 well PCR plate (Framestar®, 4titude, UK). Each pooled primer pair was diluted in a new 96 well PCR plate with water to a concentration of 20 μ M. The 96 well plates were stored at -20 °C.

The linearity of the assays was tested by real time qPCR singleplex experiments, which were performed in a 10 μ l reaction volume. The qPCR mastermix consisted of: 1 μ l 10x PCR buffer with 1.5 mM $MgCl_2$ (Qiagen, Germany), 1.6 mL 2 mM dNTPs mix (Thermo Scientific, USA), 0.5 μ l DMSO with 5x Sybrgreen® (Sigma-Aldrich, USA), 0.06 μ l HotStar Taq Polymerase (Qiagen, Germany), and 5.56 μ l water. 2 μ l of one of the three different DNAs, serially diluted (dilution factor 4, 4 calibration points, 10 ng down to 0.16 ng), and 0.8 μ l of the 20 μ M primer pool were added to the 8 μ l mastermix solution in a 384 well PCR plate (Framestar®, 4titude, UK), finally sealed with qPCR adhesive foil (4titude, UK). The reactions were on the Roche Light Cycler® 480 cycled under the following conditions: 95 °C for 15 minutes, followed by 45 cycles at 95 °C for 40 seconds, at 65 °C for 40 seconds, 72 °C for 1 min 20 seconds with a final extension of 72 °C for 7 minutes.

Due to the limited space on the 384 well PCR plate, the qPCR experiment was performed in two different runs. 28 primers and two primers for positive control (MGMT-101 bp & LUP1- 127 bp in length) were included in the first run, while the next 20 primers were tested on the following day. In addition to the 20 remained primers together with the two controls, eight assays, which showed bad results during the first run, were also reanalyzed in the second run.

2. Material and Methods

It is known that the efficiency of a multiplex PCR can be influenced by interference the other primers. In the next experiment, in order to detect a possible unbalanced amplification of the targets, a preamplification step was done before the 48 single targets have been. Therefore, a 200 nM STA (Specific Target Amplification) primer pool, consisting of 1 μ l of each primer pair (20 μ M) and 79 μ l water were mixed. The PCR mixture per sample contained 5 μ l 200 nM STA primer pool, 2 μ l 10x PCR buffer with 1.5 mM $MgCl_2$ (Quiagen, Germany), 1.6 μ l 2 mM dNTPs mix (Thermo Scientific, USA), 1 μ l DMSO (Sigma-Aldrich, USA), 0.12 μ l HotStar Taq Polymerase (Quiagen, Germany) and 5.28 μ l water to fill up the reaction to 20 μ l. 5 μ l standard DNA dilution series of two different DNAs (dilution factor 4, 4 calibration points, standard 1: 10 ng) were added to the 15 μ l mastermix solution in PCR tube strips (Eppendorf). The amplification reaction was done in the GeneAmp PCR System 2700 (Applied Biosystems) according to the following amplification protocol: heat activation at 95°C for 15 minutes, followed by 17 cycles of 95°C and 65°C for 40 seconds respectively 72 °C for 8 seconds. The program ended with a final elongation step at 72 °C for 7 minutes.

The preamplification mixture was diluted 1:8 with certified water previously adding it to the qPCR mastermix to dilute the remaining primers and to ensure the following individually analysis of all targets. The real time qPCR experiments were performed on the LightCycler® 480 using 384 well PCR plates (Framestar®, 4titude, UK). The 10 μ l reaction volume of the single primer assay contained 1 μ l 10x PCR buffer with 1.5 mM $MgCl_2$ (Quiagen, Germany), 0.8 μ l 2 mM dNTPs mix (Thermo Scientific, USA), 0.5 μ l DMSO with 5x Sybrgreen® (Sigma-Aldrich, USA), 0.06 μ l HotStar Taq Polymerase (Quiagen, Germany), 5.56 μ l water, 2 μ l diluted preamplification mixture of standard DNA and 0.04 μ l 1.5 μ M Primer Mix. The experiment was performed in Frame Star® 384 PCR plates (4titude, UK), sealed with qPCR adhesive foils (4titude, UK), with the following amplification conditions: 95 °C for 15 minutes, followed by 45 cycles at 95 °C for 40 seconds, at 65 °C for 40 seconds, 72 °C for 1 min 20 seconds with a final extension of 72 °C for 7 min.

The specificity of the amplification was controlled by conducting gel electrophore-

sis. The products were visualized using the MCE[®]-202 MultiNA Microchip Electrophoresis System (Shimadzu Biotech, Japan) using the DNA-500 Reagent Kit. According with the MultiNA Experimental Procedure, 3 ml DNA-500 Separation buffer solution was prepared by mixing 2970 μ l TE-buffer with 30 μ l 100xSybr[®] Gold Solution, obtained by 1:100 dilution of the Sybr[®] Gold Nucleic Acid Gel Stain (Invitrogen) with TE-buffer. Further, 2 μ l 25 bp DNA Ladder (Invitrogen) were added to 98 μ l TE-buffer, in order to prepare the DNA-500 Ladder Solution. 3 ml DNA-500 Separation buffer solution, 18 μ l DNA-500 Ladder Solution, 60 μ l DNA-500 Marker solution were set on the Reagent Holder together with the 96 well non-skirted PCR plate (4titude[®], UK) containing 10 μ l qPCR amplification products [Shimatzu Corporation, 2008].

2.2 Experimental setup for detection on Evaluation[™]

2.2.1 Coupling of Streptavidin on the microparticles

Streptavidin (0.74 mg/mL in PBS, Sigma-Aldrich, USA) coupling on the COOH-labeled microparticles was performed using an adapted protocol from MyCartis [Biocartis SA, 2014a]. Streptavidin was attached covalently to Evaluation[™] by a two step EDC sulfo-NHS reaction. To re-suspend the microparticles 200 μ L water were added into the original microparticle tube and thoroughly mixed. Finally the microparticles were transferred to 1.5 mL DNA LoBind safe lock tubes (Eppendorf) containing 200 μ L MEST buffer (100 mM MES (Sigma-Aldrich, USA); 0.3% Tween[®] 20 (Sigma-Aldrich, USA); pH 2.3) by holding the pipette vertically, in order to allow particles to sediment into the tube. The microparticles were washed three times by removing carefully the supernatant using 1.5 ml plastic pasteur pipette (Copan, Italy), adding 500 μ L fresh MEST buffer and vortexing. Between the washing steps the reaction tubes were leaved on the bench for few minutes in order to allow microparticles to sediment. Afterwards, the washing solution was removed and freshly prepared 500 μ L sulfo-NHS and 100 μ L EDC.HCl solutions were added to the microparticles in tubes. The sulfo-NHS solution was prepared by dis-

2. Material and Methods

solving 12.5 mg Sulfo-NHS (Sigma-Aldrich, USA) in 500 μ L MEST buffer, while EDC.HCl solution by dissolving 5 mg of EDC (Sigma-Aldrich, USA) in 100 μ L MEST buffer. After homogenization of the microparticles suspension by gently pipetting mixture up and down, the reaction tubes were placed in Rotator-Mixer (HulaMixerTM Sample Mixer, ThermoFisher Scientific), where the tubes were rotated continuously for 60 minutes according to the program shown in Table 2.1.

Table 2.1: HulaMixerTM program

	Orbital (rpm)	Reciprocal (deg)	Vibro/Pause
turning angle	45°	72°	1°
rotation time	20 s	40 s	5 s

Afterwards, the supernatant was removed and the microparticles were washed three times with 500 μ L Sodium Acetate buffer (100 mM sodium acetate, 0.3% Tween[®] 20, pH 4.8). For the coupling 540 μ L Sodium Acetate buffer, 14 μ L PBST (10 nM PBS (Life Technologies, USA), 0.3% Tween[®] 20, pH 7.2-7.4) and 46 μ L Streptavidin solution (0.74 mg Streptavidin in 1 mL PBS) were added to the DNA loBind tube containing the microparticles and placed in the HulaMixer for 30 minutes, following the rotation program shown in Table 2.1. The final wash removed the unbounded Streptavidin by washing the microparticles three times with 500 μ L PBST. The coupled microparticles were stored in 600 μ L PBST at -20 °C. 50 μ L aliquot of each code of coupled microparticle was saved for the functional test, which was used to check the quality of streptavidin coupling on the microparticles [Biocartis SA, 2014a].

2.2.2 Loading the cartridge

The loading of the microparticles to the cartridge was performed using the pumping Loading Station device. After placing the cartridge in the Loading Station, the selected inlet wells were filled with 500 μ L 100% ethanol in order to prime the channels by pumping it into the channels for 10 seconds. Using a plastic pasteur pipette (Copan, Italy), the remaining ethanol was removed before 110 μ L PBST

were added to the primed inlets and pumped in the channels. The microparticles were homogenize several times in the DNA LoBind tubes by pipetting up and down using 200 μ l pipette tips (Starlabs, Swizerland). 50 μ l of microparticles suspension were aspirated in the pipette, which was placed afterward in the Loading Station, allowing the microparticle to sediment into the inlet wells and to be pumped into the channels. At least 1 mm (corresponding to a number of 250 microparticles) of microparticles mix was loaded by pumping in one channel. All liquids from inlet and outlet wells were removed before the cartridge was insert in the EvaluationTM platform, in order to avoid liquid escape due to overfilling of the outlet wells [Biocartis SA, 2014c].

2.2.3 Streptavidin functional test

The quality characterization of the streptavidin coupling on EvaluationTM microparticles was performed using the inflow functional test, where 2.5 μ g/ml R-Phycoerythrin, Biotin-XX Conjugate (Life Technologies, USA) was used to detect the coupled streptavidin (XX= 14 atom spacer between biotin and point of attachment). 50 μ L aliquot of four different population of microparticles mentioned in subsection 2.2.1 were mixed together with 350 μ L PBST in a 1.5 mL DNA LoBind tube [MyCartis, 2014]. 1 mm of this mix was loaded in a channel of a cartridge following the loading protocol described in subsection 2.2.2. The protocol for the EvaluationTM software was set to be as shown in Figure 2.3, whereby in brief 100 μ L R-PE conjugated with biotin-XX were flushed over the streptavidin coupled microparticles for 15 minutes followed by a 3 minutes wash with PBST. The coupling efficiency of streptavidin was evaluated by measuring the fluoresce intensity of R-Phycoerythrin (R-PE) which was bound over biotin to streptavidin on the microparticles.

2.2.4 Attaching of biotinylated DNA probes

The advantage of the strong biotin-streptavidin affinity was used to attached the biotinylated DNA probes to streptavidin coupled microparticles. 100 nM oligonu-

2. Material and Methods

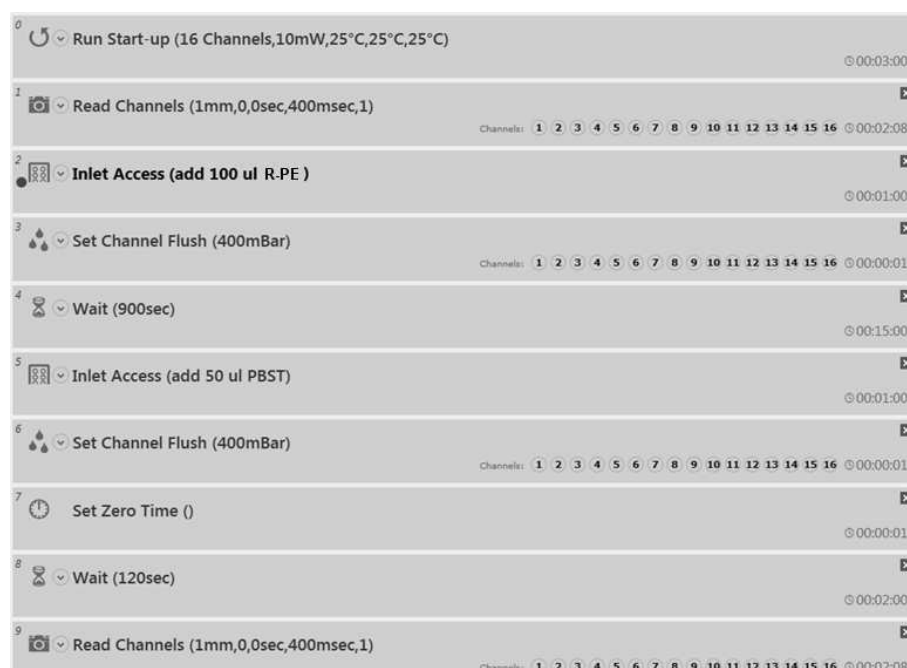


Figure 2.3: Functional test protocol for the Evaluation™ software, showing the procedure steps and the set up of their corresponding parameters. In step 0 the number of channels, the laser power (10 mW) and the temperature of the cartridge zones (25 °C for all 3 zones) were defined. Step 1 consists of the background measurement of the system (blank), whereby the microparticles are scanned before any assay at the same exposure time (400 msec) as the assay should be used. Adapted after MyCartis “Training on Evaluation: Streptavidin functional test” [MyCartis, 2014].

cleotides solution in PBST was prepared from 100 μ M stock solution of biotinylated probes (Microsynth, Switzerland). Each streptavidin coupled microparticle population was washed three times with 500 μ l PBST. Afterwards the PBST supernatant was removed and 650 μ l of the 100 nM biotinylated probes solution was added to the microparticles. The 1.5 ml DNA LoBind reaction tube was placed in Rotator-Mixer and rotated continuously for 45 minutes using the program presented in Table 2.1. Finally, the microparticles were washed three times with PBST, split in aliquots by suspending 50 μ l microparticles solution in PBST to a total volume of 500 μ l and stored at -20 °C [Biocartis SA, 2014b].

2.2.5 Flow rate assessment

The flow rate test protocol provided by MyCartis was used to assess the flow rate in Evalution™ cartridges, which is important to achieve a continuously supply of analytes and fast binding kinetics, by avoiding sample loss due to sample binding by cause of diffusion, as mention in subsection 1.3.1. The flow rate differs with the flushed buffer, temperature, number of loaded microparticles, and the pressure in the channels. The measurement principle relies on flushing the hybridization buffer for a predefined duration and under controlled conditions and subsequently weighting of the liquid quantity in the outlet wells.

The experiment was carried out with and without microparticles loaded in the channels by the same temperature in the three cartridge zones as the assay should be used, in brief 25 °C inlets zone, 95 °C denaturation zone, and 55 °C hybridization and detection zone. Figure 2.4 an exemplary protocol for flow rate determination. Necessary channels were first primed with 10µl ethanol and filled with hybridization buffer (e.g.PBST) as mentioned in subsection 2.2.2. The buffer was flushed in two empty channels, as well as in two channels loaded with 1 mm microparticles.

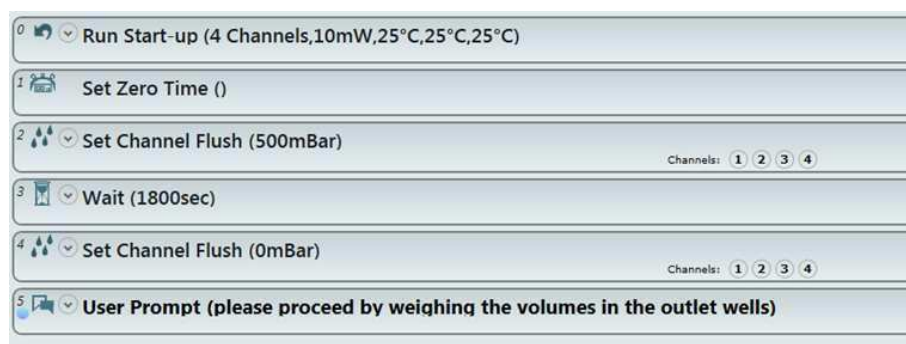


Figure 2.4: Flow rate measurement protocol

After completion of the run, the cartridge was taken out and the liquid of every inlet and outlet well was weighted. The flow rate was calculated using the following

2. Material and Methods

equation [MyCartis, 2014b]:

$$\text{Flow rate [nl/s]} = \frac{\text{measured outlet weight [mg]} * 1000}{\text{duration [s]} \text{ [MyCartis, 2014b]}}$$

The flow rate was evaluated for all hybridization buffers. All hybridization buffers and their chemical composition are listed in Table 2.2.

Table 2.2: Hybridisation buffers used for the experiments in this thesis and their chemical composition

Buffer	Composition
3x SSC	7.25 ml 20x SSC (Invitrogen, USA), 7.25 µl Proclin 300 (Sigma-Aldrich, USA), 50 mg N-Lauroylsarcosine sodium salt (Sigma-Aldrich, USA), 42.75 PCR clean water
DIG Easy Hyb	5 ml Formamide (Sigma-Aldrich, USA), DIG Easy (Sigma-Aldrich, USA)
Express Hyb PCR Buffer	20 ml Formamide, 30 ml Express Hyb buffer (Clontech Labs, USA) 2.5 ml DMSO (Sigma-Aldrich, USA), 5.5 ml 10x PCR Puffer (Qiagen, Germany), 42 ml PCR clean water
TMAC	30 ml 5 M TMAC (Sigma-Aldrich, USA), 0.25 ml 20% Sarkosyl solution (Sigma-Aldrich, USA), 1 M Tris-HCl ph 8.0 (Sigma-Aldrich, USA), 0.4 ml 0.5 M EDTA (Sigma-Aldrich, USA), 16.85 ml PCR clean water
25% Formamide	5.25 ml 20x SSC solution (Invitrogen, USA), 0.9 ml 10 % SDS (Sigma-Aldrich, USA), 7.5 ml Formamide, 16.35 ml PCR clean water
30% Formamide	5.25 ml 20x SSC solution, 0.9 ml 10 % SDS, 9 ml Formamide, 14.85 ml PCR clean water
35% Formamide	5.25 ml 20x SSC solution, 0.9 ml 10 % SDS, 10.5 ml Formamide, 13.35 ml PCR clean water
40% Formamide	5.25 ml 20x SSC solution, 0.9 ml 10 % SDS, 12 ml Formamide, 11.85 ml PCR clean water

2.2.6 Optimization of Streptavidin-Phycoerythrin concentration

At the beginning of the experiments on the EvaluationTM platform, the presence of streptavidin phycoerythrin (SAPE) aggregates on the microparticles was observed. This increased the fluorescence background signal and contributed to a reduction of detection sensitivity. In order to avoid aggregation, the optimal concentration and incubation time of SAPE was determined for different hybridization buffers, using

three 5' biotin labeled synthetic oligonucleotides (Microsynth, Switzerland). The interaction between 3xSSC, TMAC, 30% Formamide hybridization buffers and SAPE in different concentrations (1.5 µg/ml, 3 µg/ml, 5 µg/ml in hybridization buffer, and in 1:1 hybridization buffer dilution with water) was tested. The use of PBST buffer instead of hybridization buffer in the last washing step of the run was also analyzed in separate channels. Further, two negative controls were added to the experiment, one consisting in loading only SAPE without oligonucleotides and the other in loading only buffer in the channel.

For this experiment, three probes complementary to the synthetic oligonucleotides were attached first on differently encoded microparticles following the streptavidin coupling and probes attaching protocol presented in Subsection 2.2.1 and 2.2.4. The microparticle attached with three different probes were pooled together and loaded in the necessary channels according to the loading protocol presented in Subsection 2.2.2. The SAPE solutions were fresh prepared starting from the 1 mg/ml SAPE stock solution (Moss, USA), which was diluted in the first step to 30 µg/ml and further to 3 µg/ml, respectively 1.5 µg/ml. Between dilution steps, the protein conjugate solution was centrifuged briefly for 3 minutes by 10.000 rpm and only the supernatant was used for the experiment.

The inlet temperature was set to 25 °C for the beginning of that run, denaturation temperature was set to 95 °C and detection was set to 55 °C. The software run started with the scan of the channels at 400msec (blank scan for measuring the system background), continued with 2 min hybridization buffer wash (60 µl) of the channels followed by 30 minutes incubation by 250 mbar of the 100 µl SAPE dilution (1.5 µg/ml and 3 µg/ml) added in the inlets. Between two steps in the protocol, the remained liquid from the inlet well was removed with a 1.5 ml Pasteur pipette. After incubation, the temperature was decreased in all three cartridge zones to 25 °C, the remained liquid was removed from every inlet and the channels were washed for 2 min with 60 µl hybridization buffer. 100 µl SAPE was added and incubated for 10 minutes by 400 mbar, followed by a 2 minutes wash with 80 µl hybridization buffer. All channels were scanned at 400 msec.

2. Material and Methods

2.2.7 Optimization of exposure time for detection

As already mentioned in Subsection 1.3.1, EvaluationTM uses fluorescence for data readout. A suitable exposure time improves the sensibility of detection and avoids over saturation of the digitally captured images. Using the streptavidin coupling and probe attaching protocols presented in Subsections 2.2.1 and 2.2.4, one probe, complementary to one synthetic target, was attached to the microparticles. 200 nM, 100 nM, 50 nM, 10 nM dilutions of one synthetic oligonucleotides (MSH4, Microsynth, Switzerland) were made as well in 3xSSC as also in 30% formamide hybridization buffer and added into four channel, previously loaded with attached microparticles. Following the standard EvaluationTM running script presented in Appendix A-7, a 10 minutes incubation with 3 µg/ml SAPE (Moss, USA) was done. Afterward, images of the microparticles were captured with different exposure times (200 ms, 300 ms, 400 ms, 500 ms). An additional channel filled with attached microparticles was included as a negative control using only hybridization buffer instead of the target solution, in order to identify non-specific fluorescence.

2.3 Nucleic acid assay feasibility study

In order to be able to identify small amounts of specific nucleic acid sequences obtained PBMC DNA using the EvaluationTM system, parameters had to be initially optimized. To speed up the optimization processes, the experimental setup of the qPCR reaction, presented already in Subsection 2.1.2, was developed in parallel to the optimization and characterization of targets detection. Due to many non-conventional elements of the EvaluationTM system, such as manipulating of microparticles, efficient loading, managing flow rate and temperature during assays, etc., parameters optimization was done using a limited panel of nucleic acids.

2.3.1 Detection optimization using synthetic targets

To optimize the assays for the Evaluation™ system, the initial phase of nucleic acid detection was conducted using only 4 3' biotinylated synthetic oligonucleotides (Microsynth, Switzerland). The lyophilized synthetic oligonucleotides were resuspended in water to a concentration of 100 µM according to the documents provided by Microsynth.

Read-out optimization using hybridization buffers

The initial experiments, attempted to test the suitability of Evaluation™ system detection by the means of signal intensity, were performed using four synthetic oligonucleotides as targets (MSH4, TJP2, TWIST1, CHFR). In order to provide a fast, simple and functional setting for detection, only two hybridization buffers were tested, which were used for specific binding between sequences of biotinylated nucleic acid contained in the samples and nucleic acids probes fixed on microparticles. The 3x SSC hybridization buffer (7.25 ml 20x SSC (Invitrogen, USA), 7.25 µl Proclin 300 (Sigma-Aldrich, USA), 50 mg N-Lauroylsarcosine sodium salt (Sigma-Aldrich, USA), 42.75 PCR clean water) was recommended by MyCartis based on their own experience with Evaluation™ platform, while the 30% formamide buffer (5.25 ml 20x SSC solution, 0.9 ml 10 % SDS, 9 ml Formamide, 14.85 ml water) was already successfully used for DNA hybridization and detection on microarrays.

After streptavidin coupling (Subsection 2.2.1, 2.2.4, attaching of 4 biotinylated probes complementary to the synthetic targets over streptavidin on differently encoded microparticles was conducted. The microparticles were mixed together and loaded in 4 channels according to the loading protocol 2.2.2. The synthetic oligonucleotides were diluted as well in 3xSSC and respectively in 30% formamide hybridization buffer to the following concentrations: 200 nM, 100 nM, 50 nM and 10 nM.

A single synthetic target solution (100 µL) was applied to every channel containing 4 different codes of coupled microparticles and detected following the Evaluation™

2. Material and Methods

running script presented in Appendix A-7. A DNA denaturation step was performed directly in the channels, in the transit zone at 95 °C, in order to render it single-stranded. Afterwards, the single strands were flushed over with the complementary probes attached on the microparticles by flowing the denatured targets in the detection zone at 52 °C, temperature condition that favors hybridization. This process combination of denaturation followed immediately by hybridization of the targets was run for 30 minutes. After a short washing step and decrease of the temperature in the channels to 25 °C, the targets were incubated with 3 µg/ml SAPE (Moss, USA) for 10 minutes and finally detected by 300 ms exposure time.

Concentration and hybridization optimization of the formamide buffer

To investigate if the fluorescence intensity of the formamide buffer can be improved by changes in the buffer formulation, 4 hybridization buffer solutions with different percentage of formamide (25%, 30%, 35% and 40%) were tested at 55 °C, 60 °C and 65 °C and compared.

Using the standard running script (Appendix A-7), a 200 nM, 100 nM and 50 nM mixture of the 4 synthetic targets, were added to a mix of 4 microparticles codes in the channels. After denaturation at 95 °C and hybridization at 55 °C, 60 °C and 65 °C for 30 minutes, followed by a 10 minutes incubation with 3 µg/ml SAPE, the microparticle were scanned at an exposure time of 500 ms.

Alternative hybridization buffers

Use of alternative hybridization buffers can improve hybridization and detection of DNA using the Evaluation™ system. TMAC, DIG Easy Hyb, ExpressHyb buffer and a standard qPCR hybridization buffer were evaluated as possible alternatives to 3x SSC and formamide hybridization buffers, mainly focusing on optimal signal intensities, signal to blank, linearity over the concentration range and presence of SAPE aggregates. All four buffers were already used in the framework of other AIT projects for hybridization of PCR products.

DIG Easy hybridization buffer (10% formamide (Sigma-Aldrich, USA), DIG Easy Hyb buffer (Sigma-Aldrich, USA)) facilitates the lowering of the hybridization temperature, while ExpressHyb buffer (40% formamide (Sigma-Aldrich), ExpressHyb buffer (Clontech Labs, USA)) reduces hybridization times without losing sensitivity. Addition of DMSO to the 1x PCR hybridization buffer (5% (DMSO Sigma-Aldrich, USA), 10x PCR Puffer (Qiagen, Germany)) lowers the DNA strand separation and hybridization temperature [Kennedy and Oswald, 2011]. Tetramethylammonium chloride or TMAC (Table 2.2) was recommended by MyCartis as a proper hybridization buffer for nucleic acids. It is also used for the Luminex[®] platform (Thermo Fisher Scientific) by hybridization of tagged PCR products on microsphere-bound antitags. This buffer reduces the non-specific priming and increase the specificity [Kennedy and Oswald, 2011].

After loading of several cartridge channels with a mixture of different microparticles codes attached with 4 targets corresponding probes (coupling and attaching protocol in Subsection 2.2.1 and 2.2.4), 200 nM, 100 nM and 50 nM solutions of the synthetic targets (MSH4, TJP2, TWIST1, CHFR) were added into the cartridge inlets. According to the running script presented in Appendix A-7, containing a denaturation step at 95 °C, the hybridization of the targets was performed for 30 minutes in three different runs at 42 °C, 52 °C and 62 °C. The final scanning of the microparticles was done using an exposure time of 500 ms.

In an additional channel, 4 new microparticles codes attached with different probes were loaded together with the microparticles set used for detection of the 4 synthetic targets. Using the same run setting and hybridization buffers mentioned above, a 200 nM mixture of the synthetic oligonucleotides was analyzed, in order to evaluate a possible cross-hybridization.

Determination of assay specificity and sensibility

Hybridization specificity is essential for quality results. The ability of the Evaluation[™] probes to bind specific nucleic acids in a multiplex approach was assessed using a mixture made of 4 synthetic targets (MSH4, TJP2, TWIST1, CHFR),

2. Material and Methods

which was applied to the channels containing 19 microparticles populations coupled with different probes, where the same protocol mentioned above (Appendix A-7) was used. The analytical sensitivity or the limit of detection (LOD) was determined using samples of known concentration (10 nM, 5 nM, 1 nM, 0.5 nM, 0.25 nM, 0.05 nM, 0.02 nM) of synthetic oligonucleotides targets and a blank consisting only of hybridization buffer. The experiments were conducted in 3x SSC and TMAC buffer, using a hybridization temperature of 52 °C and 42 °C, respectively. The read-out was conducted with 500 ms exposure time.

2.3.2 Hybridization of qPCR products on different probes

The outline of this experiment was to test the feasibility of the EvaluationTM platform to detect multiple nucleic acids targets isolated from blood, using a multiplexed approach.

For this experiment, 38 probes were attached via streptavidin to different microparticle populations following the standard protocols already presented in Subsection 2.2.1, 2.2.4 and 2.2.3. In order to facilitate a proper storage and efficiently cartridge loading, two pools of microparticles were prepared so that each mixture contained 19 microparticle codes attached with different probes.

Isolation of PBMC DNA from 1 mL plasma was conducted using the QIAamp Circulating Nucleic Acid Kit (Qiagen, Germany), followed by quantification of DNA contained in the sample by NanoDropTM ND-1000 Spectrophotometer (PepLab, Germany).

Preamplification of the limited amount of cDNA isolated from plasma was necessary for the analysis of the 19 nucleic acid assays. 19 primers were amplified in single target reactions. 39.8 µL qPCR mastermix for one reaction, containing 4 µL 10x PCR buffer with 1.5 mM MgCl₂ (Qiagen, Germany), 3.2 µL 2 mM dNTPs (Thermo Scientific, USA), 2 µL DMSO (Sigma-Aldrich, USA), 0.24 µL HotStar Taq Polymerase (Qiagen, Germany), 27.36 µL water, was combined in a single tube of the PCR tube strip (Eppendorf) with 0.2 µL of a single primer pair (20 µM) and

3 μ L DNA (60 ng/ μ L). A negative control reaction containing the mastermix and primers was also added to the assay. After homogenization by short vortexing, the preamplification reactions were performed in VWR Duo Cyclor (VWR, USA) according to the following protocol: heat activation at 95 °C for 15 minutes followed by 35 cycles of denaturation at 95 °C and 65 °C for 40 seconds respectively and 72 °C for 80 seconds. The program was completed with a final 7 minutes elongation step at 72 °C. Products of the preamplified targets were controlled in a 2% agarose gel. For agarose gel, 6 g peqGold Universal Agarose (Peqlab, Germany) were dissolved in 300 mL 1xTBE buffer (TRIS-Borate-EDTA, Sigma-Aldrich, USA). 30 μ L SYBR[®] Safe DNA Gel Stain in DMSO (Life Technologies, USA) were added to the gel for trans-illumination. 2 μ L samples were diluted in 8 μ L water and 2 μ L 6x Loading Dye (Thermo Scientific, USA). The GeneRuler[™] 100 bp DNA Ladder (Thermo Scientific, USA) was used as a DNA marker. The gel electrophoresis was performed in PerfectBlue Gel System Maxi S Plus (Peqlab, Germany) for 60 minutes with 180 V supplied by the PeqPower 250 Powerstation (Peqlab, Germany). The separated bands were visualized at a wavelength of 515-570 nm. The gel images were captured with BioSpectrum[®] 310 Imaging System (UVP, Canada) using VisionWorksLS Image Acquisition and Analysis Software (UVP, Canada).

After confirmation of successful targets amplification, all products were pooled together. 20 μ L, 10 μ L, 5 μ L and 2 μ L of the samples mixture were added to hybridization buffer to a volume of 100 μ L. According to the standard loading protocol presented in Subsection 2.2.2, the cartridges were loaded with the microparticle pool which contained 19 attached probes corresponding to the 19 amplified targets. The hybridization approach was run with 3x SSC, TMAC (1.5 X TMAC hybridization solution, Table 2.2), 35% Formamide and 1x PCR buffer with 5% DMSO buffers at 42 °C, 52 °C and 62 °C. Apart from the changed hybridization temperature, the standard running script presented in Appendix A-7 was followed. Sample solutions were analyzed along with two negative controls (preAmp negative control and hybridization buffer) and a positive control (5 nM mixture of 4 synthetic oligonucleotides MSH4, TJP2, CHFR, TWIST1). In order to check cross reactivity, an additional channel was loaded with the second microparticle pool, containing 24 probes that theoretically should not bind the targets. For detec-

2. Material and Methods

tion, a SAPE concentration of 3 $\mu\text{g/mL}$ prepared in hybridization buffer, which was previously diluted 1:1 with water, was used for incubation. The read-out was performed with an exposure time 500 ms.

Protein assay

Recognizing the potential of the multiplex technology based on digitally encoded microparticle in microfluidic channels as a potential molecular diagnostic tool, we evaluated its significance in detecting proteins.

A schematic representation of the protein assay design is depicted in Figure 2.5. The developed indirect immunoassay involves the following elements: MyCartis microparticles bearing carboxyl groups on the surface, antigens acting as probe for sample antibodies and a detection antibody. The carboxylated microparticles capture specific IgG molecules which are label by a secondary antibody. NEUROD2 and NFIX, taken from a *E. coli* based expression library (UniPEX), were selected as antigens based on a previous auto-antibody project conducted by Austrian Institute of Technology. Both include an N-terminal 6x-His-tag in order to make their identification and purification from *E. coli* possible. Sample detection was performed using goat-anti-human-IgG conjugated to R-Phycoerythrin specific against Fab and Fc γ IgG fragments.

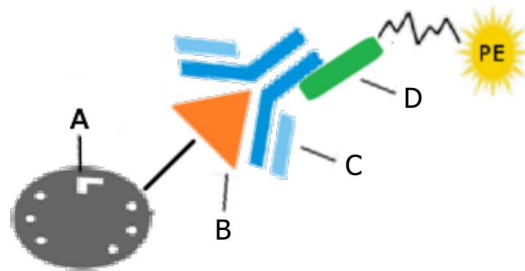


Figure 2.5: Schematic set up representation of an indirect immunoassay composed of carboxylated microparticle (A), an antigenic protein (B) acting as a probe, IgG from sample (C) and a detection antibody labeled with phycoerythrin (PE) (D).

2. Material and Methods

2.4 pH screening for antigen coupling

Strongly acidic or basic conditions can influence phycoerythrin detection reaction [Liu1 et al., 2009]. Before performing the assay it was important to check if aggregation of the Streptavidin-Phycoerythrin occurs and how pH influences the fluorescence intensity. For this, antigens were covalently bound to Evaluation™ COOH labeled microparticles by a two-step EDC sulfo-NHS reaction, explained in brief in Figure NHS. Immediately after coupling of the protein of interest under varying pH conditions per channel, the process was evaluated by measuring fluorescence of a reporter protein. The protein coupling was performed according to the Immunoassay Protocol provided by MyCartis directly in the cartridge, which is explained in detail in the following paragraph [MyCartis, 2014a].

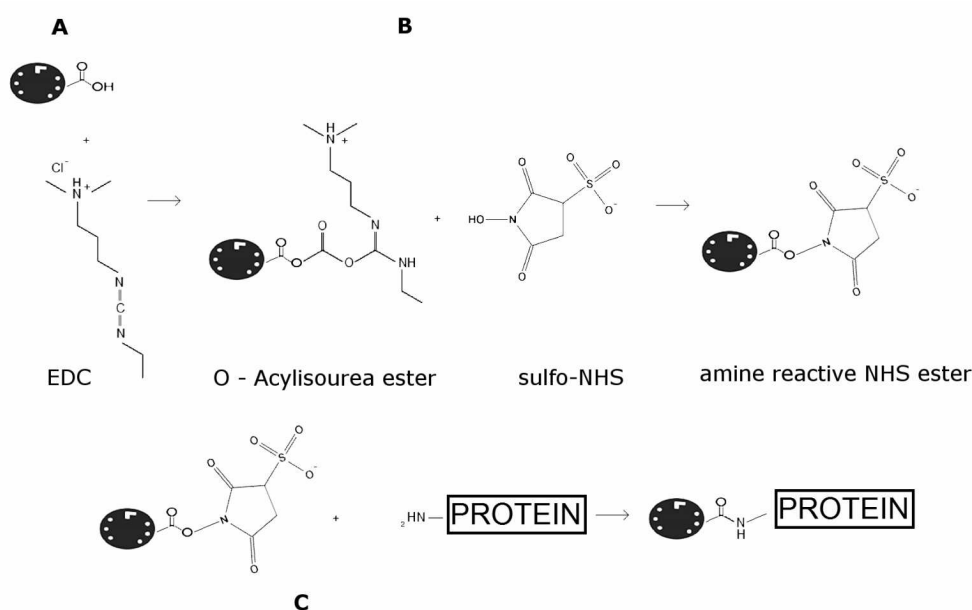


Figure 2.6: Schematic set up representation of the EDC/sulfo-NHS activation of COOH-microparticles. The COOH-microparticles were activated by mixing them together with sulfo-NHS and EDC (a dehydrating agent). In the first step of reaction EDC forms with the COOH group of the microparticle an unstable ester intermediate (A). The addition of sulfo-NHS stabilizes this intermediate by converting it in to an amine-reactive NHS ester (B), which then react with the amino groups of the protein and form a covalent bound (C). [Gmeiner, 2015]

This experiment was conducted using the IgG samples P125 (1.04 mg/mL) and P225 (0.64 mg/mL), purified using Melon Gel Kit (Thermo Scientific) from human serum. After thawing the frozen samples, they were brought to a concentration of 0.1 μ g IgG/ μ L in LowCross buffer (Candor, Germany). The coupling of the microparticles was carried out using NEUROD2 (2 mg/mL) and NFIX (0.48 mg/mL) antigens as probes. The coupled antigens bound the IgG antibody from the flushed samples forming a protein complex that was detected by measuring the fluorescence of a reporter conjugated to goat anti-human IgG. R-Phycoerythrin AffiniPure F(ab')₂ Fragment Goat Anti-Human IgG (Jackson ImmunoResearch, USA) stucked to the Fab portion of human IgG that was already captured to the microparticles through the antigen binding.

The pellets of COOH-labeled microparticles codes (MyCartis, Switzerland) were suspended in the original package tube in 200 μ L water. 100 μ L were aspirated into the pipette tip and immediately transferred by sedimentation into a 1.5 mL Protein LoBind tube (Eppendorf, Germany) containing 100 μ L MEST buffer (100 nM MES (Sigma-Aldrich, USA); 0.3%(v/v) Tween[®]20 (Sigma-Aldrich, USA); pH 3.5). After carefully removing the supernatant using 1.5 mL plastic pasteur pipette, the microparticles were washed 3x by vortex homogenization in 250 μ L MEST buffer and finally re-suspended with 1 mL MEST buffer (pH 3.5).

Before starting the cartridge loading, the antigen solutions were diluted for pH screening to a concentration of 2 μ g/ μ L in each of the following buffers: MEST pH 3.6, Sodium Acetate pH 4.9, MEST pH 6.5, MEST pH 7.3 and MEST pH 8.1. 12 channels of the cartridge were loaded with 1.5 mm COOH-labeled microparticles in MEST pH 3.5. Shortly before cartridge insert, a mixture of 200 μ L 50 mg/mL EDC.HCl (Sigma-Aldrich, USA) and 1 mL 10 mg/mL sulfo-NHS solutions were prepared in MEST buffer (pH 3.5). After setting the flow pressure at 350 mbar for all experimental steps, 50 μ L of this mixture was flushed for 10 minutes in each channel. After removing the content of the inlets, the wells were washed twice with MEST buffer (pH 3.5), followed by a 2 minutes channels flush with 70 μ L of the same buffer. After removing the remaining solution from inlets, the coupling of the antigens was conducted flushing 90 μ L of the antigen solutions for 20

2. Material and Methods

min and was finally completed after a 5 minutes wash with 70 μ L PBST (10 nM PBS (Life Technologies, USA), 0.3% (v/v) Tween[®]-20 (Sigma-Aldrich, USA, pH 7.2-7.4). 50 μ L of each sample were added into the inlet wells and flushed for 10 minutes in 6 channels corresponding to one antigen. After a short 1 minute wash of the channels with PBST, 50 μ g/mL of a 0.5 μ g/mL solution of Biotin goat anti-human IgG (diluted in LowCross buffer (Candor, Germany)) was added and flushed for 5 minutes. After 1 minute channel wash with PBST, the microparticles were scanned by increasing the exposure time every 20 ms, from 20 ms up to 250 ms. A screen-shot of the EvaluationTM Software representing the running script for the pH screening experiment is illustrated in Figure 2.7.

2.5 Immunoassay feasibility study of EvaluationTM

In this section the protocol used for the standard coupling procedure in protein LoBind Tubes and the antigen coupling confirmation via a non functional test will be explained. Further, a comparison of the fluorescence intensities between purified human IgG and serum human IgG was conducted and the feasibility of the LowCross buffer and 1x PBS (pH 7.4) - 1% BSA (10x PBS, pH 7.4 (Life Technologies, USA)) as assay buffers on EvaluationTM system was evaluated with different concentration of detection antibody, amount of IgG present in the sample as well as using several sample incubation times.

2.5.1 Antigen coupling in tubes

In order to save time, instead of proceeding the coupling direct in the cartridge during every run, a bigger amount of microparticles were coupled with antigens in protein LoBind tubes. Preparation of COOH-microparticles for protein coupling in tubes was accomplished similar to the coupling of nucleic acids presented in the previous chapter.

After re-suspending 5 different microparticles pellets in their original package tubes

2. Material and Methods

0	Run Start-up (16 Channels,10mW,25°C,25°C,25°C)	00:03:00
1	Inlet Access (add EDC sulfo-NHS)	00:01:00
2	Set Channel Flush (350mBar)	00:00:01
3	Wait (600sec)	00:10:00
4	Inlet Access (wash inlets 2x then add activation wash buffer)	00:01:00
5	Set Channel Flush (350mBar)	00:00:01
6	Wait (120sec)	00:02:00
7	Inlet Access (add antigen solutions)	00:01:00
8	Set Channel Flush (350mBar)	00:00:01
9	Wait (1200sec)	00:20:00
10	Inlet Access (wash inlets 2x then add coupling wash buffer)	00:01:00
11	Set Channel Flush (350mBar)	00:00:01
12	Wait (300sec)	00:05:00
13	Inlet Access (Functional test: add sample solutions)	00:01:00
14	Set Channel Flush (350mBar)	00:00:01
15	Wait (600sec)	00:10:00
16	Inlet Access (Functional test: add assay wash buffer)	00:01:00
17	Set Channel Flush (350mBar)	00:00:01
18	Wait (60sec)	00:01:00
19	Inlet Access (Functional test: add anti-human Ab)	00:01:00
20	Set Channel Flush (350mBar)	00:00:01
21	Wait (300sec)	00:05:00
22	Inlet Access (Functional test: add assay wash buffer)	00:01:00
23	Set Channel Flush (350mBar)	00:00:01
24	Wait (60sec)	00:01:00
25	Set Channel Flush (350mBar)	00:00:01
26	Set Zero Time ()	00:00:01
27	Read Channels (1mm,0.0sec,200msec,1)	00:02:08

Figure 2.7: Screenshot of the pH Screening standard run protocol for protein assay adapted after [MyCartis, 2014a]. Activation buffer = MEST buffer pH 3.5; antigen solutions = NFIX and NEUROD2 in assay buffer; wash buffer = PBST; sample solutions = purified IgG from P125 and P272 samples of human serum; anti human Ab = goat anti-human IgG labeled with SAPE.

using 200 μ L water, the microparticle suspension was immediately let to sediment by gravitation into a Protein LoBind tube containing 100 μ L MEST buffer (pH 3.5). After removing the supernatant using a plastic pasteur pipette, the microparticles were washed 3x with 600 μ L of the same buffer and suspended finally in 1 mL buffer. MEST buffer was removed from the tubes and freshly prepared 500 μ L of 10 mg/mL sulfo-NHS (Sigma-Aldrich, USA) together with 100 μ L 50 mg/mL EDC

2. Material and Methods

(Sigma-Aldrich, USA) solution were added to the reaction tube followed by short vortexing. Tubes were placed in a HulaMixer™ and mixed continuously for 60 minutes using the program shown in Table 2.1. Subsequently to the mixture, the microparticles were washed 3x times with MEST buffer (pH 5.4). 520 µL of the same wash buffer was used to re-suspend the washed microparticles.

The coupling was carried out using 10 µg of NEUROD2 (2 mg/mL) and NFIX (0.48 mg/mL) as antigens pro microparticle code and *E. Coli* lysate (0.2 mg/mL), HSA (10 mg/mL) and Protein G (1 mg/mL) as controls. In order to have the possibility to compare Evaluation™ with another standard multiplex immunoassay platform, as already mentioned, NEUROD2 and NFIX antigens as well as the human serum samples P125 and P272 were selected for this experiments based on data from an another AIT project. Within this previous project the Luminex® platform was used to quantify the amount of serum IgG antibodies against several antigens including NEUROD2 and NFIX.

80 µL of the antigen solution (10 µg protein/20.000 microparticle) were added into the tube containing the corresponding microparticles code. After 60 minutes homogenization in HulaMixer™ (Table 2.1), the microparticles were washed 3 times with 600 µL PBST buffer and finally stored in 500 µL of the same buffer at -20 °C. 50 µL aliquots were saved for coupling control.

2.5.2 Non-functional test

The aim of this experiment was to asses the efficiency of the antibody coupling on Evaluation™ microparticles. This was performed by co-flowing biotin labeled anti-His tag antibody and SAPE simultaneously and detecting fluorescence in real time (Figure 2.8). NEUROD2 and NFIX are proteins carrying a 6xHis tag modification, a polyhistidine motif that consists of at least six histidine residues. By binding to a protein's His tag, Penta · His Biotin Conjugate (Qiagen, Germany) forms a complex, which can be detected with a fluorescently labeled streptavidin. For this, a mixture of 2 µg/mL Penta · His Biotin Conjugate (Qiagen, Germany) and 1 µg/mL SAPE (Moss, USA) in LowCross buffer (Candor, Germany) was done.

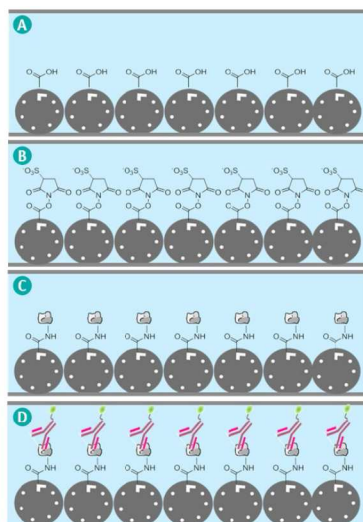


Figure 2.8: Uncoupled microparticles are loaded into a channel of a cartridge (A). By an active flow of EDC/NHS solution the microparticles are activated (B). The formed reactive NHS ester can bound covalently over its amine to the protein (C). Addition of a fluorescently labeled antigen allows visualization of the coupled process (D). [MyCartis, 2015]

One channel of a cartridge was loaded with 1 mm of a mix made of each coupled microparticles populations according to the loading protocol presented in the amino acids Subsection 2.2.2. The cartridge was loaded into the platform and using the running script presented in Figure 2.9, a blank scanning of the microparticles was performed. After removing the inlet content with a plastic Pasteur pipette, 50 μ L of detection solution was flushed continuous through the channels, while the fluorescence was measured in real-time.

2.5.3 Human serum IgG detection

The aim of the following experiments, performed after successful coupling confirmation, is to assess the performance of NEUROD2 and NFIX coupled microparticles in a 2-plex functional assay using LowCross and PBST-1%BSA as assay buffers. The role of both buffers is to minimize nonspecific binding, cross-reactivities and matrix effects of the assay. 1x PBST (pH 7.4) - 1% BSA buffer

2. Material and Methods

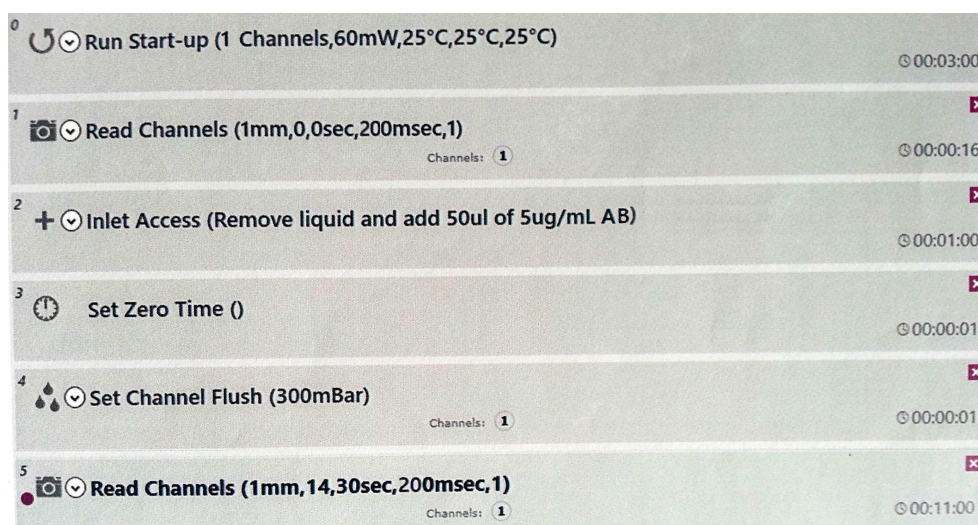


Figure 2.9: Screen shot of the running script for a Non-functional test. The detection antibody (AB) was flushed continuous through the channels, while the microparticle fluorescence was measured in real-time

(10x PBS (Life Technologies, USA); 0.3% (v/v) Tween[®]-20 (Sigma-Aldrich, USA); pH 7.4) was already successfully used as sample and antibodies diluent for immunoassay analyzed in several AIT projects on the Luminex[®] platform, while LowCross buffer (Candor, Germany) was recommended by MyCartis.

The coupled microparticle aliquots were thawed at room temperature and finally split in two solution. The supernatant was carefully removed and replaced with 500 μ L LowCross buffer and respectively PBST-BSA buffer. By preparing the microparticles mixture for multiplex detection was taking in consideration that every channel has to be loaded with at least 250 coupled microparticle (=1 mm). Further, for each population between 20 and 80 microparticles has to be present in order to guarantee a proper detection. 100 μ L of the homogenized suspension of each population was transferred in one fresh LoBind tube containing 100 μ L LowCross or PBST-BSA buffer. According to the loading protocol presented in Subsection 2.2.2, every channel of the cartridge was loaded with 1 mm microparticles.

All experiments were conducted using frozen samples (P125 and P272) of human serum IgG, respectively purified serum IgG, provided from a previous work at AIT, where the purification of IgG was conducted using Melon[™] Gel. Assuming an aver-

age IgG concentration of 8 g/L in serum, serum IgG was diluted 1:200 in LowCross buffer, while purified samples were diluted to a concentration of 0.04 mg/mL in LowCross buffer. The detection protein solution was prepared by dilution of the Goat Anti-Human IgG labeled with phycoerythrin (0.5 mg/mL) to 2 μ g/mL. All proteins used for this experiments were centrifuged 2 minutes at maximum speed. PBST was used in these experiments as wash buffer.

In the first experiment, the detection of unpurified human serum IgG was compared with purified IgG. 4 channels were loaded with the microparticle mix prepared in LowCross buffer following the standard loading protocol. 100 μ L of the samples were pumped with 200 mbar trough the channels for 30 minutes. After 1 minute wash with 50 μ L, 100 μ L of detection antibody was incubated by a 30 minutes continuously flush. Finally, after 1 minute wash the microparticles were scanned with an exposure time of 500 ms.

As a next step, cross reactivity between the assay buffer and detection antibody was analyzed. For this, 6 channels were loaded with the microparticle mixture. All inlets were loaded with 100 μ L solutions, two of them with purified IgG, followed by other two with unpurified serum IgG and two with negative control (only LowCross buffer). The incubation was performed in 30 minutes using a 300 mbar flow. After 1 minute wash, the detection antibody was added and incubated for 30 minutes. After the final 1 minute wash the microparticles were scanned for 500 ms.

Aggregation of the samples was observed on the captured images of the last experiment. In order to remove aggregation, two different detection antibody concentrations were analyzed using LowCross as well as PBST-1% BSA assay buffer. Further, the protein samples underwent an additional centrifugation step for 5 minutes. 10 channels were loaded with microparticles. 8 channels were flushed with 100 μ L purified IgG samples. The last two channels served as negative control, therefore assay buffer was flushed through the channels. After 30 minutes incubation time, followed by 1 minute wash with PBST, the goat anti human IgG detection antibody in two different concentrations (2 μ g/mL and 5 μ g/mL) was flushed for 30 minutes into the channels. The microparticles read out was conducted using an exposure time of 500 ms.

2. Material and Methods

In final experiment, the sample concentration of the purified IgG was reduced to 0.02 mg/mL. Further, a comparison of 15 minutes vs. 30 minutes incubation time of the samples was conducted within a single run. 5 channels were loaded with microparticles. 100 μ L purified IgG samples were flushed in 4 channels for 15 minutes. In the remaining channel a negative control was conducted with PBST-1% BSA assay buffer. After 15 minutes, 2 of the 4 channels together with the control channel were incubated for another 15 minutes. Further, a 2 mg/mL solution of detection antibody was incubated for 30 minutes and finally washed previous to the detection of the captured IgGs. The microparticles were scanned with two different exposure times 500 ms and 1000 ms.

3 Results

Nucleic acid assay

3.1 Design and performance of the qPCR assay

To achieve optimal primer performance in accordance to MIQE guidelines stated by Bustin et al [Bustin et al., 2009] and mentioned in Section 2.1, a total of 48 PCR primers were redesigned. The characteristics of the designed primers and their corresponding probes are summarized in the table shown in Appendix A-1.

Successfully designed assays were evaluated by qPCR experiments using standard DNA isolated from blood. The first experiment was conducted in singleplex reactions without primary target enrichment and followed by a second experiment with a 17 cycles multiplex PCR preamplification step before single qPCR. The assays were classified as failed, when the PCR efficiency was situated outside the range of 80%-100%, when the correlation coefficient of the calibration curves (R^2) was smaller then 0.95 or the fluorescent signal of the first standard (10 ng) was not detected before a C_p value of 30. Further, regarding the specificity of the assays for their target, none of the assays resulted in two melting points.

Detailed data about PCR efficiency, theoretical 1 ng detection, slope and correlation coefficient of calibration curves for 4-point serial dilutions, resulted from both experiments is available in Appendix A-2 (without preamplification) and Appendix A-3 (17 cycles preamplified DNA). From a total number of 48 assays tested without preAmp step, 5 targets didn't provide C_p values, while 6 provide C_p values over 30 and 3 showed low reaction efficiency. The linearity of the calibration curves was for all assays within the required parameter of 0.99 ± 0.02 . In the next approach, which included a 17 cycle preamplification step, no C_p values were provided for 6 targets (3 were the same as in the experiment without preAmp), 3 assays showed bad efficiency and 2 high C_p values over 30. The average correlation coefficient

obtained from the standard curves was still over the required value of 0.95, but it decreased to 0.97 ± 0.02 for the experiment with the preamplified DNAs.

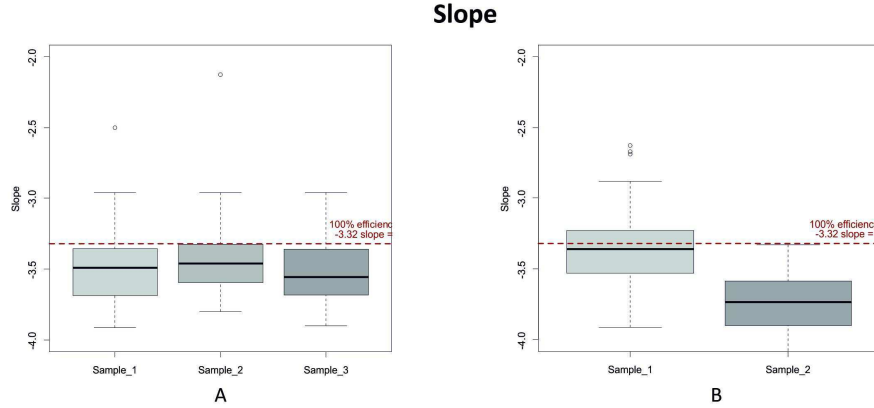


Figure 3.1: Slopes of the log-linear phase of the qPCR experiment without primary target amplification (A), and with the 17 cycles preamplification step (B) respectively. The boxplots show the median values as line across the box. Lower and upper boxes indicate the first and the third quartile. Whiskers represent the maximum and minimum values. The red line marks the ideal efficiency of 100% corresponding to a slope of -3.32.

The median slope of the assays, for which we performed preAmp was -3.47 with a standard deviation of ± 0.33 , respectively -3.49 ± 0.19 for the experiment without preAmp. The formula used to calculate the assay efficiency was already mentioned in Figure 2.2 in Subsection 2.1.2. A slope of -3.32 indicates a PCR efficiency of 100%. Slopes with values below -3.32 indicates reactions with efficiencies below 100%, while slopes with higher values -3.32 indicate sample quality or pipetting problems. Reactions with a slope between -3.93 and -3.3 [Bustin et al., 2009] corresponding respectively to an efficiency of 80% and 120 % are acceptable. Introducing the preamplification step yielded a decrease of the calibration slope towards the 100% efficiency line (Figure 3.1), which corresponds to optimal PCR condition, when the amount of DNA doubles with every cycle. Therefore, the same trend was observed also for the performance parameters calculated from the calibration curve and showed in Figures 3.2 and 3.3. The averaged efficiency was 93.91 ± 5.72 for the normal qPCR, while for preamplified qPCR a slighting decrease to 91.48 ± 7.56 was observed.

3. Results

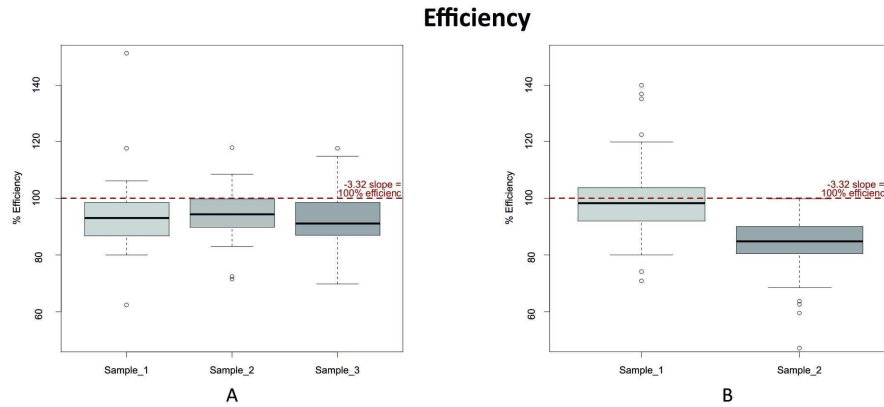


Figure 3.2: Amplification efficiency of the qPCR experiment without primary target amplification(A), and with the 17 cycles preamplification step (B) respectively. The boxplots show the median values as line across the box. Lower and upper boxes indicate the first and the third quartile. Whiskers represent the maximum and minimum values. The red line marks the ideal efficiency of 100% corresponding to a slope of -3.32.

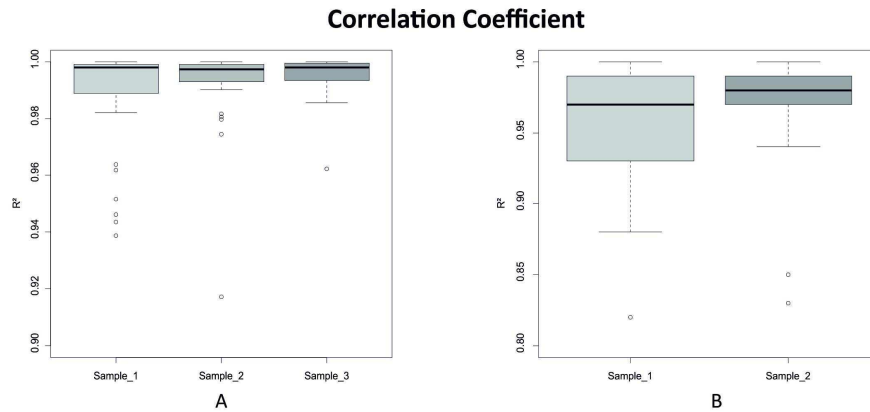


Figure 3.3: Boxplots of the correlation coefficients (R^2) obtained from the linear regressions of the standard curves generated from the qPCR experiment without primary target amplification(A), respectively with the 17 cycles preamplification step (B). The median values are shown as line across the box. Lower and upper boxes indicate the first and the third quartile. Whiskers represent the maximum and minimum values. Note: R^2 axis of the two approaches has different scales.

The images of the agarose gels, presented in Appendix 4 (without preamplification) and Appendix 5 (with 17 cycles preAmpl), allowed a visual control of the qPCR

products and as expected, they reflected the results of the qPCR performed on LightCycler®. 5, respectively 6 failed assays from both experiments, which didn't provided Cp values during the qPCR quality test, show no bands on gel, while all other assays were detected in the expected size ranges, confirming amplification of the desired targets. As expected, the control genes MGMT (109 bp) and LUP1 (127 bp), used in the qPCR experiment without preamplification step, showed that the assays provide the requested parameters efficiencies: 80%- 120%.

As Figure 3.4 shows, there is a significant difference between both experiments regarding the 1 ng detection, resulting in a Cp value of 26.46 ± 3.54 for the normal qPCR, respectively, 19.2 ± 4.73 for the preamplified approach. This shift resulted in a improvement of nearly 7 Cp-values, meaning that the same amount of input DNA can be detected 7 cycles earlier by introducing a 17 cycles preAmp step. Due to the exponential nature of qPCR, 7 Cp-values ($2^7=128$) allows the detection of much lower DNA concentration in the input sample.

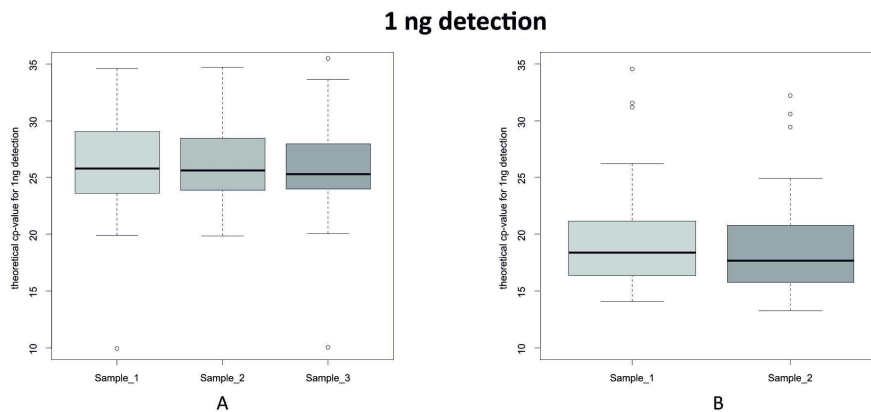


Figure 3.4: Boxplots show the median value of the theoretical 1 ng detection as line across the box for the qPCR experiment without primary target amplification(A) and with the 17 cycles preamplification step (B). Lower and upper boxes indicate the first and the third quartile. Whiskers represent the maximum and minimum values.

The reproducibility of both experiments was determined by running two qPCR with a 17 cycles preamplification step and three qPCR without, on different days, using the same technical design and different blood DNA dilution series. The

3. Results

calculated efficiencies and the standard deviations, which give the interassay variation, are illustrated in Appendix A-6. Ten randomly selected qPCR assays are also exemplary shown in Table 3.1. Evaluating the efficiencies of both experiments, it revealed that 26 assays showed lower standard deviation values in the standard qPCR as in the experiment with the additional amplification step. The reproducibility of the qPCR without preamplification, with a median interassay variation of 5.59%, is similar to that of the qPCR with the prior target enrichment, which was found to be 5.54%.

Table 3.1: Reproducibility and repeatability of 10 randomly selected qPCR assays tested on serial dilutions of blood DNA with 17 cycles and without preamplification including the calculated standard deviation (SD).

	no preAmp efficiencies [%]				preAmp efficiencies [%]		
Primer	Run1	Run2	Run3	SD \pm	Run1	Run2	SD \pm
BOLL	92.43	90.28	84.42	4.15	89.16	79.49	6.84
CHFR	104.04	89.89	80.39	11.90	102.85	93.51	6.61
FMR1	106.26	103.30	102.86	1.85	93.58	86.99	4.65
JUB	98.31	96.72	95.06	1.62	91.90	84.63	5.14
MSH4	95.88	96.53	91.03	3.01	100.22	87.47	9.01
S100A2	98.98	99.66	98.44	0.61	102.49	89.60	9.11
SNRPN	97.71	100.99	91.08	5.05	110.13	89.77	14.40
TFPI2	93.33	83.94	97.37	6.89	109.47	99.32	7.18
TP53	97.51	93.33	100.36	3.53	89.94	89.77	0.12
XIST	92.79	100.08	90.45	5.02	94.68	82.00	8.97

The results described above show that for the most of the primers the performance on serial dilutions was reproducible between different experiments. Further, an expected parallel translation of the Cp values between non and preamplified serial dilution was observed.

3.2 Experimental setup for DNA hybridization

3.2.1 Flow rate assessment

The flow rates were calculated as described in subsection 2.2.5 for all buffers used in the course of experiments (PBST, DIG Easy, TMAC, DMSO, 3xSSC, Formamid

buffer), in order to avoid running out of the analytes, which would lead to air presence in the channels and changes in the reaction conditions. An exemplary calculation of the flow rate using PBST as buffer is shown in Table 3.2. The pressure in the channels was set taking into consideration the 100 μ l total sample volume added in the inlet wells and the 30 minutes flushing time. The suitability of several buffers for microfluidic environment and their flow rate were evaluated at different temperatures (data not shown). DIG Easy, due to its viscosity, was the only not suitable buffer for the EvaluationTM platform.

Table 3.2: Exemplary flow rate assessment for PBST buffer by 25 °C and 52 °C. In order to avoid running out of the inlet wells, a pressure of 350 mbar was set for the experiments conducted at 25 °C, while for 52 °C a pressure of 250 mbar.

Pressure	Flow rate [μ l in 30 min]	
	25 °C	52 °C
500 mbar	119,16	169,20
350 mbar	83,41	118,5
250 mbar	59,58	84,6

3.2.2 Streptavidin functional test

The functional test was done in order to characterize the quality of the streptavidin coupling on the microparticles using the protocol described in subsection 2.2.3. The coupling of streptavidin was considered successful when the saturated fluorescence (i.e. >250 a.u.) was confirmed as well by the software images, as also by the microparticles data. Figure 3.5 presents an image of the scanned microparticles, while the Table 3.3 contains the fluorescence values provided by the software after an exemplary streptavidin functional test.

After each coupling of microparticles, a functional test was conducted. Throughout the experiments, there were four microparticle population, which showed always a significant lower fluorescence value (around 150 a.u.) compared with other populations. This microparticles codes of this populations were reported to MyCartis and not further used for the experiments.

3. Results



Figure 3.5: Exemplary image of streptavidin coupled microparticles with over-saturated fluorescence as required for a successful functional test.

Table 3.3: Microparticles data of an exemplary streptavidin functional test. Fluorescence is oversaturated in all channels (>250 a.u.).

Channel	Capture molecule	Exposure time [ms]	Particle count	Mean [a.u]
A2	[Undefined-520]	400	461	255
B2	[Undefined-990]	400	219	255
C2	[Undefined-462]	400	261	254
D2	[Undefined-816]	400	327	255

3.2.3 Streptavidin R-Phycoerythrin detection

The results, presented in Figure 3.6 and 3.7, indicates that the optimal way to avoid SAPE aggregates and increase the sensitivity of the detection is to use, in addition to the briefly protein centrifugation, an optimized concentration of SAPE. An incubation time of 10 minutes for SAPE was used as recommended by MyCartis. The preparation of SAPE, which gave the best results for all three tested buffer (3x SSC, TMAC, 30% formamide) was the 3 $\mu\text{g}/\text{ml}$ solution, obtained in a 1:1 dilution of hybridization buffer with water. Unlike the other two buffers, 30% formamide hybridization buffer didn't show any interaction with the detection solution and therefore no SAPE aggregates, but it delivered lower fluorescence levels.

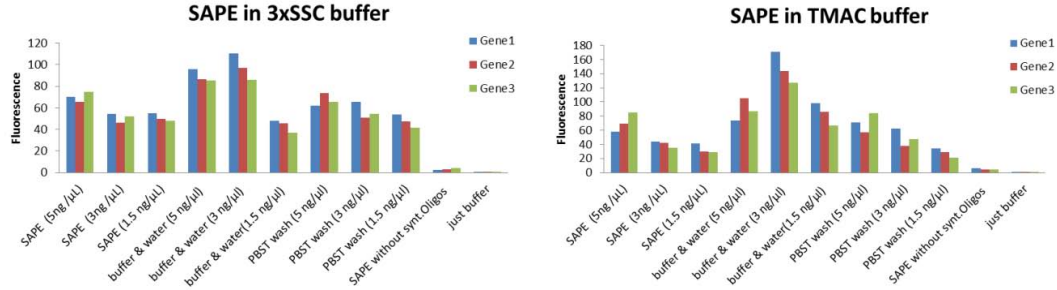


Figure 3.6: An exemplary result comparison of the concentration optimization of Streptavidin R-Phycoerythrin conjugate in 3x SSC (right) and TMAC (left) hybridization buffers. From the chart, it can be seen, that the optimal SAPE detection was achieved with a 3 $\mu\text{g}/\text{ml}$ SAPE solution, prepared in hybridization buffer, which was first diluted 1:1 with water.

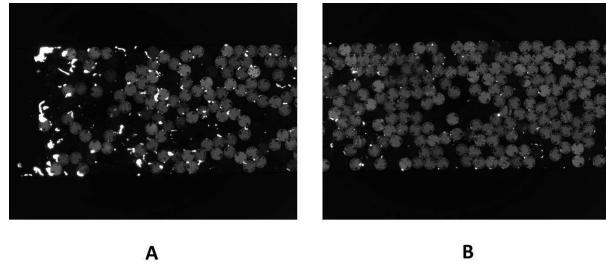


Figure 3.7: Exemplary images of the microparticles before and after optimization of SAPE in 3x SSC hybridization buffer. In the left image (A), captured before SAPE optimization, several aggregates are present. The applied SAPE solution was diluted in two steps in 3x SSC hybridization buffer to a concentration of 3 $\mu\text{g}/\text{ml}$. In the right image (B), the aggregates problem was solved by using for detection a 3 $\mu\text{g}/\text{ml}$ SAPE solution, which was made in two dilution steps, using 3x SSC buffer mixed 1:1 with water.

3. Results

3.2.4 Optimal exposure time

The 4 dilutions of the synthetic oligonucleotides targets, made in 3x SSC and 30% formamide hybridization buffer, were scanned by setting the exposure time at 200 ms, 300 ms, 400 ms and 500 ms. The Evaluation™ software calculated and displayed the amount of fluorescence emission from the captured images. The fluorescence output is linear to concentration of the target solution. After subtracting the blank values, measured in the negative control channel, the linearity of the fluorescence intensity was determined by calculating the R^2 value. R^2 is a measure of correlation degree between fluorescence and concentration. A correlation coefficient of one means perfect correlation. The comparison of the relative intensities of the fluorescence measured at different exposure times is shown in Figure 3.8. The correlation coefficients obtained were high, with ranges between 0.95 and 0.96 for 3xSSC buffer and 0.96 up to 0.99 for formamide buffer. These high correlation values indicates a minimal dependence of the used exposure time on the fluorescence intensity of the microparticles. The best trade-off between signal intensity and linearity was calculated and used for an optimal detection in all further experiments. This was for 3x SSC buffer at an exposure time of 300 ms, while for hybridization in 30% formamide buffer at 500 ms.

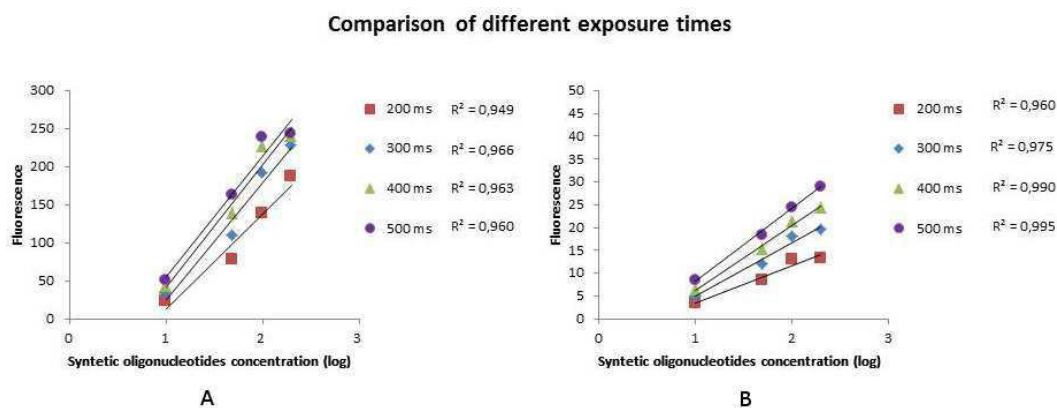


Figure 3.8: Comparison of different exposure times. The optimal exposure time was determined by plotting the log concentration of the synthetic targets on the x axis versus fluorescence values on the y axis and calculating the R^2 values. For hybridization in 3x SSC buffer (A) the optimal exposure time is 300 ms, while for hybridization in 30% formamide buffer (B) at 500 ms.

In the case of hybridization in 3x SSC buffer, the fluorescence values of the negative control, i.e the background signal, were very low in comparison with the high fluorescence signals of the targets. Compared to 3x SSC buffer, the use of formamide buffer for hybridization led to approximately eight times lower intensity of the fluorescence, where the values of the 10 nM target solution couldn't be distinguished from the negative control. In conclusion, for further experiments conducted in 3x SSC buffer, removal of the blank signal is not necessary, while for formamide buffer the blank values have to be taken always into consideration.

3.3 Nucleic acid assay feasibility study

3.3.1 Detection optimization using 4 synthetic targets

In order to test and to evaluate the optimal detection conditions of PBMC-DNA using the EvaluationTM System from MyCartis, 4 biotinylated synthetic oligonucleotides solutions of known concentration were initially analyzed in 3x SSC hybridization buffer, followed by a test carried out in 30% formamide buffer. The dilutions, which were hybridized by 52 °C in 3x SSC buffer, were successfully detected by an exposure time of 300 ms. The amount of fluorescence emission, calculated by the EvaluationTM software, correlates directly with increasing concentration of the synthetic oligonucleotides as shown in Figure 3.9. Even though the background signal was relatively high, with values from 5 up to 49, all targets could be clearly identified.

After hybridization in formamide buffer, the targets with a concentration of 10 nM and 50 nM were not distinguishable from the control microparticles (fluorescence <4 a.u.), but for the 100 nM and 200 nM solutions the signal was clearly significant (data not shown). By hybridization in formamide buffer, a high target specificity was noticed, but the fluorescence was very low, with less than 30 units, even after increasing the exposure time to 500 ms. Formamide hybridization buffer yielded lower signal intensities (about between 5 and 30 a.u.), but increased the linear detection range (R^2 value of 0.99 for formamide compared to 0.96 for 3x SSC

3. Results

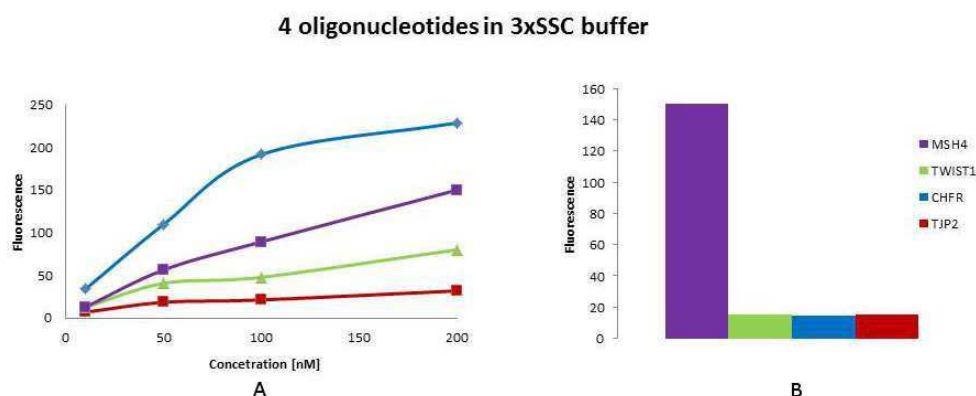


Figure 3.9: Fluorescence values vs. concentration curve of the 4 target solutions in 3xSSC hybridization buffer (A). Exemplary selected assay (MSH4) showing the specific target signal vs. background signal (B)

bufer). However, the signal intensities measured after hybridization in 3x SSC buffer were still considerably stronger (about between 5 and 250 a.u.).

3.3.2 Hybridization optimization in formamide buffer

Despite the very low signal of fluorescence intensity, the use of formamide buffer for targets hybridization showed an increased linear detection range compared to 3x SSC buffer. Several formamide buffer concentrations (25%, 30%, 35% and 40%) were examined throughout hybridization at temperatures of 55 °C, 60 °C and 65 °C, in order to improve the hybridization reaction as well as the detection process using this buffer. Information on the linearity correlation between the concentration of the four oligonucleotides solution and measured fluorescence are available in Table 3.4. Hybridization in the presence of 35% formamide at 55 °C showed an almost perfect linearity (correlation coefficient: mean $R^2=0.9995\pm0.0005$). Therefore, all further experiments involving targets hybridization in formamide buffer, were conducted using a 35% formamide concentration and a hybridization temperature of 55 °C.

Table 3.4: Determination of optimal formamide buffer concentration and the corresponding hybridization temperature using four synthetic oligonucleotides of known concentration as targets. The table shows the linear correlation coefficients (R^2) between target concentration and measured fluorescence value.

Hybridization temperature	Formamide concentration	Linearity coefficient R^2			
		CHFR	MSH4	TJP2	TWIST1
55 °C	25 %	1.000	0.998	0.999	0.998
	30 %	0.858	0.960	0.950	0.936
	35 %	1.000	0.999	1.000	0.999
	40 %	0.999	0.992	0.977	0.990
60 °C	25 %	0.997	0.999	0.996	0.987
	30 %	0.984	0.976	0.970	0.984
	35 %	0.985	0.989	0.999	0.998
	40 %	0.985	0.998	0.995	0.981
65 °C	25 %	0.948	0.970	0.961	0.973
	30 %	0.790	0.850	0.774	0.894
	35 %	0.950	0.930	0.926	0.986
	40 %	1.000	0.990	0.954	0.999

3.3.3 Alternative hybridization buffers

A variety of different buffer reagents is available for hybridization. Because no hybridization reagent is appropriate for all systems, empirical testing is essential. When changing buffer contents and/or hybridization temperature or the target, a diminished signal or increased background can result, simply because the hybridization buffer was not optimal for the system. TMAC, DIG Easy Hyb, ExpressHyb buffer and a standard qPCR buffer were evaluated at 42 °C, 52 °C and 62 °C to determine their efficacy as hybridization buffers.

Due to its high viscosity and difficulty of pipetting, ExpressHyb buffer with 40% formamide showed that it is not suitable for the EvaluationTM system, even low fluorescence signals were measured at 42 °C. The use of 1x PCR buffer with 5% DMSO and TMAC buffer for 30 minutes hybridization resulted in strong signal intensities for the synthetic oligonucleotides targets, whereas no signals were obtained using DIG Easy Hyb buffer at the same settings. Further, hybridization at 62 °C resulted in poor signal quality with low fluorescence values for all tested

3. Results

buffers, that couldn't be quantified.

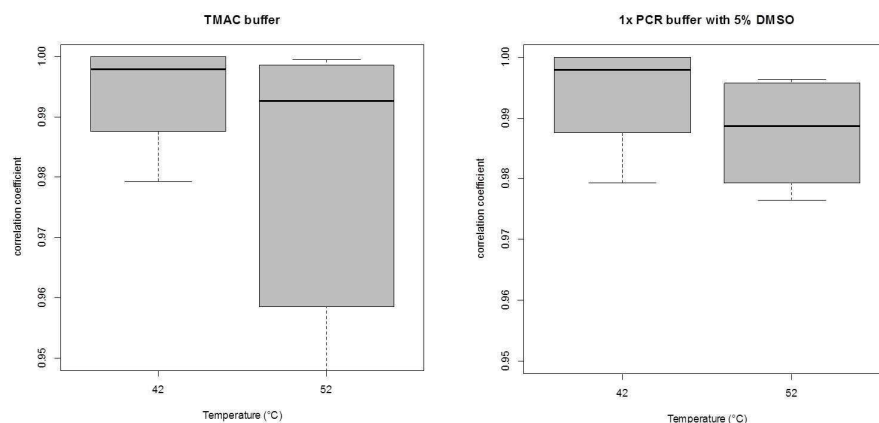


Figure 3.10: 1x PCR with 5% DMSO and TMAC hybridization buffer comparability. The boxplots illustrate the correlation coefficients of the 4 synthetic targets and the linearity of their concentration range in both buffers at 42 °C and 52 °C, indicating that hybridization worked better in both buffers at 42 °C.

The fluorescence data of 1x PCR and TMAC buffers was plotted. R^2 was calculated for the three concentrations of the 4 targets and two hybridization temperatures. The box plots (Figure 3.10) illustrate that R^2 values of both buffers vary only very little at the lower temperature, indicating that 42 °C is the best temperature for target hybridization with 1x PCR and TMAC buffer.

The fluorescence signals measured after hybridization with TMAC buffer were remarkably higher than the signals measured with 1x PCR buffer. Further, blanks signals obtained from microparticles processed with TMAC buffer were unusually high with an average value of 31.5. This could be caused by SAPE aggregation or cross-reactivity of the targets. The presence of SAPE aggregates was checked by visualizing the captured fluorescence images of the microparticles during the detection. Figure 3.11 illustrates the assessed cross-hybridization.

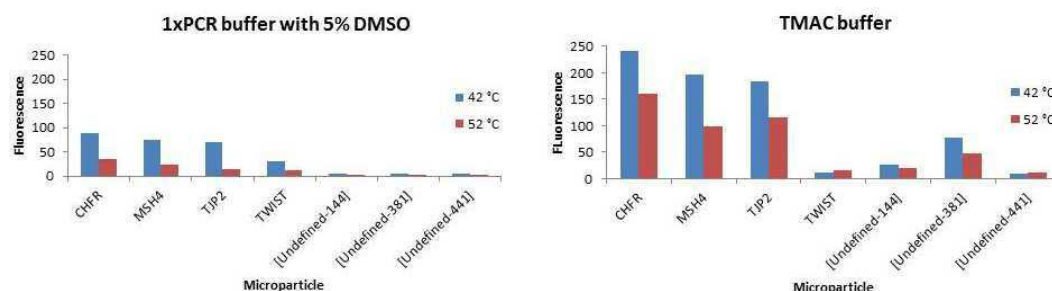


Figure 3.11: Cross-hybridization in 1x PCR with 5% DMSO and TMAC buffer. On the X-axis are reported the microparticles producing a fluorescent signal after hybridization at 42 °C and 52 °C. The fluorescence intensity signals are reported on the histogram bars.

3.3.4 Assay specificity and sensitivity

In order to determinate the limit of detection and a possible cross-hybridization, 4 synthetic oligonucleotides targets with known concentration were applied to a microparticle pool coupled with 19 different probes. A blank was measured by flushing hybridization buffer instead of the samples. Overlapping of the signal intensity of the blank and low concentration of the samples is a statistical reality and makes blank a reasonable starting point for LOD estimation. The average value of the blank signals measured in TMAC (13.47 ± 14.92) is four time higher than the average blank 4.01 ± 2.70 measured in 3x SSC buffer, indicating a high cross reactivity between TMAC buffer and probes or/and streptavidin coupled on the microparticles. Independent of the used hybridization buffer, higher oligonucleotides concentrations increased the background signal, yielding a lower overall signal to background ratio, while low concentration resulted in lower overall signal intensity.

As expected, the obtained median fluorescence intensity increased with the concentration of the synthetic nucleotides. The difference in signal intensities between background signal and samples was very low for synthetic nucleotide solutions with a lower concentration than 0.25 nM, irrespective of the used hybridization buffer. Therefore, targets with a concentration below this level can not be detected due to the high level of background signal. The high cross-hybridization presented in this

3. Results

multiplex approach is illustrated in Figure 3.12. TMAC buffer showed a higher cross-hybridization than 3x SSC buffer.

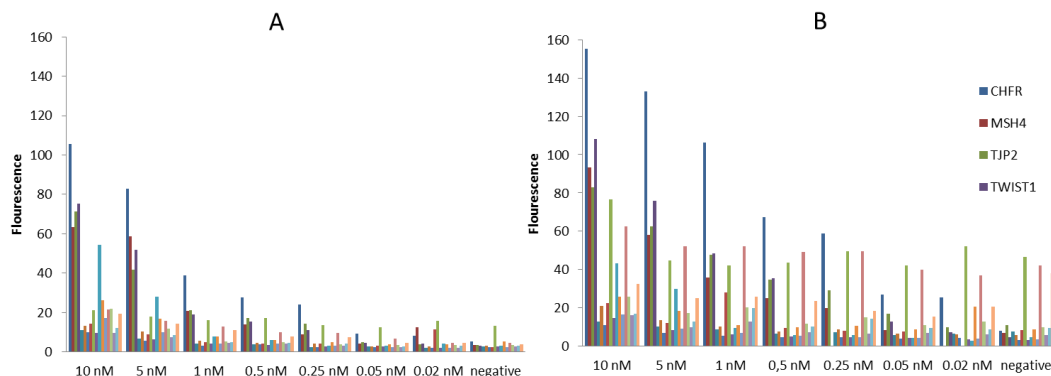


Figure 3.12: Hybridization sensibility of the multiplex assay was evaluated by comparing the signal intensities of synthetic nucleotides in 3xSSC buffer(A) and TMAC buffer (B), after subtracting the blank values. A relatively high level of cross hybridization were noted in both buffers.

3.3.5 Hybridization of qPCR products on different probes

Due to the small amount of DNA after extraction from plasma, an amplification of the target sequences previous to the multiplex detection was necessary. The quality control of the PCR products was checked using agarose gel electrophoresis (Figure 3.13). It revealed a successful amplification for 17 out of 19 targets. The two reactions without visible products on the gel correspond with the failed qPCR reaction performed on Lightcycler[®] and were already described in Section 3.1. Quality of the reaction components or DNA, presence of primer interactions as well as competition for the reagents contribute considerably as a possible error in multiplex assays [Chan et al., 2011]. Since the other reactions worked optimal, low quality of the assay components or DNA can't be the failure source. These failed assays are likely to be related to an improper assay design and will be subjected to a redesign.

All 19 targets previously amplified in single reactions were pooled together and diluted in the corresponding hybridization buffer (1:40, 1:20, 1:10, 1:5). A com-

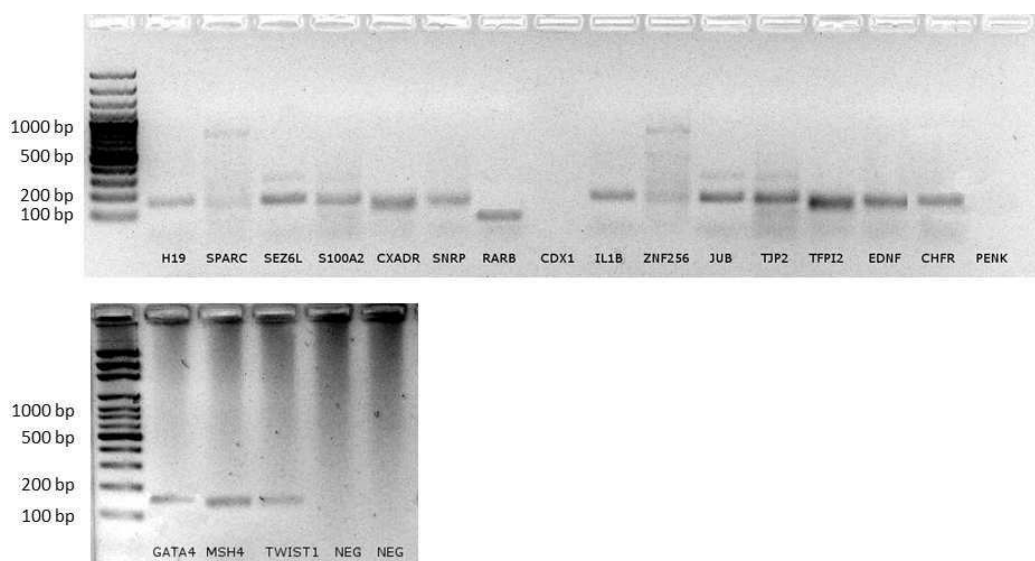


Figure 3.13: PCR products control on agarose gel. DNA bands show a successful amplification for 17 out of 19 target sequences. The gel shows also a DNA ladder containing DNA fragments of defined length for sizing the bands and two negative controls

parison and evaluation of three hybridization temperatures and four hybridization buffer was performed. Aim was to confine the choice of buffers, which could be used in the final Evaluation™ runs. Signal intensities for each target dilution and control assay were determined from the median intensities of a microparticle code and corrected by subtracting the blank intensities (data not shown), which were measured at the beginning of the run by scanning of the cartridge containing only microparticles in loading buffer. Even for the highest target concentration, hybridization in 35% Formamide and 1x PCR with 5% DMSO buffers registered very low signal intensities, mostly under the corresponding negative control level. Therefore, this two hybridization buffers were found to be inappropriate for detection of low amounts of DNA targets and will not be discussed further here.

As illustrated in Figure 3.14, the best linearity concentration over median intensity was given for both buffers after hybridization at 52 °C, even the measured signal intensities of the cDNA targets were low. It was shown that 62 °C is an inappropriate hybridization temperature as it led to assay failure in both buffers and also to bad linearity. The measured fluorescence intensities after using 3x SSC buffer

3. Results

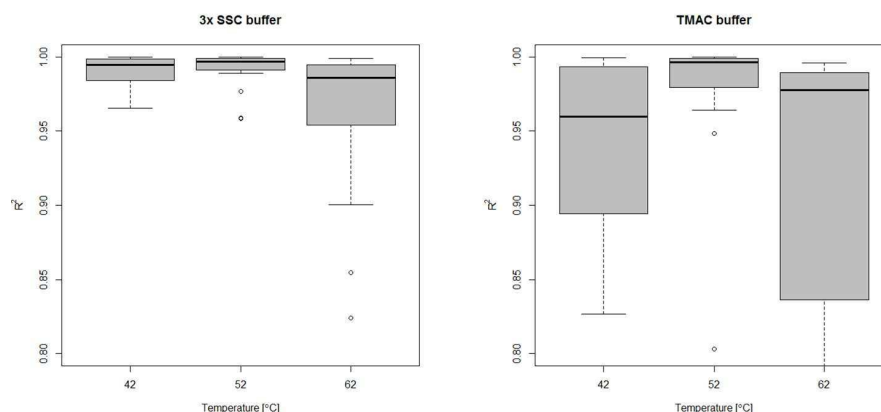


Figure 3.14: R^2 of all target concentrations showing the linearity of the analyzed concentration range in 3x SSC and TMAC hybridization buffer at three different temperatures. 52 °C was determined to be the optimal hybridization temperature for both buffers.

for hybridization were in a range between approximately 4 and 43 a.u. at 42 °C and 4 and 63 a.u. at 52 °C. R^2 of 0.98 ± 0.011 , respectively 0.99 ± 0.009 stated an almost perfect linear relationship between signal intensity and target concentration for hybridization with 3x SSC buffer at both temperatures, while linearity of TMAC buffer was achieved only at 52 °C ($R^2 = 0.98 \pm 0.025$). Hybridization at 42 °C in TMAC buffer resulted for the last three lowest concentrations by 10 of the assays in intensities almost on the or even below the blank level, indicating a low sensitivity of the TMAC assay at this temperature. A special attention was drawn to the signal-to-background (SBR) ratio. High values of SBR at lowest target concentration indicates best detection results. The signal-to-background ratios were calculated for all sample concentrations as the ratio between the specific intensity of a captured target and the signal of the negative control, performed using hybridization buffer instead of samples. At 52 °C, across the lowest concentration samples, the average on-target signal was approximately 3 times greater than the average off-target background signal for 3x SSC buffer, and only one time greater for TMAC buffer, while across the highest DNA standard concentrations 14 times for 3x SSC and 5 times higher for TMAC buffer, respectively.

The increase of fluorescence intensity and signal to blank ratio indicates that ap-

plied concentration of the targets were in range of where they could get detected, after a hybridization conducted at 52°C in 3x SSC and TMAC buffer. However, the 3x SSC hybridization buffer lead to higher signal-to-background ratios and better linearity than TMAC buffer.

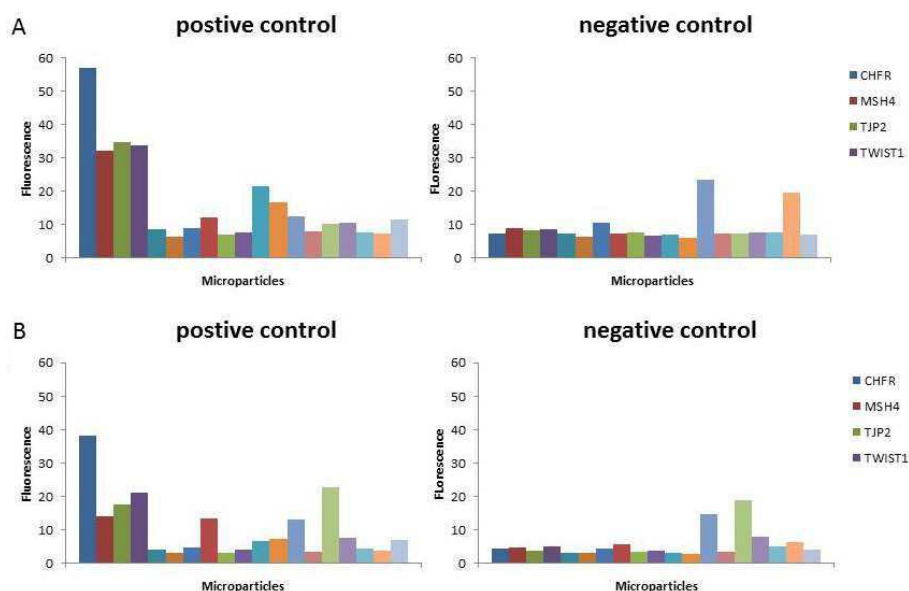


Figure 3.15: Signals of the positive and negative control in 3x SSC hybridization buffer (A) and TMAC hybridization buffer (B). Positive control was conducted using four synthetic oligonucleotides of known concentration. The negative control was obtained flushing the samples over the second microparticle pool containing non-complementary probes.

The evaluation of the positive and negative controls, used to verify the suitability of the detection system, is presented in Figure 3.15. A positive control containing of four synthetic oligonucleotides of known concentration was flushed over the microparticle pool containing, among others, also the probes complementary to the oligonucleotides, while the negative control was obtained flushing the samples over the second microparticle pool containing 19 non-complementary probes. Figure shows the measured signals of the negative control are similar to the values of the background signal present in the positive control. Although the background signal levels varied on different microparticles codes, high specific signals of the four synthetic targets could be clearly distinguished from the background after hybridization at 52°C using 3x SSC hybridization buffer.

3. Results

Taking this results together, it has been observed that hybridization temperature, hybridization buffer and target concentration played a crucial role in optimization of fluorescence signal intensity and signal-to-background ratio. Especially minimization of non-specific binding of detection probes is a key step to improve detection sensitivity. By increasing the efficiency with which target sequences are captured, higher signal intensities could be obtained and therefore also the sensitivity could be improved. This could be achieved by enhancing the affinity of the capture probes for their targets by refining the sequence design and their optimal hybridization temperature.

3.3.6 Limit of detection

Limit of detection or the analytical sensitivity of the method is given by the minimal amount of target DNA which can be detected with a clear distinction between sample and blank. LOD was determined by comparison of two different experiments with synthetic oligonucleotides samples of known concentration, respectively blood DNA. The lowest concentration at which synthetic targets can be accurately distinguished from the background signal was determined in Subsection 3.3.4 and was at 0.5 nM for 3x SSC and for TMAC hybridization buffer. The sequence lengths and the molecular weights of the four synthetic oligonucleotides were all in the same range. Therefore, the calculation of LOD was conducted based upon CHFR as a target, with a molecular weight of 19.49 kDa, respectively a mass of 3.24×10^{-8} 0.25 pg per one copy. According this, the target amount of the 0.25 nM sample solution (100 μ L) is 4.87 μ g, representing the 4.87 ng/ μ L observed LOD. Assuming that the start PCR reaction contains just one DNA copy, after 35 PCR cycles a number of 3.43×10^{10} copies and 1.11 ng of the target amount should be available for detection in 40 μ L reaction volume. Based on the calculation presented in Table 3.5, the expected LOD was determined to be at 0.5 pg/ μ L. Therefore, the expected vs. observed LOD diverges by the factor of 10000x. Increased exposure time can not overcome this discrepancy, but its reason may have something to do with the dynamic range limitation of the Evalution™ detection system. However, this difference explains the low fluorescence intensities measured from amplified

PBMC-DNA, but also the high background signals.

Table 3.5: Limit of detection of the nucleic acid assay. The expected LOD was calculated theoretical upon CHFR as a reference target, while observed LOD was determined by measuring fluorescence intensity of the synthetic CHFR target solutions of known concentration. A difference between observed and expected LOD by the factor of 10000x was observed.

Dilution	Nr. of targets [copies/ μ L]	Target amount [ng/ μ L]	Obs. vs. Exp. LOD
1:5	1.71E+08	5.54E-03	1:885
1:10	8.57E+07	2.77E-03	1:1739
1:20	4.28E+07	1.38E-03	1:3478
1:40	1.71E+07	0.55E-03	1:9740

Protein assay

3.4 pH screening for antigen coupling

The pH of the assay buffer can influence the coupling efficiency of the procedure as well as the intensity of the phycoerythrin fluorescence used for detection of the targeted proteins. In order to determinate an optimal pH for coupling, a pH screening was performed.

Both samples showed massive protein aggregation more or less independent of the pH, as also illustrated in Figure 3.16. This might be most likely due to precipitates from the antigen and antibody solutions. For the next experiments all protein solution were spun down by maximum speed before usage. Despite the aggregation problem, which makes a clear interpretation hard, the purified serum samples showed significant high signals, indicating that the coupling as well as the assay worked. The identification of optimal pH for antigen coupling was not possible due to the abundant presence of SAPE aggregates. For further experiments a pH of 5 was set for coupling procedure. This is the current pH used also by AIT for similar coupling experiments on Luminex™ COOH-microspheres.

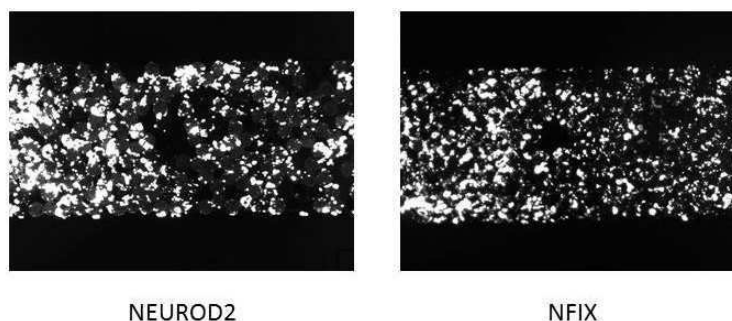


Figure 3.16: Image of the capture microparticles. Both samples show high protein aggregation.

The procedure of antigen coupling direct in the cartridge was presented in Section 2.4 and used for in-flow pH screening for optimal coupling conditions. Its advantage compared to the standard procedure performed in protein LoBind tubes is its

simple work flow with minimal hands-on-time that allows a significant acceleration of the immunoassay work flow. The entire experiment took around 1 hour and 15 minutes. The run of the same experiment using external coupling would be lasting for at least 3 hours, where only the coupling in tubes would be taking around 2 hours.

3.5 Antigens coupling confirmation

Before the coupled microparticles were further used for binding and detecting of serum IgG, it was necessary to confirm the efficiency of the coupling procedure. This was accomplished by performing a non-functional test, where both coupled 6x His tag antigens were detected with a co-flow of SAPE and monoclonal mouse anti-His antibodies. The successful coupling was confirmed through the intensity signals of the fluorescence, measured from all microparticles coupled with NEUROD2 and NFIX antigens. The signals were high and increased constantly with the exposure time. Further, the coefficient of variation between NEUROD2 and NFIX signals measured at the same exposure time was in a very low range (median % CV was by 6.44%). Low variation between those signals implied that the microparticles were coupled with antigens in an equal way. Figure 3.17 confirms the successful coupling of the antigen to the Evaluation™ microparticles.

3.6 Purified IgG vs. Serum IgG detection

The aim of this experiment was to test if incubation of the antigens with whole human serum samples influences the quality of the detection compared to the standard procedure, which uses purified IgG from serum. Human serum is obtained from blood of an immunized host after removing the clotting proteins and red blood cells. It contains not only IgG (most abundant protein in serum), but also many other types of antibodies, present due to immunological history or an autoimmune reaction [Virella, 2007]. Therefore whole human serum samples can

3. Results

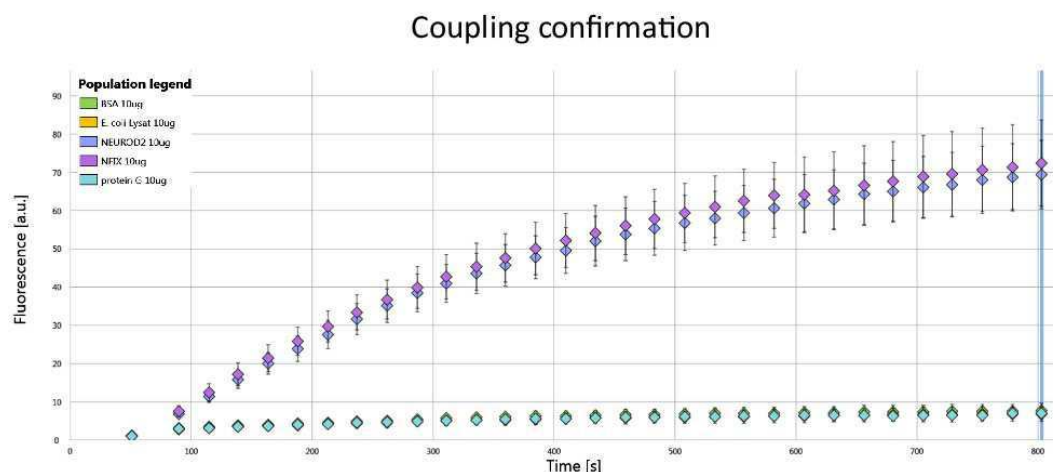


Figure 3.17: Successful coupling of antigens on the Evaluation™ microparticles is indicated by the high fluorescence signals in a similar intensity range of NEUROD2 and NFIX, which increase constantly with the extended exposure time. *E. coli* lysat, Protein G and HSA, which do not have a his tag modification, can not be detected and therefore show no signals.

sometimes react non-specifically in immunological assays, but otherwise skipping the purification step the working time could be reduced significantly. Figure 3.18 presents the detection results after incubation with whole human serum samples versus incubation with purified IgG samples.

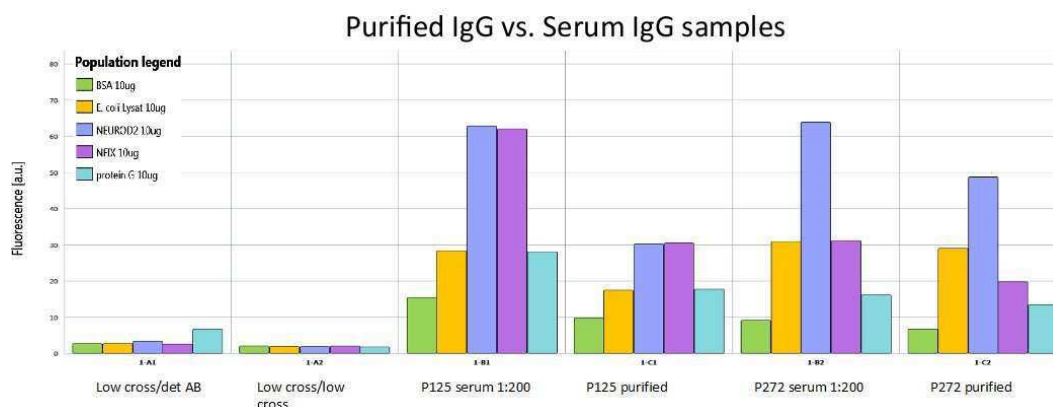


Figure 3.18: Purified IgG vs. Serum IgG samples. Diluted serum samples worked as good as purified samples and gave generally higher signals. A little cross-reactivity of detection antibody with protein G can be observed from the graphic LowCross/det AB

Fluorescence of the purified samples resulted in 1.2 to 1.6 times lower signal intensities for sample P125, and 1.1 to 1.8 for P275 (Table 3.6). At the same time, the signal ratio remained the same as shown in 3.18. Taken together, these lead to the conclusion that serum samples work as good as purified samples for IgG detection and suggest that using whole human serum could avoid an extra labor intense and costly purification step.

Table 3.6: Table shows the fluorescence values of IgG obtain obtained on the one hand from diluted serum samples and on the other from purified samples. Purified samples showed lower fluorescence values.

	P125			P275		
	diluted 1:200	purified	signal ratio	diluted 1:200	purified	signal ratio
BSA	16.04	10.38	1.6	11.61	9.09	1.3
<i>E. coli</i> lysat	33.07	20.41	1.6	41.49	38.91	1.1
NEUROD2	75.40	43.84	1.7	99.60	75.94	1.3
NFIX	76.30	42.30	1.8	50.76	31.64	1.6
Protein G	24.67	20.10	1.2	17.69	16.28	1.1

As in other previous immunoassays performed by AIT, Protein G was used as a positive control for the assay. This binds with high specificity the Fc region of IgG leading to high fluorescence intensity (>250 a.u.). Interestingly, Protein G shown a lower fluorescence signal as expected. The low fluorescence intensity of Protein G may be linked to a possible protein degradation since the used Protein G comes from a very old AIT internal stock. Further, a little cross-reactivity between Protein G and detection antibody was present, which can be also observed in Figure 3.18.

The choice of NEUROD2 and NFIX as antigens, based on data from a previous AIT project, allows a comparison of fluorescence intensity between two systems. In the previous work both antigens were incubated with IgG purified from human serum samples P125 and P272 and analyzed using the Luminex[®] FLEXMAP 3D[®] (Luminex Corporation) platform. P125 showed high fluorescence signals after binding of both antigens, whereas P272 gave high signals with NEUROD2 and low signals with NFIX antigen (data presented in Table 3.7). Further in the previous project, the analysis of the samples resulted in no signal for HSA and over-saturated signal for *E. coli* lysat and Protein G, which were used as assay

3. Results

controls. A similar trend of the measured fluorescence was observed also in the serum IgG detection using the EvaluationTM system.

Table 3.7: This table compares immunoassay detection on MyCartis EvaluationTM platform with Luminex[®] FM3D platform. Luminex[®] fluorescence data was provided from a previous AIT project, while for EvaluationTM the serum vs. purified IgG results were used. 250 a.u. is the maximum possible fluorescence signal on EvaluationTM, 300.000 a.u on FM3D[®]. Both systems show a similar trend.

		Luminex [®]	Evaluation TM
P125	NEUROD2	51.000	63
	NFIX	51.000	62
P272	NEUROD3	100.000	64
	NFIX	10.000	32

3.7 LowCross and PBST-1%BSA buffers

LowCross and PBS-1% BSA assay buffers were tested and compared mainly focusing on optimal signal intensities, signal ratio trend and sample aggregation. Further, the influence of increased detection antibody concentration and intensive samples spinning was checked. The results are presented in Figure 3.19.

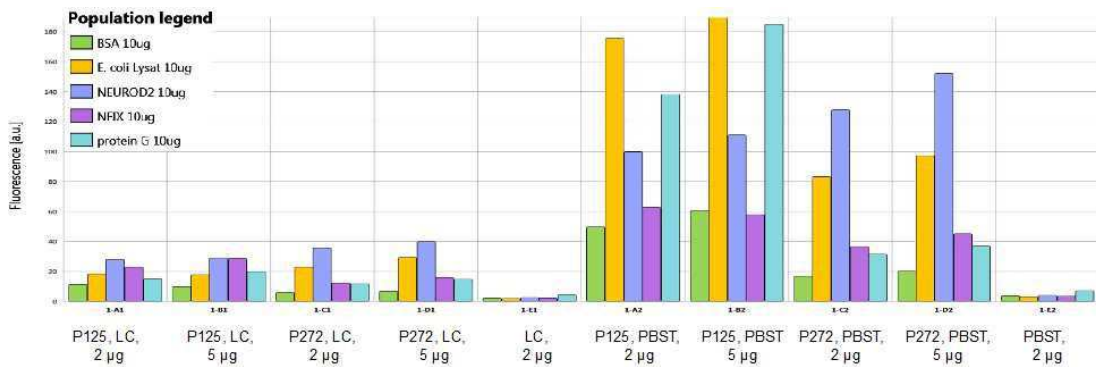


Figure 3.19: 2 µg vs 5 µg detection antibody in LowCross and PBST assay buffer. Samples as well as controls show high signal intensity differences between both buffers. Increasing detection antibody concentration led to minor differences.

Both purified serum IgG samples, NEURDOD2 and NFIX, were analyzed in two different assay buffers using two concentrations of detection antibody (2 $\mu\text{g}/\text{ml}$ and 5 $\mu\text{g}/\text{ml}$). The fluorescence signals of the standard Luminex[®] assay buffer (PBST (pH 7.4) - 1% BSA) were remarkably stronger (up to 7 times) than that of the LowCross buffer, but also formation of slightly more aggregates was observed after using PBST-1% BSA as samples diluent and incubation buffer (Figure 3.20).

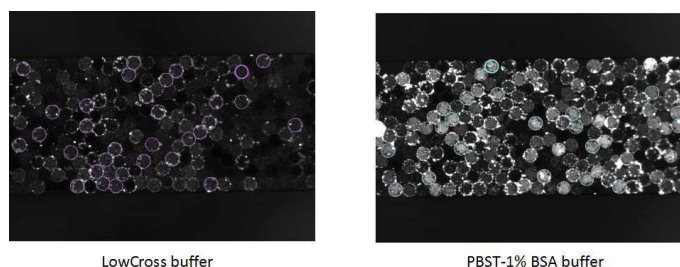


Figure 3.20: Samples aggregation in LowCross buffer vs. PBST-1% BSA buffer. LowCross buffer show less aggregates, but also less signal intensity up to maximum of 25 a.u.

This aggregation of the samples happens very likely also on Luminex[®], but compared to Evaluation[™] the system doesn't have the ability to visualize the microparticles. The possibility to access captured images of the microparticles during and after assays detection on Evaluation[™] provides helpful information about the quality of the assay. The signal differences of both different assay buffers were remarkably high for the control samples. While incubation in LowCross buffer of the samples with Protein G and *E.coli* lysat resulted in low signal intensities (values between 18 and 25 a.u.), in PBST-1%BSA buffer signal intensities of the same controls were much higher than the two antigens intensities. Incubation of the sample P125 with PBST lead to over-saturated signals for *E. coli* lysat and for P272 to fluorescence intensity between 80 and 100 a.u.. HSA control show with sample P272 low signal intensities and with P125 high signals in both buffers. Further, the signal ratio of two antigens changes depending of the used assay buffer. Increasing the detection antibody concentration led to minor differences in the signal intensities and seems to have no influence of the sample aggregation.

In order of decreased aggregation, samples as well as the detection antibody were

3. Results

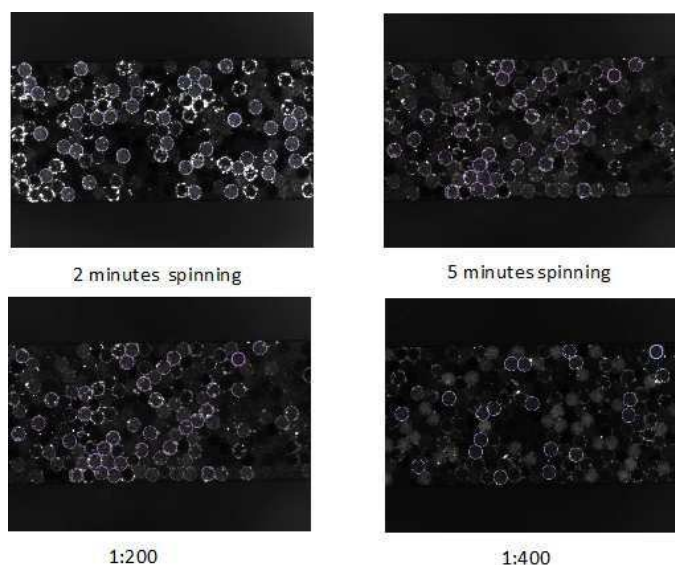


Figure 3.21: Optimization of aggregation in PBST-1% BSA buffer. Comparison of 2 minutes vs. 5 minutes spinning and 1:200 vs. 1:400 sample dilution. Both approaches were conducted using purified IgG samples and 2 $\mu\text{g}/\text{mL}$ detection antibody. Increased spinning duration, as well as using a higher sample dilution, reduced aggregation of the proteins.

centrifuged at maximum speed for 5 minutes and compared with the results obtained after 2 minutes spinning. Further, in an additional approach, samples containing purified IgG were diluted in PBST-1% BSA buffer prior to the experiment to 1:200 and 1:400, respectively, assuming an average IgG concentration of 8 g/L in serum. The results comparison of both experiments are summarized in Figure 3.21. The 5 minutes spinning decreased the aggregation, but did not completely resolved it. The 1:400 sample dilution contained less aggregates, but showed also lower signal intensities. These were compensated by scanning of the microparticles with a higher exposure time, e.g. 1000 ms.

4 Discussion

To review, the overall aim of the master thesis was to evaluate the suitability of the Evalution™ platform for DNA Methylation and protein based multiplexed biomarker detection and to set up a bead based nucleic acid assay for potential use in the early diagnostic of colon cancer. The setup should be minimally invasive, easy to use, highly sensitive and specific.

4.1 Nucleic acid assay

The focus of this part of the thesis was the development of a microparticle based multiplex assay suitable for detection of Methylation biomarkers in human blood on Evalution™ platform. The assay design relied on a biomarker panel targeting 48 genes, which were found to be aberrant methylated in colon cancer during a previous project conducted by AIT. Since the DNA methylation biomarker panel was derived from targeted microarrays based screening, the same probes as on the microarray were used and adapted to the specifications of the MyCartis system. The readout was based on a Streptavidin Phycoerythrin detection in combination with biotinylated PCR primers. Therefore, forward primers targeting the sequence of interest of the existing panel were completely redesigned in order to obtain shorter products for microfluidic environment, while the 5' biotinylated reverse primers remained for the most of the targets the same. Several parameter which can influence the amplification success (e.g. T_m, GC content, sequence length of the primer and product) were taken in consideration for the design set up. On one side, in order to avoid mispriming or formation of primer dimers, on the other side to increase PCR efficiency and sensibility, particular attention has been paid to primer length and their annealing temperature together with the length and GC content of the targeted sequence. For design and as well as for qPCR control of the assay the MIQE quality criteria were followed, which helped to set up reliable qPCR experiments and generate transparent results [Bustin et al., 2009].

The performance of the 48 successful designed assays was controlled in single as well as in multiplexed qPCR reactions, following the MIQE guidelines quality criteria [Bustin et al., 2009]. Therefore, linearity (R^2), specificity and sensitivity of the DNA assays were determined. The same number of failed assays were observed in the singleplex testing as in the multiplex approach (5), the last containing an additional preamplification step. The results were also confirmed with the gel electrophoresis. Three of the failed assays (PENK, PITX2, SERPINB2) were the same in both experiments. The fact that the two failed assay of the singleplex qPCR (CDX1, CLIC4) showed perfect results during the multiplex approach can be explained by increased fluorescence signal of the targets due to their presence in a higher amount after 17 additional PCR cycles performed during the multiplex approach. On the contrary, the two failed multiplex assays resulted independent of the target dilution in high fluorescence intensities and therefore Ct values higher than 40 after inclusion of the preamplification step. This high values showed that the PCR reaction has been saturated due to high accumulation of products and has reached the plateau phase level, where the real-time measurement of the target is not possible anymore.

Another important finding was the Cp shift of nearly 7 Cp values for the theoretical 1 ng detection, meaning that the same input amount of DNA can be detect 7 cycles earlier within the multiplex approach. This effect is caused by the additional 17 performed PCR cycles prior to qPCR. Since amplification in PCR is an exponential reaction, 7 Cp values correspond to a huge difference of 128, which enables the tracing of much lower DNA amount. Minimal amount of targets contained in the samples are an important limitation in current diagnostic work-flows. High-throughput qPCR systems operate with very low sample volume. In order to overcome this limited material, a robust sample preamplification is required to generate sufficient nucleic acids concentration for detection [Vermeulen et al., 2009]. However, the number of preamplification steps cannot be endlessly increased due to the limitation of qPCR. Limiting reagents, accumulation of inhibitors, or inactivation of the polymerase influence the efficiency of amplification. Too many amplification cycles would lead to a decrease of qPCR efficiency and would introduce unintentionally bias in the experiment [Stahlberg and Ku-

4. Discussion

bista, 2014]. Therefore, the implementation of the preamplification step explains also the greater deficiencies for the efficiency parameter in the multiplex approach compared to the singleplex. While efficiency below 80% is mostly associated with poor annealing of the primers or unfavorable reaction condition, efficiency higher than 120% are caused by an excess of targets due to a nonlinear PCR reaction [Bustin et al., 2009]. If amplification of unspecific products (given by T_m values) or bad correlation coefficient ($R^2 < 0.95$) can be excluded, the cause of this bad efficiencies could be a bad primer, especially the related annealing temperature, unanticipated variants within the target sequence or the presence of inhibitory effects occurring during the amplification reaction.

Nevertheless, we ended up with 41 assays fulling the selection criteria and showing a constant performance and good reproducibility throughout the singleplex as well as throughout the multiplexed qPCR experiments. Their compatibility with the microfluidic, bead based multiplex detection was evaluated using the EvaluationTM platform from MyCartis.

In order to be able to detect the preamplified biotinylated targets, an assay design based on biotin-streptavidin interaction was defined. More exactly, probes consisting of biotinylated synthetic oligonucleotides were attached to the streptavidin molecules, which have been already coupled covalently to the carboxyl groups of the silicon-based microparticles. Different encoded microparticles were used for each individual probe. The nucleic acid targets, preamplified using reverse biotinylated primers and denatured previously in flow to single stranded DNA can hybridize to the probes and finally be detected by streptavidin phycoerythrin conjugate, which can bind to the target's biotin.

Attaching of biotinylated probes on the microparticles takes more than one step and is the time-determining step in the whole detection procedure on EvaluationTM, accounting for about of two third of the total analysis time. Based on MyCartis biotin coupling and probes attaching protocols, a faster, general and simple detection protocol was set up and optimized, which improved the practicability of the EvaluationTM platform drastically and shortened the time to detection by approximately one hour. Further, a number of parameters independent of the

biomarker panel were initially optimized. To avoid run out of the sample in the inlet wells, which is associated with the formation of air bubbles, the optimal flow rate and flow time was assessed for each hybridization buffer used in the frame of this work with regard to channel pressure, number of loaded microparticles and temperature. Another important parameter for the sensitivity of the detection is streptavidin-R-phycoerythrin, used for the last step of detection, which was observed to aggregate with 3x SSC and TMAC hybridization buffers. To eliminate any protein aggregates that may be formed between microparticles and thereby to reduce the non specific background staining, several concentrations of SAPE and incubation times were analyzed. The optimal incubation time was determined to be 10 minutes, while the appropriate staining dilution was 3 µg/mL SAPE prepared in hybridization buffer prior diluted 1:2 with water. In order to increase the detection sensibility (signal to ratio) when imaging low-fluorescent levels, e.g after hybridization in formamide buffer, it was advantageous to set the exposure time to 500 ms. This ensured the detection of smaller target amounts and avoided over saturation of the images.

After implementation of the standard protocol for probe coupling and attaching as well as setting important run parameter, an optimization of buffer condition for optimal target hybridization was performed. In order to test efficiently the suitability of the EvaluationTM system for detecting nucleic acids, the first evaluation experiments were performed with a reduced target panel of four synthetic oligonucleotides of known concentration. A four multiplex nucleic acid assay was produced and analyzed towards signal intensity and sensitivity signal with different hybridization buffers and times. Hybridizations conducted at different temperatures indicated that good sensitivities were obtained after 30 minutes incubation at 55 °C in the presence of 3x SSC, TMAC or 35% formamide hybridization buffers.

For detection of specific DNA sequences in complex, heterogeneous samples, the multiplex level of the nucleic acid assay was finally increased to a 19-plex assay and analyzed using synthetic nucleotides as well as PCR amplicons. In comparison with 3x SSC and TMAC buffer, 35% formamide buffer showed a lower detection sensitivity due to weaker signal intensities, but minimal cross-hybridization, re-

4. Discussion

sults which are explained by the fact that formamide, a DNA helix destabilizer, disrupts poorly hybridized molecules preventing non-specific hybridizations [Blake and Delcourt, 1996]. In consequence, 35% formamide hybridization buffer can be successfully use for detection of synthetic nucleotides down to a target concentration of 10 nM. Due to their higher limit of detection and therefore a better sensitivity compared to formamide buffer, 3x SSC and TMAC hybridization buffers could be able to detect very small amounts of DNA (up to 0.02 nM) present in the sample, if the non-specific binding of the targets could be reduced. Taking in consideration cross hybridization, the smallest target concentration that could be clearly detected was observed to be at 0.25 nM or 4.87 ng/ μ L. The theoretical LOD of PCR products amplified within 35 PCR cycles was calculated to be at 0.5 pg/ μ L. A comparison of the expected and observed LOD reveals a difference by the factor of 10000, which makes detection of PCR-products impossible. This limitation could be overcome in future by increasing the initial sample volume of the analyzed blood or by minimalism undesirable cross-hybridization.

Cross-hybridization is a major issue of multiplex hybridization reactions causing false positive signals, lowering specificity and sensitivity. Ideally, each single DNA strand from a multiplex reaction should bind with only its perfectly matched and complementary single strand. However, depending of the target sequence, many of the single strands anneal in reality also with wrong sequences resulting in cross-hybridization and mismatched duplex formation. Low background signal and therefore minimal cross-hybridization are more difficult to achieve in a multiplex approach than in a singleplex assay, because of the complexity of the multiplex environment and the resulting competition between perfect match and mismatch strands, which influence hybridization kinetic as well as equilibrium. Even cross-hybridization is well known as a major problem in multiplex hybridization, the molecular interactions responsible for it are not totally elucidated yet [Fish et al., 2007].

Although further work is required to overcome the sensibility challenge of the nucleic acid assay (e.g. by reducing cross-hybridization), the multiplex capability of the EvalutionTM platform is a powerful tool for detection of nucleic acid

based biomarkers from blood samples as well as for detection of synthetic oligonucleotides.

4.2 Protein assay

In the second part of this master thesis the capability of EvaluationTM system to detect specific proteins from a multiplex complex was evaluated on the basis of an indirect immunoassay. In this assay, a His tag modified antibody (NEUROD2 and NFIX) was first immobilized covalently to the carboxylated microparticles using a two step EDC sulfo NHS cross linking reaction. Detection of the auto-antibody of interest, present in human serum (samples P125 and P272), was performed using a conjugated secondary antibody (Goat Anti-Human IgG labeled with Phycoerythrin) and measuring its fluorescence signal. In order to achieve a correct detection, the secondary antibody responsible for detection, has to bind specific only to the antibody contained in the sample and not to the coupled antigen on the microparticles. This was achieved by using antigenic proteins expressed in *E. coli* together with samples' antibodies isolated from human serum. One of the main advantages of this assay design consists in the non labeled sample antibody, which guaranties its high immunoreactivity and increases signal amplification and therefore also sensitivity due to the several epitopes that can be bound by the detection antibody [ThermoFisher Scientific, 2015].

The coupling efficiency of the immobilized 6x His tag antigens to the carboxylated microparticles was confirmed by flowing simultaneously SAPE and monoclonal mouse anti His antibodies in the channels. All assays exhibited high signal intensities, which increased also proportional with the incubation time. Similar signal intensity ranges were measured, fact which showed that the microparticles were coupled in an equal proportion with both antigens. As expected, no signals were obtained for the controls proteins *E. coli* lysat, Protein G and HSA. Their detection and therefore their coupling was not possible because these do not present a His tag on their surface.

4. Discussion

Before conducting the evaluation experiments, a pH screening test was performed directly in the cartridge. This was important for determination of the optimal pH range of the applied buffer, which was used for sample dilution and antibody incubation and could influence phycoerythrin detection reaction and its aggregation. For this, the purified IgGs from both human serum samples were added to the microparticles previously coupled with the two antigens and detected using a phycoerythrin labeled detection antibody. Independent of pH, both samples showed massive protein aggregation making estimation of the optimal pH impossible. This might be most likely due to precipitates from the antigen and antibody solutions. Despite the aggregation problem, which makes a clear interpretation hard, the measured fluorescence of the microparticles were very high, indicating that coupling and assay worked. Therefore, based on similar experiments conducted within another AIT project conducted on Luminex[®] platform, the assay buffer pH was set at pH 5, which is also in line with MyCartis protocols.

The comparison between whole serum samples and purified IgG samples resulted in higher signals for unpurified IgG. The whole human samples contained due to immunological history beside the targeted IgG also other antibodies that could also react and therefore explain the higher, eventually non specific fluorescence signal. Non specific reaction as a possible reason for higher signals can be excluded taking into consideration the similar trend of the measured fluorescence (same signal ratio) observed after comparison of the Evaluation[™] results with data obtained from the antibodies screening project conducted by AIT on Luminex[®], which used only purified IgGs as samples. On both systems, independent of the purification level, P125 showed high fluorescence binding specific both antigens, while for P272 high intensity was registered after capture on NEUROD2 and low signals on NFIX. Also the three controls (*E. coli* lysat, Protein G and HSA) behaved in both experiments similar. Therefore, serum samples work as good as purified samples and give generally higher signals. The use of whole serum samples with an adequate level of dilution could avoid an extra labor intense and costly purification step.

Evaluation of two different coupling buffers, focused on optimal signal intensities, signal to noise ratio and sample aggregation, showed that PBS-1%BSA buffer

gave higher fluorescent signals than Low Cross buffer and lead also to stronger aggregation. Aggregates are also most likely present on Luminex® assays, but the system is not able to visualize them. A main advantage of the Evaluation™ system is given by the possibility of visualization of the capture images of the microparticles during (real time) as well as after assay detection. This ability of the system provides helpful qualitative information about the assay quality. Whereas the increase of detection antibody's concentration did not lower aggregation level, spinning the samples with high rotation, reduced considerably aggregation, but did not completely solve it.

However, it has been shown that the Evaluation™ system is able to detect specific antibodies within short assay times and has a competitive analytical sensitivity compared to other multiplex technologies. Further optimization work is necessary to make the use of the immunoassay more suitable for molecular diagnostics, e.g. coupling optimization for each antigen with higher/lower antigen amounts, optimization of run conditions regarding pressure and flow times, improving buffer composition, increasing multiplex level, etc.

4.3 Conclusion

In conclusion, this thesis addressed implementation and sensitivity issues of a novel multiplexed detection platform provided by MyCartis. It has been shown that Evaluation™ platform is a valuable alternative to state-of-the-art methods used for multiplex nucleic acid and protein detection from blood and serum, being best suited to simultaneously detect multiple biomarkers in very low concentrations, which could prevent patients from unnecessary invasive diagnostic procedures, saving time and costs.

List of Figures

1.1	Application of molecular diagnostics in clinical field	6
1.2	Amplification of DNA by PCR technique	7
1.3	Evalution™ detection schemes	9
1.4	Digitally encoded microparticles	10
1.5	Microfluidic assay plate	10
1.6	Evalution™ bench top instrument	11
2.1	Nucleic acid assay design for Evalution™	15
2.2	PCR efficiency equation	17
2.3	Software protocol for functional test	24
2.4	An exemplary flow rate measurement protocol [MyCartis, 2014b]. In the protocol of this work the cartridge zone temperatures were changed to 25 °C, 95 °C and 55 °C, while other parameters as well as all steps remained unchanged	25
2.5	Indirect Immunoassay	35
2.6	EDC/sulfo-NHS activation of COOH-microparticles	36
2.7	Screenshot of the pH Screening standard run protocol for protein assay adapted after [MyCartis, 2014a]. Activation buffer = MEST buffer pH 3.5; antigen solutions = NFIX and NEUROD2 in assay buffer; wash buffer = PBST; sample solutions = purified IgG from P125 and P272 samples of human serum; anti human Ab = goat anti-human IgG labeled with SAPE.	39
2.8	Schematic set up of the non functional test	41
2.9	Non-functional test protocol script	42
3.1	Slope of the log-linear phase of the PCR	47
3.2	qPCR efficiency	48
3.3	Correlation coefficient of the standard curves	48

3.4	Theoretical 1 ng detection	49
3.5	Exemplary fluorescence image of streptavidin coupled microparticles	52
3.6	Results of Streptavidin RPE optimization	53
3.7	Capture images of SAPE optimization results	53
3.8	Comparison of exposure times	54
3.9	4 sythetic oligonucelotides in 3xSSC buffer	56
3.10	Alternative hybridization buffers	58
3.11	Cross-hybridization of TMAC and 1x PCR buffers	59
3.12	Multiplex hybridization sensibility	60
3.13	PCR products control	61
3.14	Linearity box plots of cDNA concentration	62
3.15	Positive and negative control for cDNA samples	63
3.16	Protein aggregation after pH screening	66
3.17	Antigens coupling confirmation	68
3.18	Purified IgG vs. Serum IgG samples	68
3.19	LowCross vs PBS buffer and 5 µg vs 2 µg detection antibody	70
3.20	Aggregation in LowCross and PBST-1% BSA buffers	71
3.21	Optimization of aggregation in PBST-1% BSA buffer	72
4.1	Control electrophoresis gel of standard qPCR	98
4.2	Control electrophoresis gel of standard qPCR	99
4.3	Control electrophoresis gel of qPCR with preAmp step	100
4.4	Standard Evaluation TM running script for nucleic acid assays	102

List of Tables

2.1	HulaMixer™ program	22
2.2	List of the hybridisation buffers	26
3.1	Assays reproducibility and repeatability of randomly selected qPCR assays	50
3.2	Exemplary flow rate assessment for PBST	51
3.3	Data example functional test	52
3.4	Optimal hybridization temperature and concentration of formamide buffer	57
3.5	Limit of detection	65
3.6	IgG diluted from serum vs. purified IgG	69
3.7	Evalution™ vs. Luminex® detection	70
4.1	Assay parameters	95
4.2	Performance parameter of qPCR assay without preamplification . .	96
4.3	Performance parameter of qPCR assay with preamplification step .	97
4.4	Assays reproducibility of both qPCR experiments	101
4.5	Multiplex synthetic oligonucleotides assay in TMAC buffer	103
4.6	Multiplex synthetic oligonucleotides assay in 3x SSC buffer	103

References

- Alberts, B., A. Johnson, J. Lewis, M. Raff, K. Roberts, and P. Walter. 2008. *Molecular Biology of the Cell*. Garland Science, New York, USA. 5 edition. ISBN 978-0-8153-4105-5.
- Biocartis SA. *Training on Evalution: Protocol for the Coupling of Streptavidin*. Lausanne, Switzerland, 2014a.
- Biocartis SA. *Training on Evalution: Protocol for the Attaching of Biotinylated DNA probes*. Lausanne, Switzerland, 2014b.
- Biocartis SA. *Training on Evalution: Loading of a Cartridge*. Lausanne, Switzerland, 2014c.
- Biomarkers Definitions Working Group. 2001. Biomarkers and surrogate endpoints: preferred definitions and conceptual framework. *Clinical Pharmacology & Therapeutics*, 69:89–95.
- Blake, R. D. and S. G. Delcourt. 1996. Thermodynamic effects of formamide on dna stability. *Nucleic Acids Res*, pages 2095–2103.
- Bustin, S. A., V. Benes, J. A. G. J. Hellemans, J. Huggett, M. Kubista, R. Mueller, T. Nolan, M. W. Pfaffl, G. L. Shipley, J. Vandesompele, and C. T. Wittwer. 2009. The MIQE guidelines: Minimum information for publication of quantitative real-time PCR experiments. *Clinical Chemistry*, 55.
- Chan, M., M. W. Chan, T. W. Loh, H. Y. Law, C. S. Yoon, S. S. Than, J. M. Chua, C. Y. Wong, W. S. Yong, Y. S. Yap, G. H. Ho, P. Ang, and A. S. G. Lee. 2011. Evaluation of nanofluidics technology for high-throughput Snp genotyping in a clinical setting. *The Journal of Molecular Diagnostics*, 13.
- Costello, J., M. C. Fruehwald, D. J. Smiraglia, L. J. Rush, G. P. Robertson, X. Gao, F. a. Wright, J. D. Feramisco, PaeviPeltomaeki, J. C. Lang, D. E. Schuller, L. Yu, C. D. Bloomfield, M. A. Caliguri, A. Yates, R. Nishikawa, H.-J. S. Huang, N. J. Petrelli, X. Zhang, M. S. O’Dorisio, W. A. Held, W. K.

- Cavenee, and C. Plass. 2000. Aberrant cpg-island methylation has non-random and tumour-type-specific patterns. *Nature Genetics*, 24:132–138.
- Debnath, M., G. Prasad, and P. Bisen. 2010. *Molecular Diagnostics: Promises and Possibilities*. Springer, Heidelberg, Germany. ISBN 978-90-481-3261-4.
- Falconnet, D., J. She, R. Tornay, E. Leimgruber, D. Bernasconi, L. Lagopoulos, P. Renaud, N. Demierre, and P. van den Bogaard. 2015. Rapid, sensitive and real-time multiplexing platform for the analysis of protein and nucleic-acid biomarkers. *Analytical Chemistry*, 87:1582–1589.
- Filion, M. 2012. *Quantitative Real-time PCR in Applied Microbiology*. Caister Academic Press, Norfolk, UK. ISBN 978-1-908230-01-0.
- Fish, D. J., M. T. Horne, R. P. Searles, G. P. Brewood, and A. S. Benight. 2007. Multiplex snp discrimination. *Biophysical Journal*, pages 89–91.
- Gmeiner, E. 2015. Evaluation of micropshere-based anitgenic peptide arrays for the early detection of breast cancer. Master’s thesis, BOKU, Vienna.
- Gormally, E., E. Caboux, P. Vineis, and P. Hainaut. 2007. Circulating free dna in plasma or serum as biomarker of carcinogenesis: Practical aspects and biological significance. *Mutation Research*, 635:105–117.
- Jain, K. 2009. *Textbook of Personalized Medicine*. Springer Science, Basel, Switzerland. ISBN 978-1-4419-0768-4.
- Jain, K. 2010. *The Handbook of Biomarkers*. Springer, New York, USA. ISBN 978-1-60761-685-6.
- Jung, K., M. Fleischhacker, and A. Rabien. 2010. Cell-free dna in the blood as a solid tumor biomarker - a critical appraisal of the literature. *Clinica Chimica Acta*, 411:1611–1624.
- Karlen, Y., A. McNair, S. Perseguers, C. Mazza, , and N. Mermoud. 2007. Statistical significance of quantitative pcr. *BMC Bioinformatics*, 8.

REFERENCES

- Kennedy, S. and N. Oswald. 2011. *PCR Troubleshooting and Optimization: The Essential Guide*. Caister Academic Press, Norfolk, UK. ISBN 978-1-904455-72-1.
- Levenson, V. V. 2011. Dna methylation as universal biomarker. *Expert Rev Mol Diagn*, 10:481–488.
- Liu1, L.-N., H.-N. Su1, S.-G. Yan, S.-M. Shao, B.-B. Xie, X.-L. Chen, X.-Y. Zhang, B.-C. Zhou, and Y.-Z. Zhang. 2009. Probing the pH sensitivity of R-phycoerythrin: Investigations of active conformational and functional variation. *Biochimica et Biophysica Acta*, 1787.
- Mackay, I. 2007. *Real-time PCR in Microbiology: From Diagnosis to Characterization*. Caister Academic Press, Norfolk, UK. ISBN 978-1-904455-18-9.
- MyCartis. *Evaluation training: Immunoassay Protocol*. Lausanne, Switzerland, 2014a.
- MyCartis. *Flow rate measurement protocol*. Lausanne, Switzerland, 2014b.
- MyCartis. *Training on Evaluation: Streptavidin functional test*. Lausanne, Switzerland, 2014.
- MyCartis. 2015. *Technical notes - Lightening the black box by visualization of the reaction*. MyCartis NV, Zwijnaarde, Belgium.
- Najeeb, Q., R. Pandey, and N. Bhaskar. 2012. Personalized Medicine versus era of "Trial and Error". *Journal of Pharmaceutical and Biomedical Science*, 19:1–5.
- National Institute of Health, 2010. FACT SHEET - Human Genome Project. <http://report.nih.gov/nihfactsheets/ViewFactSheet.aspx?csid=45>. Accessed: September 2015.
- Platforma europeana de dezvoltare, 2013. Medicina personalizata, sansa ta la viata! http://issuu.com/edp-org.com/docs/brosura_mp_ok_new. Accessed: September 2015.
- Pothier, K., R. Woosley, A. Fish, and T. Sathiamoorthy. 2013. The essentials of diagnostics: Introduction to molecular diagnostics. Technical report, AdvamedDx & DxInsights. Accessed: September 2015.

- Schmitz, G. and D. Anz. 2008. *Biomarker: Bedeutung für medizinischen Fortschritt und Nutzenbewertung*. Schattauer, Stuttgart, Germany. ISBN 978-3-7945-2614-7.
- Schwarzenbach, H., D. Hoon, and K. Pantel. 2011. Cell-free nucleic acid as biomarkers in cancer patients. *Nature Reviews Cancer*, 11:426–437.
- Shimatzu Corporation. *Microchip Electrophoresis System for DNA/RNA Analysis MCE-202 MultiNA Instruction Manual*. Kyoto, Japan, 2008.
- Stahlberg, A. and M. Kubista. 2014. The workflow of single-cell expression profiling using quantitative real-time PCR. *Expert Rev. Mol. Diagn.*, 14.
- Strimbu, K. and J. Tavel. 2010. What are biomarkers? *Current opinion in HIV and AIDS*, 5:463–466.
- Sveca, D., A. Tichopadb, V. Novosadova, M. W. Pfaffld, and M. Kubista. 2015. How good is a PCR efficiency estimate: Recommendations for precise and robust qPCR efficiency assessments. *Biomolecular Detection and Quantification*, 3.
- ThermoFisher Scientific, 2015. Overview of elisa. <https://www.thermofisher.com/at/en/home/life-science/protein-biology/protein-biology-learning-center/protein-biology-resource-library/pierce-protein-methods/overview-elisa.html>. Accessed: March 2016.
- Tost, J. 2010. Dna methylation: an introduction to the biology and the disease-associated changes of a promising biomarker. *Mol. Biotechnol.*, 44:71–81.
- Vermeulen, J., S. Derveaux, S. Lefever, E. D. Smet, K. D. Preter, N. Yigit, A. D. Paepe, F. Pattyn, F. Speleman, and J. Vandesompele. 2009. RNA pre-amplification enables large-scale RT-qPCR gene-expression studies on limiting sample amounts. *BMC Research Notes*, 2.
- Virella, G. 2007. *Medical Immunology, Sixth Edition*. CRC Press, New York, USA. ISBN 978-0849396960.
- Wink, M. 2011. *Molekulare Biotechnologie: Konzepte, Methoden und Anwendungen*. Wiley-VCH. ISBN 9783527326556.

REFERENCES

Worm, J., A. Aggerholm, and P. Guldberg. 2001. In-tube DNA methylation profiling by fluorescence melting curve analysis. *Clinical chemistry*, 47.

Eigenständigkeitserklärung

Hiermit bestätige ich, dass ich die vorliegende Arbeit selbständig verfasst und keine anderen als die angegebenen Hilfsmittel benutzt habe. Die Stellen der Arbeit, die dem Wortlaut oder dem Sinn nach anderen Werken (dazu zählen auch Internetquellen) entnommen sind, wurden unter Angabe der Quelle kenntlich gemacht. Weiterhin versichere ich, dass die Arbeit bisher weder in gleicher noch in ähnlicher Form einer anderen Prüfungsbehörde vorgelegt und auch nicht veröffentlicht wurde.

Appendix

A-1

Table 4.1: Assay parameters. The table contains information about lengths of the targets, probes, primers and products, GC content and melting point.

Gene	Length (base pairs)					GC content (%)		Melting point (°C)	
	Probe	Target	PCR Product	Forward Primer	Reverse Primer	Forward Primer	Reverse Primer	Forward Primer	Reverse Primer
TJP2	63	106	141	24	21	70.83	80.95	77.21	77.72
TFPI2	50	97	108	19	20	84.21	80.00	77.97	79.16
H19	59	101	119	22	22	72.73	72.73	77.48	77.96
PITX2	58	108	144	22	21	72.73	85.00	75.38	77.92
SPARC	50	213	118	24	23	70.83	69.57	76.37	77.29
SEZ6L	50	243	127	21	24	76.19	70.83	77.91	77.74
GDNF	61	104	140	22	20	72.73	80.00	77.69	76.93
PITX2	57	91	115	21	22	80.95	77.27	78.02	77.89
S100A2	62	110	126	22	25	71.43	64.00	77.94	75.00
CHFR	64	108	119	27	24	59.26	58.33	75.15	76.31
PENK	58	105	133	23	20	69.57	75.00	77.72	77.18
ZNF502	58	101	116	23	22	69.57	77.27	75.45	77.28
CXADR	64	90	153	24	25	54.17	68.00	68.2	76.88
SNRPN	57	105	124	20	23	75.00	65.22	77.08	76.57
RARB	61	101	90	23	23	61.54	69.57	76.17	76.05
CDX1	50	101	150	22	22	68.18	68.18	77.27	76.22
GATA4	52	105	138	23	20	68.18	80.00	75.12	78.19
IL1B	64	92	99	24	25	56.67	60.00	75.49	72.21
ZNF256	57	109	108	23	20	65.22	75.00	77.74	77.63
JUB	65	101	91	23	5	69.57	65.52	75.18	77.44
CALCA	57	100	83	22	23	72.73	65.22	77.11	76.32
DAPK1	57	105	147	20	20	80.00	75.00	77.9	77.57
SERPINB2	62	107	96	22	28	77.27	60.71	77.71	76.67
CLIC4	59	120	105	22	30	72.73	56.67	77.07	75.72
RHOXF1	51	108	102	22	25	77.27	60.00	77.99	76.02
IRF4	64	100	128	31	33	54.84	51.52	76.88	76.44
S100A8	65	102	116	23	27	69.57	62.96	76.88	76.33
SALL3	54	100	113	20	21	80.00	71.43	76.37	77.69
CD24	60	100	114	22	22	72.73	77.27	76.58	77.04
TMEFF2	51	106	131	22	24	77.27	70.83	76.03	76.97
PTGS2	61	101	98	22	27	72.73	66.67	76.92	77.89
BOLL	53	107	119	21	25	80.95	64.00	77.84	76.06
MSH4	64	109	150	23	20	65.22	80.00	76.57	76.96
TWIST1	50	100	143	23	24	72.73	62.50	77.66	76.79
SFRP2	57	108	123	19	25	78.95	68.00	75.76	76.39
FMR1	58	82	148	22	20	72.73	85.00	77.02	78.05
DCC	64	92	105	23	27	73.91	62.96	76.98	76.78
TCEB2	62	102	150	20	20	80.00	80.00	78.89	77.84
HLA-G	58	99	133	22	23	72.73	69.57	75.62	77.22
NKX2-1	50	104	95	22	22	77.27	72.73	77.27	77.94
ESR1	52	98	93	22	22	68.18	72.73	77.35	77.53
SRGN	70	105	110	30	28	53.57	60.71	76.26	76.97
MYOD1	50	97	95	22	19	77.27	78.95	77.22	77.96
TBP	55	101	101	18	21	83.33	71.43	75.14	74.54
WT1	64	110	101	26	20	65.38	80.00	77.54	77.96
TP53	56	108	127	22	23	68.18	73.9	77.85	77.2
THBD	50	94	109	24	22	66.67	72.73	75.64	77.09
XIST	62	108	148	27	24	55.56	66.67	76.00	76.56

4. Appendix

A-2

Table 4.2: Performance parameters of qPCR assay without preamplification. Slope of a 4-point calibration curve, theoretical 1 ng detection, correlation coefficient (R^2), and deduced efficiency are shown. "X" represents a failed assay

Gene	DNA1				DNA2				DNA3			
	Slope	1 ng detection[Cp]	R^2	Efficiency[%]	Slope	1 ng detection[Cp]	R^2	Efficiency[%]	Slope	1 ng detection[Cp]	R^2	Efficiency[%]
BOLL	-3.52	26.31	0.99	92.43	-3.58	26.44	1.00	90.28	-3.76	26.04	1.00	84.42
CALCA	-3.54	24.60	1.00	91.72	-3.49	24.61	1.00	93.45	-3.55	24.68	1.00	91.32
CD24	-3.52	24.36	0.99	92.49	-3.65	24.34	1.00	87.90	-3.67	24.22	1.00	87.26
CDX1	x	x	x	x	x	x	x	x	x	x	x	x
CHFR	-3.23	25.37	1.00	104.04	-3.59	25.32	1.00	89.89	-3.90	25.35	0.99	80.39
CLIC4	-4.75	9.96	0.98	62.37	x	x	x	x	x	x	x	x
CXADR	-3.31	25.23	0.99	100.36	-3.42	25.38	1.00	96.14	-3.86	24.63	1.00	81.45
DAPK1	-3.20	30.06	0.99	105.26	-3.59	29.81	1.00	90.06	-3.51	29.82	0.99	92.79
DCC	-3.68	23.30	1.00	86.84	-3.67	23.44	1.00	87.37	-3.57	23.28	1.00	90.62
ESR1	-3.77	27.73	1.00	84.18	-3.55	28.28	1.00	91.20	-3.66	27.40	1.00	87.47
FMR1	-3.18	30.62	0.94	106.26	-3.25	30.50	0.97	103.30	-3.26	30.40	1.00	102.86
GATA4	-2.96	27.24	0.98	117.81	-3.53	27.44	1.00	92.14	-3.38	27.04	0.99	97.64
GDNF	-3.60	24.53	0.99	89.44	-3.13	23.83	1.00	108.57	-2.96	24.26	1.00	117.71
H19	-3.89	33.35	0.95	80.61	-3.80	31.71	0.84	83.19	-3.27	32.97	1.00	102.12
HLA-G	-3.43	21.38	1.00	95.82	-3.24	21.55	1.00	103.67	-3.56	22.20	1.00	90.80
IL1B	-3.65	19.93	1.00	88.01	-3.75	19.87	1.00	84.73	-3.65	20.07	1.00	87.79
IRF4	-3.82	24.47	0.95	82.71	-3.64	24.68	1.00	88.39	-3.55	25.05	1.00	91.14
JUB	-3.36	25.50	1.00	98.31	-3.40	25.63	0.99	96.72	-3.45	25.21	1.00	95.06
LUP1	-3.46	26.26	0.99	94.37	-3.44	23.96	1.00	95.38	-3.36	24.05	1.00	98.51
MGMT	-3.86	30.95	1.00	81.53	-3.38	28.60	1.00	97.64	-3.30	28.34	1.00	101.06
MSH4	-3.42	23.17	1.00	95.88	-3.41	23.23	1.00	96.53	-3.56	23.19	1.00	91.03
MYOD1	-3.68	32.83	0.96	86.99	-2.13	31.48	0.92	194.64	-3.01	36.61	1.00	114.78
NKX2-1	-3.84	26.06	1.00	82.05	-3.60	26.35	1.00	89.72	-3.86	25.76	0.99	81.58
PENK	x	x	x	x	x	x	x	x	x	x	x	x
PITX2	x	x	x	x	x	x	x	x	x	x	x	x
PITX2	-2.50	34.58	0.99	151.21	-2.96	33.84	0.86	117.90	-3.85	35.45	0.87	82.00
PTGS2	-3.45	23.98	1.00	94.81	-3.42	24.06	1.00	96.08	-3.41	24.07	1.00	96.46
RARB	-3.28	24.59	1.00	101.78	-3.57	24.72	1.00	90.51	-3.47	24.84	1.00	94.25
RHOXF1	-3.61	24.99	1.00	89.38	-3.52	26.00	1.00	92.43	-3.72	26.15	1.00	85.85
S100A2	-3.35	23.48	1.00	98.98	-3.33	23.57	0.99	99.66	-3.36	23.89	1.00	98.44
SA1008	-3.62	24.56	1.00	88.77	-3.95	26.44	1.00	79.05	-3.66	24.68	0.99	87.52
SALL3	-3.43	31.16	1.00	95.68	-3.74	31.52	0.89	85.08	-3.32	30.99	0.99	100.15
SERPINB2	x	x	x	x	x	x	x	x	-3.67	10.09	1.00	87.25
SEZ6L	-3.91	33.90	1.00	80.17	-4.23	34.70	0.98	72.41	-3.77	33.64	0.96	84.33
SFRP2	-3.69	32.42	0.96	86.63	-4.27	33.33	0.99	71.51	-4.18	32.17	1.00	73.55
SNRPN	-3.38	24.11	1.00	97.71	-3.30	24.00	1.00	100.99	-3.56	24.14	1.00	91.08
SPARC	-3.34	23.26	1.00	99.25	-3.41	23.37	0.99	96.46	-3.34	23.26	1.00	99.25
SRGN	-3.73	23.12	1.00	85.54	-3.55	23.16	1.00	91.14	-3.62	23.17	1.00	88.88
TBP	-3.75	28.40	1.00	84.88	-3.22	29.04	0.98	104.50	-3.69	27.73	0.99	86.68
TCEB2	-3.70	27.80	1.00	86.37	-3.36	28.13	1.00	98.63	-3.33	26.34	0.99	99.46
TFPI2	-3.49	29.66	0.94	93.33	-3.78	28.63	0.98	83.94	-3.39	28.78	0.99	97.37
THBD	-3.46	23.20	1.00	94.69	-3.46	23.17	1.00	94.37	-3.46	23.40	1.00	94.62
TJP2	-3.27	27.45	0.99	102.42	-3.30	26.97	1.00	101.06	-3.02	27.24	1.00	114.56
TMEFF2	-3.30	27.02	0.99	100.99	-3.16	25.96	0.87	107.44	-3.60	27.09	0.99	89.61
TP53	-3.38	23.22	1.00	97.51	-3.49	23.17	1.00	93.33	-3.31	23.14	1.00	100.36
TWIST1	-3.51	28.19	0.99	92.60	-2.65	28.35	0.99	138.35	-4.35	28.21	0.72	69.82
WT1	-3.59	27.15	1.00	89.94	-3.78	27.65	1.00	83.98	-3.40	27.61	0.99	96.85
XIST	-3.51	22.49	1.00	92.79	-3.32	24.71	0.99	100.08	-3.57	24.72	1.00	90.45
ZNF256	-3.49	23.72	1.00	93.33	-3.41	23.81	1.00	96.46	-3.53	23.98	1.00	92.08
ZNF502	-3.64	24.46	1.00	88.39	-3.50	24.13	1.00	93.21	-3.73	24.37	1.00	85.44

A-3

Table 4.3: Performance parameters of qPCR assay with a preamplification step with 17 cycles. Slope of 4-point calibration curves, theoretical 1 ng detection, correlation coefficient (R^2), and deduced efficiency are shown. "X" represents a failed assay

Gene	DNA1				DNA2			
	Slope	1 ng detection [Cp]	R^2	Efficiency[%]	Slope	1 ng detection [Cp]	R^2	Efficiency[%]
BOLL	-3.61	22.93	1.00	89.16	-3.94	22.24	0.98	79.49
CALCA	-3.38	18.54	0.96	97.51	-3.78	17.85	0.98	83.88
CD24	-2.88	18.63	0.95	122.45	-3.75	17.66	0.97	84.92
CDX1	-2.97	31.18	0.97	116.96	-3.38	28.32	0.95	97.40
CHFR	-3.26	20.69	0.97	102.85	-3.49	18.96	0.97	93.51
CLIC4	-2.69	6.89	0.97	135.08	-4.05	7.89	1.00	76.50
CXADR	-2.94	21.49	0.91	118.96	-3.59	20.23	0.97	89.94
DAPK1	-4.29	15.62	0.90	70.98	-3.76	16.50	0.98	84.63
DCC	-3.27	16.72	0.98	102.28	-3.76	16.23	0.99	84.53
ESR1	-3.23	14.84	0.99	103.82	-3.33	14.38	1.00	99.80
FMR1	-3.49	21.18	0.99	93.58	-3.68	21.04	1.00	86.99
GATA4	-3.66	16.38	0.98	87.47	-3.64	16.09	0.99	88.23
GDNF	x	x	x	x	x	x	x	x
H19	-3.44	18.98	0.95	95.38	-3.80	18.08	0.99	83.19
HLA-G	-3.48	25.73	0.99	93.63	-3.59	13.27	0.99	90.06
IL1B	-2.92	22.91	1.00	119.98	-3.95	22.47	0.85	79.23
IRF4	-3.39	24.76	0.93	97.31	-3.89	23.37	0.94	80.84
JUB	-3.53	18.69	0.97	91.90	-3.76	17.86	0.98	84.63
MSH4	-3.32	16.44	0.96	100.22	-3.66	15.59	0.99	87.47
MYOD1	-3.36	17.48	0.92	98.30	-4.67	17.08	0.96	63.76
NKX2-1	-3.30	26.24	0.93	101.06	-4.19	24.94	0.97	73.35
PENK	x	x	x	x	x	x	x	x
PITX2	x	x	x	x	x	x	x	x
PITX2_	-3.91	17.41	1.00	80.07	-3.91	17.21	0.99	80.16
PTGS2	-3.68	16.37	0.99	86.89	-3.80	16.01	0.99	83.30
RARB	x	x	x	x	x	x	x	x
RHOXF1	x	x	x	x	-3.76	21.71	0.94	84.42
S100A2	-3.26	18.12	0.96	102.49	-3.60	17.40	0.98	89.60
S100A8	-3.33	17.87	0.97	99.66	-3.75	17.11	0.98	84.93
SALL3	-3.61	19.32	0.93	89.22	-3.52	19.53	0.98	92.25
SERPINB2	x	x	x	x	x	x	x	x
SEZ6L	-3.43	19.24	1.00	95.70	-4.25	18.50	0.99	72.01
SFRP2	-4.15	31.56	0.82	74.11	-3.58	30.56	1.00	90.27
SNRPN	-3.10	19.88	0.91	110.13	-3.59	18.99	0.98	89.77
SPARC	-3.03	16.15	0.98	113.94	-3.51	15.35	0.99	92.85
SRGN	-3.51	34.52	0.90	92.85	-3.47	32.22	0.83	94.12
TBP	-3.28	16.34	0.97	101.99	-3.39	15.56	0.99	97.37
TCEB2	-2.67	17.00	0.94	136.96	-4.93	16.57	0.98	59.59
TFPI2	-3.11	18.39	0.95	109.47	-3.34	17.74	0.97	99.32
THBD	-3.53	15.93	0.98	91.96	-3.42	15.41	1.00	96.01
TJP2	-3.33	14.56	0.99	99.60	-3.37	14.09	1.00	98.10
TMEFF2	-3.42	14.07	1.00	96.14	-3.62	13.50	1.00	88.99
TP53	-3.59	14.89	0.99	89.94	-3.59	14.28	1.00	89.77
TWIST1	-2.63	21.16	0.91	139.81	-3.19	31.57	0.79	105.95
WT1	-3.36	15.53	0.98	98.24	-3.65	15.04	0.99	88.01
XIST	-3.46	18.20	0.97	94.68	-3.85	17.37	0.94	82.00
ZNF256	-3.42	20.45	0.92	95.88	-3.72	19.71	0.97	85.74
ZNF502	-3.84	23.78	0.99	82.25	-4.73	20.86	0.98	62.68

4. Appendix

A-4

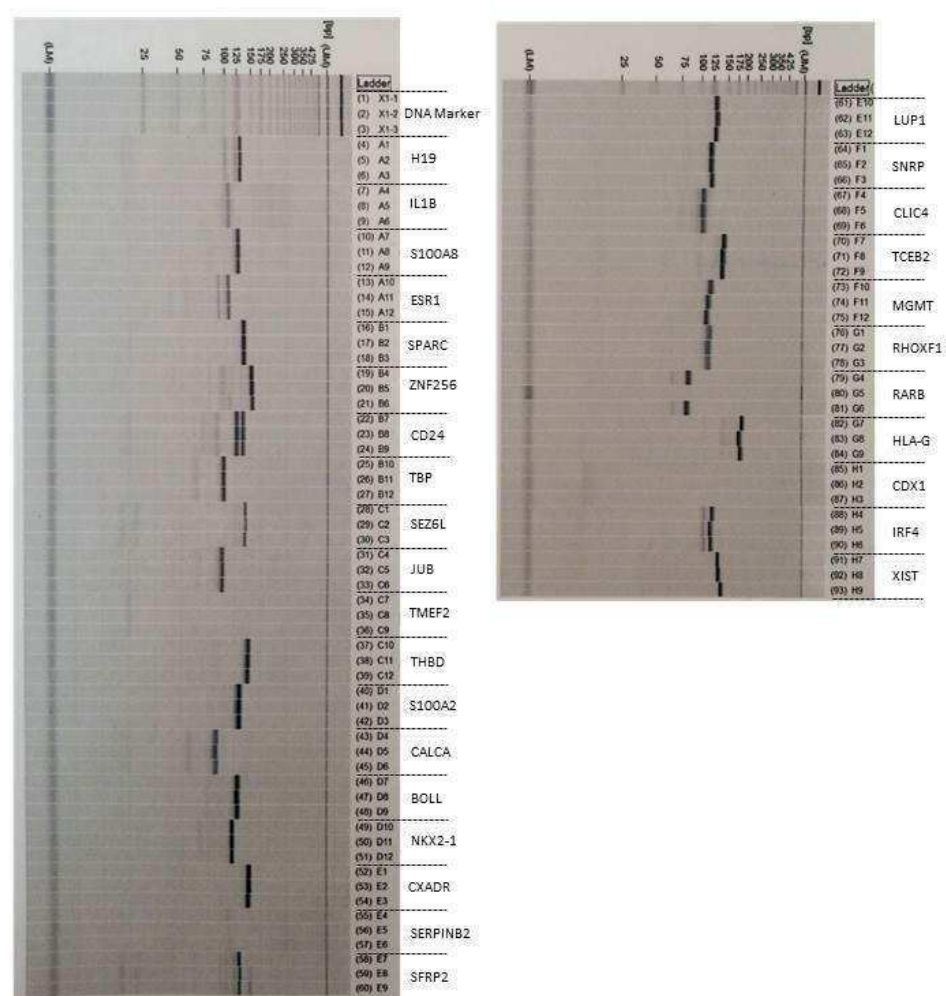
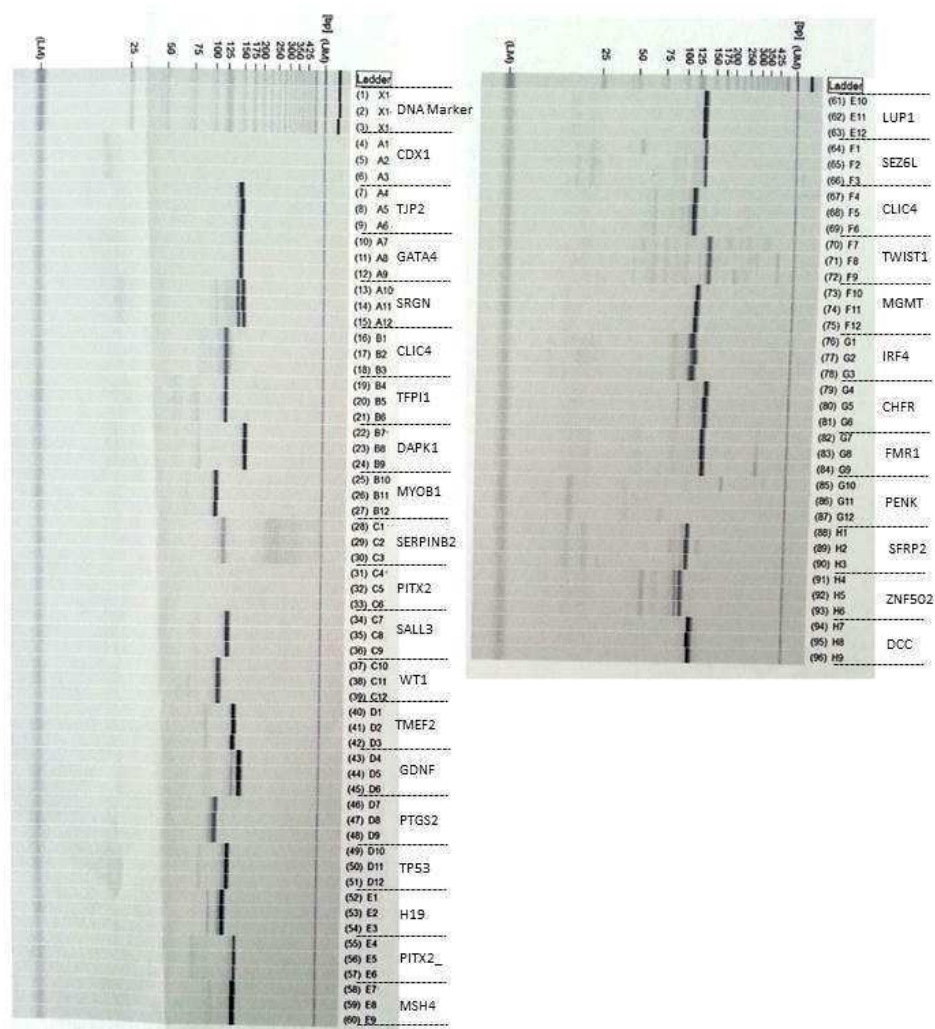


Figure 4.1: Control electrophoresis gel of the PCR assay without preamplification (first part)

Figure 4.2: Control electrophoresis gel of the PCR assay without preamplification (second part)



4. Appendix

A-5

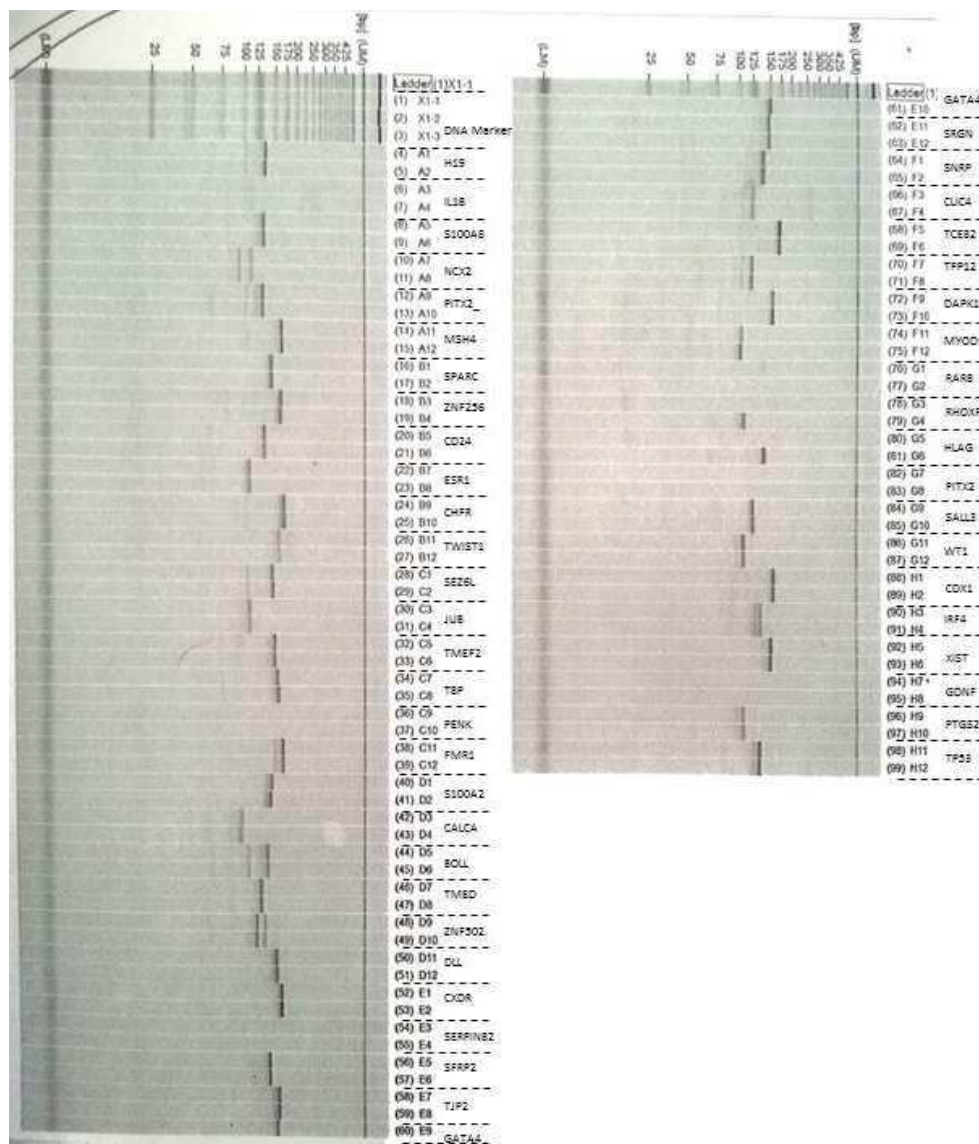


Figure 4.3: Control electrophoresis gel of the PCR assay including a preamplification step

A-6

Table 4.4: Reproducibility and repeatability of the 48 assays tested on serial dilutions of blood DNA with 17 cycles and without preamplification. SD=standard deviation, x= failed assay.

	no preAmp efficiencies [%]				preAmp efficiencies [%]		
Primer	Run1	Run2	Run3	SD \pm	Run1	Run2	SD \pm
BOLL	92.43	90.28	84.42	4.15	89.16	79.49	6.84
CALCA	91.72	93.45	91.32	1.14	97.51	83.88	9.63
CD24	92.49	87.90	87.26	x	122.45	84.92	26.54
CDX1	x	x	x	x	116.96	68.60	34.19
CHFR	104.04	89.89	80.39	11.9	102.85	93.51	6.61
CLIC4	62.37	x	x	x	135.08	76.50	41.42
CXADR	100.36	96.14	81.45	9.93	118.96	89.94	20.52
DAPK1	105.26	90.06	92.79	8.10	70.98	84.63	9.65
DCC	86.84	87.37	90.62	2.05	102.28	84.53	12.55
ESR1	84.18	91.20	87.47	3.51	103.82	99.80	2.84
FMR1	106.26	103.30	102.86	1.85	93.58	86.99	4.65
GATA4	117.81	92.14	97.64	13.52	87.47	88.23	0.53
GDNF	89.44	108.57	117.71	14.43	x	x	x
H19	80.61	83.19	102.12	11.75	95.38	83.19	8.62
HLA-G	95.82	103.67	90.80	6.49	x	90.06	x
IL1B	88.01	84.73	87.79	1.84	119.98	79.23	28.81
IRF4	82.71	88.39	91.14	4.30	97.31	80.84	11.65
JUB	98.31	96.72	95.06	1.62	91.90	84.63	5.14
MSH4	95.88	96.53	91.03	3.01	100.22	87.47	9.01
MYOD1	86.99	194.64	114.78	55.89	98.30	63.76	24.42
NKX2-1	82.05	89.72	81.58	4.57	101.06	73.35	19.60
PENK	x	x	x	x	x	x	x
PITX2	x	x	x	x	x	x	x
PITX2_	151.21	117.90	82.00	34.61	80.07	80.16	0.06
PTGS2	94.81	96.08	96.46	0.86	86.89	83.30	2.54
RARB	103.89	90.51	94.25	6.91	x	x	x
RHOXF1	89.38	92.43	85.85	3.30	x	84.42	x
S100A2	98.98	99.66	98.44	0.61	102.49	89.60	9.11
S100A8	88.77	79.05	87.52	5.29	99.66	84.93	10.42
SALL3	95.68	85.08	100.15	7.74	89.22	92.25	2.15
SERPINB2	x	x	87.25	x	x	x	x
SEZ6L	80.17	72.41	84.33	6.05	95.70	72.01	16.75
SFRP2	86.63	71.51	73.55	8.20	74.11	90.27	11.43
SNRPN	97.71	100.99	91.08	5.05	110.13	89.77	14.40
SPARC	99.25	96.46	99.25	1.61	113.94	92.85	14.91
SRGN	85.54	91.14	88.88	2.82	92.85	94.12	0.90
TBP	84.88	104.50	86.68	10.84	101.99	97.37	3.26
TCEB2	86.37	98.63	99.46	7.33	136.96	59.59	54.71
TFPI2	93.33	83.94	97.37	6.89	109.47	99.32	7.18
THBD	94.69	94.37	94.62	0.16	91.96	96.01	2.87
TJP2	102.42	101.06	114.56	7.43	99.60	98.10	1.05
TMEFF2	100.99	107.44	89.61	9.03	96.14	88.99	5.05
TP53	97.51	93.33	100.36	3.53	89.94	89.77	0.12
TWIST1	396.68	852.85	69.82	393.29	139.81	47.29	65.42
WT1	89.94	83.98	96.85	6.44	98.24	88.01	7.23
XIST	92.79	100.08	90.45	5.02	94.68	82.00	8.97
ZNF256	93.33	96.46	92.08	2.26	95.88	85.74	7.17
ZNF502	88.39	93.21	85.44	3.92	82.25	62.68	13.84

4. Appendix

A-7

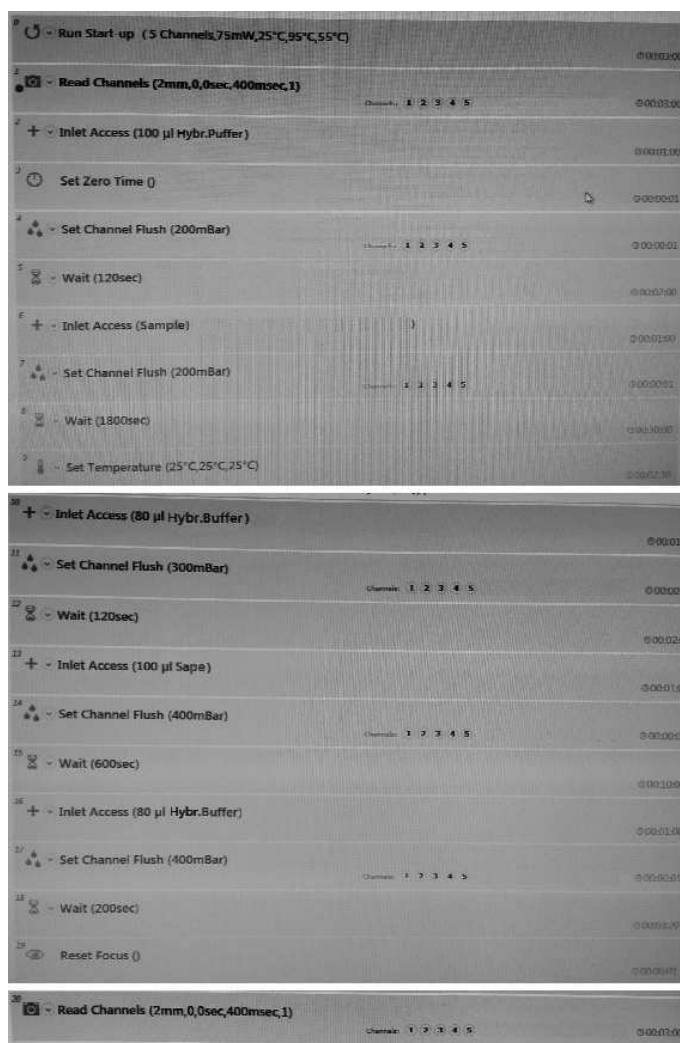


Figure 4.4: Screen shot representing the standard running script for the detection of nucleic acids sequences on Evaluation platformTM. It consists of 30 minutes sample hybridization followed by a 10 minutes incubation with Streptavidin PE and finally target detection. After each main step of the run, a short wash of the channels with hybridization buffer has to be performed in order to wash out unbounded reactants.

A-8

Table 4.5: Results of the nucleic assay sensitivity evaluation using synthetic oligonucleotides of known concentration and TMAC buffer. "X" represents a failed assay.

Targets	Target concentration							blank
	10 nM	5 nM	1 nM	0,5 nM	0.25 nM	0.05 nM	0.02 nM	
CHFR	147.31	125.19	98.58	59.66	50.83	19.12	17.53	7.89
MSH4	86.22	51.18	28.99	18.00	12.91	x	1.48	6.96
TJP2	72.16	51.48	36.78	23.64	18.16	6.08	0.00	10.93
TWIST1	103.56	71.34	43.94	30.91	x	8.27	2.57	4.70
TFPI2	82.31	25.16	23.53	17.30	14.90	8.22	16.19	26.81
GNDF	5.27	2.78	1.24	0.00	0.00	0.00	0.00	7.59
IIIB	14.84	7.58	4.36	1.57	2.87	0.61	0.03	6.02
S100A2	7.56	3.48	2.27	1.25	1.26	0.45	1.08	3.36
ZNF256	13.86	3.43	19.51	0.96	0.00	x	0.00	8.61
H19	29.98	0.00	0.00	0.00	0.00	0.00	5.50	46.64
PENK	11.27	5.10	2.98	1.88	1.30	0.93	0.11	3.37
SNRPN	38.48	25.37	4.80	1.33	1.23	0.00	0.00	4.68
GATA4	16.93	9.71	2.31	1.20	1.89	0.00	11.94	8.89
RARB	12.96	5.58	3.37	1.60	0.88	0.76	0.30	3.74
SEZ6L	20.46	9.92	10.19	7.19	7.46	0.00	0.00	42.16
CXADR	15.86	7.42	10.13	1.59	4.90	0.95	2.68	10.04
CDX1	10.21	4.08	6.94	1.57	0.82	0.93	0.15	5.91
JUB	7.47	3.24	10.47	0.83	4.63	0.14	x	9.58
SPARC	x	x	x	x	x	x	x	38.11

Table 4.6: Results of the nucleic assay sensitivity evaluation using synthetic oligonucleotides of known concentration and 3x SSC buffer. "X" represents a failed assay.

Targets	Target concentration							blank
	10 nM	5 nM	1 nM	0,5 nM	0.25 nM	0.05 nM	0.02 nM	
CHFR	100.25	77.58	33.58	22.37	18.80	3.75	2.81	5.41
MSH4	60.09	55.28	17.43	10.56	5.49	0.87	9.25	3.36
TJP2	67.71	38.06	17.62	13.57	10.89	1.35	0.25	3.49
TWIST1	72.12	48.61	15.71	12.04	7.72	1.41	0.85	3.25
TFPI2	17.89	10.75	7.23	6.25	5.71	2.08	2.36	5.52
GNDF	8.30	3.73	1.32	1.02	0.00	0.11	0.00	2.81
IIIB	10.26	7.22	2.78	1.62	1.21	0.00	0.00	2.95
S100A2	7.40	3.14	0.46	1.49	0.05	0.04	0.00	2.50
ZNF256	11.97	6.43	2.62	1.71	1.72	0.63	9.27	2.32
H19	7.83	4.81	2.76	3.93	0.36	x	2.67	13.24
PENK	6.99	3.59	1.28	0.83	x	x	0.00	2.75
SNRPN	51.04	24.79	4.75	2.79	0.13	x	0.87	3.16
GATA4	21.10	11.44	2.44	0.75	0.00	0.00	x	5.23
RARB	14.60	7.57	1.80	1.61	0.43	0.00	x	2.56
SEZ6L	16.90	10.98	8.07	5.29	4.85	1.93	x	4.67
CXADR	18.55	8.44	2.00	1.53	0.49	0.22	0.25	3.35
CDX1	7.01	4.62	2.01	1.64	0.38	x	x	2.73
JUB	9.07	5.65	2.07	1.73	1.20	x	0.23	2.99
SPARC	15.58	10.51	7.14	3.90	3.55	0.78	0.68	3.93